Tseng, Susan Yu

MORPHOLOGICAL STUDY OF TRANS 1,4-POLYBUTADIENE CRYSTALS GROWN FROM SOLUTION

City University of New York PH.D. 1983

PLEASE NOTE:

In all cases this material has been filmed in the best possible way from the available copy. Problems encountered with this document have been identified here with a check mark ✓.

1. Glossy photographs or pages ✓
2. Colored illustrations, paper or print _____
3. Photographs with dark background ✓
4. Illustrations are poor copy _____
5. Pages with black marks, not original copy _____
6. Print shows through as there is text on both sides of page _____
7. Indistinct, broken or small print on several pages ✓
8. Print exceeds margin requirements _____
9. Tightly bound copy with print lost in spine _____
10. Computer printout pages with indistinct print _____
11. Page(s) _____ lacking when material received, and not available from school or author.
12. Page(s) _____ seem to be missing in numbering only as text follows.
13. Two pages numbered _____. Text follows.
14. Curling and wrinkled pages ✓
15. Other _____

MORPHOLOGICAL STUDY OF TRANS 1,4-POLYBUTADIENE CRYSTALS GROWN FROM SOLUTION

By

Susan Y. Tseng

A Dissertation Submitted to the Graduate Faculty in Chemistry in Partial Fulfillment of the Requirements for the Degree of Doctor of Philosophy, The City University of New York.

1982

This manuscript has been read and accepted for the Graduate Faculty in Chemistry in satisfaction of the dissertation requirement for the degree of Doctoral of Philosophy.

October 12, 1982
date

Arthur E. Woodward
Chairman of Examining Committee

12 October 1982
date

David C. Lorden
Executive Officer

George Odian

Yaw-Ming Yang

Arthur E Woodward
Supervisory Committee

The City University of New York

ABSTRACT

Molecular weight fractions of trans 1,4-polybutadiene, prepared by fractional crystallization, were characterized by gel permeation chromatography and were found to have $\bar{M}_n$'s of 4.7×10^3 to 1.2×10^5 and $\bar{M}_w/\bar{M}_n$ of 1.3 to 2.7. The morphologies of self-seeded solution crystallized samples prepared from these fractions were studied by photomicroscopy and electron microscopy. The physical properties were studied using small angle X-ray scattering, density measurement, differential scanning calorimetry and chemical reaction at the crystal surface with m-chloroperbenzoic acid in toluene solution. These properties are related to the % crystallinity, the distribution of the disordered fraction and the type of chain folding in the TPBD crystals.

Single lamellas with few screw dislocations were found for crystals grown from dilute solutions (0.01% to 0.02%). A more complicated multilamella supermolecular structure was found for concentrated solution (1% to 10%) grown crystals. (An increase in lamellar thickness, L, vs. crystallization temperature were discovered in this research.) For dilute solution grown crystals the heat of transition from DSC was found to be proportional to the specific volume. For crystals prepared from one fraction ($\bar{M}_n = 2.8 \times 10^4$) secondary endotherms in the crystal-crystal transition region were observed. These secondary endotherms are attributed to nonisothermal crystallization and crystallization of an adsorbed polymer layer. Other types of crystal defect/disordered fraction and their relationship to the amorphous density are discussed.

The number of monomer units per chain fold, U, and the number of monomer units per chain end, c/2, were obtained from an equation that

relates these two parameters to the crystal thickness, L_c, the fraction of double bonds at the crystal surfaces, F_s, the crystal repeat distance along the polymer chain, R, and $\bar{M}_n$. It is concluded that the length of chain ends in each molecule is proportional to the lamellar thickness, 0.79 L/R, and the number of monomer units per chain fold, U, decreases with decreasing crystallization temperature and molecular weight.

A method of using ^{13}C nmr spectrum to study chain folding is discussed. Satisfactory agreement of U values from F_s with those from direct measurement was found.

ACKNOWLEDGEMENTS

I wish to express, first of all, my deepest gratitude and sincere appreciation to my mentor, Dr. A. E. Woodward for his precious time frequently given to me; his most competent guidance and excellent advice on my entire research project; and his untiring efforts in directing and assisting me going through various aspects of academic life throughout my graduate study.

I would like to thank Dr. G. Odian for his inspiration and encouragement especially during my early years as a graduate student. To Dr. N. L. Yang, I am thankful for his critical readings and constructive suggestions on my thesis.

A word of thanks is due to Dr. F. Naider and Dr. H. Haubenstock for their stimulating lectures on the advanced courses which have considerably broadened my required knowledge in the field of polymer chemistry.

I am much obliged also to Mr. and Mrs. S. Parello's family who have been most helpful in taking excellent care of my son, Alan, over the past five years.

I should like to take this opportunity to extend my grateful thanks to my parents, Mr. and Mrs. T. K. Yu, who helped me lay down an academic foundation in my early life; to my parents in law, Mr. and Mrs. C. T. Tseng, for their understanding and spiritual support during my research years.

Finally, I find it hard to express adequately my indebtedness to my husband, Jason, for his unfailing patience and long standing

and staunch support; to my six-year old son, Alan, for his remarkable understanding and awareness as well as his joyful personality. Without their love and willing cooperation the completion of my dissertation would not have been possible.

TABLE OF CONTENTS

	Page
INTRODUCTION	1
EXPERIMENTAL	21
Samples	21
Sample Characterization	23
Crystal Preparation	24
Photomicroscope and Electron Microscope Observation	25
Low Angle X-Ray Scattering (LAXS)	26
Density Measurement	26
Differential Scanning Calorimetry (DSC) Measurement	27
Epoxidation Reaction	31
^{13}C NMR Measurements	35
RESULTS	39
Gel Permeation Chromatography	39
Photomicroscope and Electron Microscope Observation	43
Differential Scanning Calorimetry	54
Density Measurement	60
Epoxidation Reaction	60
Low Angle X-Ray Scattering	61
^{13}C NMR Measurement	63
DISCUSSION	66
Temperature Gradient Fractionation	66
Crystallinity and Crystal Defects	67
Multiple Endotherms In the Crystal-Crystal Transition Region	73

TABLE OF CONTENTS (Continued)

Page

Chain Folding

(A) Calculation of the Monomer Units Per Chain Fold and Chain End 78

(B) Independent Calculation of Monomer Units Per Chain Fold From ^{13}C NMR Spectrum 88

CONCLUSIONS 91

APPENDIX 93

^{13}C NMR Spectroscopic Study of Epoxidized TPBD Crystals and Model Compounds 93

The Chain Tilt Correction in the Calculation of U Values From Equation (7) 124

Solution of Equation (7) 126

REFERENCES 128

TABLES

Table Number	Caption	Page
1	Comparison of Epoxidation and IR Results for TPBD Single Crystals	13
2	Disordered Fraction in TPBD Single Crystals	16
3	Characteristics of TPBD Samples	22
4	Chemical Shifts of Polybutadiene and Epoxypolybutadiene	34
5	Epoxidation Data for Wet and Dry Single Crystals UH45	36
6	Preparation of TPBD Crystals	40
7	Calorimetric, Density, Epoxidation and Lamellar Thickness Results for Dilute Solution-Grown TPBD Crystals	52
8	The Transition Temperature, Heat of Transition and the Non-crystalline Fraction for TPBD Grown From Solution at Various Concentration	59
9	^{13}C NMR Measurement for Epoxidized TPBD Crystals...	65
10	Calculation of Number of Monomer Units per Fold for TPBD Crystals	84
11	Disordered Fraction and U Value for TPBD Crystals	86
12	^{13}C NMR Measurement for Epoxidized TPBD Crystals ..	90

FIGURES

Figure No.	Caption	Page
1	Model of Fold Plane Illustrating Chain Folding with Imperfections which May Occur in the Structure	4
2	(a) DSC Scan of TPBD Single Crystals (VH53) (b) Conformation of TPBD Form I and Form II Crystals	10
3	Mixing Device for a Density Column	28
4	Typical Calibration Curve of a Density Gradient Column	29
5	Differential Scanning Calorimetry Scans for Dilute Solution Grown Crystals From Three TPBD Fractions: (1) F1H55; (2) F2H36; (3) F3H29	30
6	100 MHz ^{1}H NMR Spectrum of Partially Epoxidized TPBD Sample	33
7	Gel Permeation Chromatograms for TPBD Fractions: (1) F1; (2) F2; (3) F3; (4) UH45; (5) F1H55; (6) VH53; (7) WH62	41
8	Gel Permeation Chromatograms for TPBD Fractions: (1) F1b; (2) F2b; (3) F3b	42
9	Electron Micrograph of TPBD Crystals, F3H29	44
10	Electron Micrograph of TPBD Crystals, F2H36	45
11	Electron Micrograph of TPBD Crystals, F1H55	46
12	Electron Micrograph of TPBD Crystals, VH53	47
13	Electron Micrograph of TPBD Crystals, WH62	48
14	Electron Micrograph of TPBD Crystals, F1H29	49
15	Electron Micrograph of TPBD Crystals, F1T15	50

FIGURES (Continued)

		Page
16	Electron Micrograph of TPBD Crystals, UH45	51
17	Photomicrograph of TPBD Crystals, 5% F1bH60	53
18	Electron Micrograph of TPBD Crystals, 5% F1bH60	55
19	Enthalpy of Crystal-Crystal Transition vs. Specific Volume for Dilute Solution-Grown TPBD Crystals	56
20	DSC Scans for TPBD Crystals Grown from Concentrated Solution: (a) 5% F1bH60; (b) 5% F1bH55; (c) 1% F1bH55; (d) 5% F1bH29; (e) 5% F2bH36; (f) 5% F2bH42; (g) 5% F3bH29; (h) F3bH40; (i) 10% F3bH29	58
21	Schematic Representation of Crystalline and Associated Noncrystalline Region	62
22	Different Kinds of Defects in the Crystalline Region ...	68
23	Proposed Model of Adjacent Reentry Fold with an Amorphous Phase that Consists of Polymer Molecules that are Physically Adsorbed on the Fold Surface	69
24	Models of the Fold Region for TPBD Crystals Grown From Two Different Preparations, (a) Heptane Grown Crystals; (b) Toluene Grown Crystals	72
25	Schematic Representation of Chain Folds, Chain Ends and Crystal Stems of a Polymer Molecule	79
26	Determination of the Average Number of Monomer Units per Fold and the Average Number of Monomer Units per Chain End for Dilute Solution-Grown TPBD Crystals	82

INTRODUCTION

Polymer crystals often have crystal habits characteristic of their crystallization condition. Lamellar habits are frequent for crystals slowly grown from polymer melts or solutions.[1] The simplest and first discovered lamellar habits of polymer crystals are polymer single crystals grown from dilute solutions.[2-4] Subsequent work[5,6] showed similar lamellae to be the basic structural element in spherulites - a common morphological entity obtained from melt-grown crystals. In an attempt to elucidate the morphology and to understand crystallization from the melt, the detailed studies of polymer crystals grown from dilute solution as well as concentrated solution - the latter exhibiting a complexity between that of crystals grown from dilute solution and those grown from the melt - are necessary.

In the year of 1957, three papers published nearly simultaneously by Keller,[2] Fischer[3] and Till[4] in England, Germany and the U.S., recongized that isolated single crystals of a polymer, polyethylene, with thin platelet lamella could be grown. All three papers reported the use of electron microscopy to examine the structure of linear polyethylene crystallized from dilute solution. The single crystals observed were platelets on the order of 10 nm in thickness and 1-50 μm in lateral dimension. Further investigations[7-12] found that any flexible linear backbone polymer which is sterically regular can be crystallized from solution in platelet form using appropriate solvent and temperature conditions. However, the most extensive studies to date on morphology and polymer properties have been carried out using polyethylene.

The thickness of polyethylene single crystals obtained from dilute solution are very sensitive to crystallization temperature and the solvent used.[13-22] The thickness varies from 100 to 200Å depending on the crystallization conditions. The uniformity of thickness was deduced from detailed examination with the electron microscope and from small angle X-ray scattering, SAXS, maxima of a collection of such crystals. The orientation of the chain molecules within the platelet have been determined from selected area electron diffraction studies.[2,3,10,23] Detailed analysis indicated that the chain axis is preferentially oriented perpendicular to the wide face of the crystals; the a and b crystallographic axes are preserved throughout the platelet structure, so that the term "single crystal" has been commonly given to such structures.

Knowing the long chain nature of polymers, it becomes clear that during crystallization a given molecule must traverse the crystallite many times to satisfy the requirements of a linear long chain. Chain folding in polymer crystallization is thus well established. However, the nature of the fold region has been the subject of intensive study and controversy.

Some workers[24-26] reported that polymer single crystals are perfectly regular crystalline entities and the polymer chains regularly undergo adjacent reentry. Fischer and Lorenz,[27] Jackson et al.[28] and Flory[29] measured the density of single crystal mates of polyethylene and arrived at a conclusion in favor of random irregular polymer chain reentry - the nonadjacent reentry or switchboard model. Several

later studies[30-33] support models in which there is a distribution of fold sizes, ranging from very short tight folds to very long loose folds. Regardless of the controversy concerning the exact nature of chain folding, it can be concluded that the thin platelet lamella contains two portions - a crystalline portion and an amorphous portion. As shown in Fig. 1, polymers form thin lamella with a thickness of L, as observed using the electron microscope and from low angle X-ray scattering. The lamella contains a crystalline core with average crystallite thickness, L_c. Since the molecules are not of infinite length, there will be chain end (cilia). Infrared studies[34-36] on polyethylene found that chain ends are outside the crystal lattice. Therefore, the surface component is composed of chain folds and chain ends for perfect single crystals.

On changing the crystallization conditions by lowering T_c, therefore increasing the degree of undercooling, more and more defects become incorporated and remain in the crystals. One such defect which leads to multilayer crystals is the spiral growth[37,92-94] induced by screw dislocations in the parent lamella formed during the preparation of single crystals. Other more complicated morphologies[27,92,38-40] of polyethylene grown from solutions have been reported; however, the lamellar nature of polymer crystals have been found to be fundamental. Disorder in the crystal interior can

occur, a shown in Fig. 1, due to irregularities in packing, dislocations or numerous other imperfections.

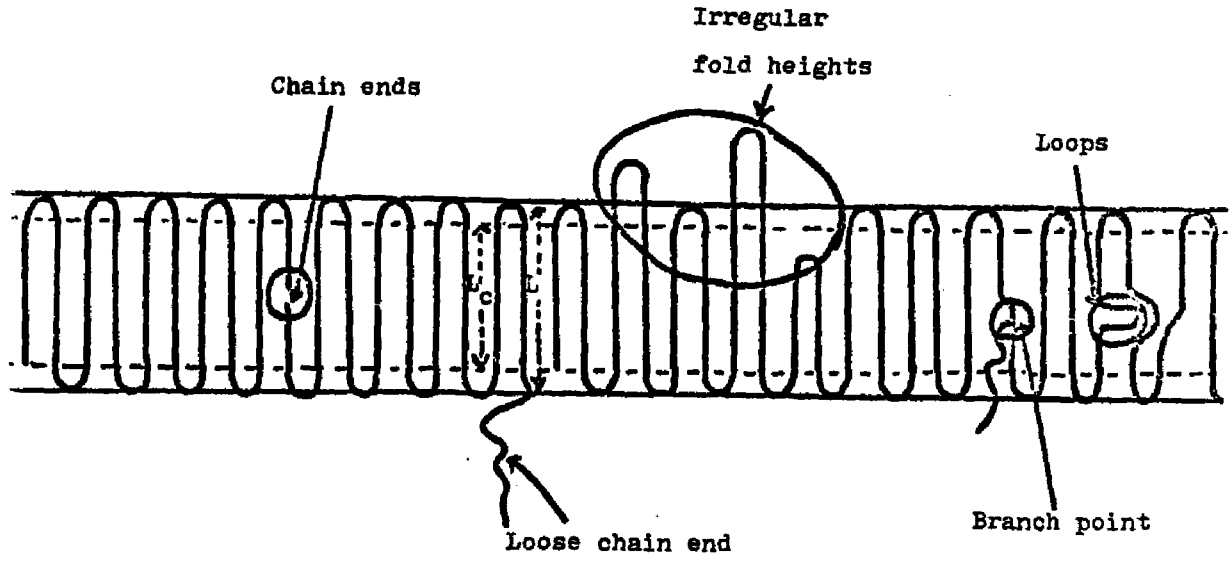

Fig. 1. Model of fold plane illustrating chain folding with imperfections which may occur in the structure.

For the interpretation of physical properties of polymer crystals the percent crystallinity has been considered to be primary. Using the floatation, or density gradient method, measurements of polyethylene crystals[34,41,42] showed that densities obtained lie somewhere between those for the perfect unit cell as obtained from X-ray crystallography and the melt, the latter being corrected for temperature. Assuming that the sample is composed of a relatively perfect crystalline phase and a completely amorphous noncrystalline phase, a percent crystallinity of these crystals were calculated. Although the separated two phase system assumed for a crystal may be an oversimplification, a systematic decrease in the percent crystallinity with both increasing molecular weight (10^4-$4x10^5$) and decreasing crystallization temperature were reported.[42]

Several workers[43,49] analyzed the broad-line n.m.r. spectra of sedimented polymer crystals and tried to correlate the absorption line shape with the polymer chain mobility in the crystalline and amorphous regions of a crystal. Bergman and Nawotki[43] gave a quantitative account for the spectra obtained - the broad component was characteristic of segmental motion within the crystalline region and the narrow component resulted from the motions within the liquid-like amorphous regions. Madelkern[50] compared the crystallinities from broad-line n.m.r. with those from the density for linear polyethylene at room temperature and concluded that the degree of crystallinity can be quantitatively observed from broad-line n.m.r.

The heat of fusion determined calorimetrically for polymer

crystals has been studied.[42,52-54] Wunderlich and Carmier[51] reported that the heat of fusion of polyethylene solution grown crystals increased with increasing lamellar thickness. An opposite relationship[52] was observed by keeping the lamellar thickness constant but increasing the molecular weight and molecular weight distribution which are possibly affecting the regularity of polymer crystals. Using the floatation method, X-ray diffraction and differential scanning calorimetry, DSC, Hamada et al.[42] compared the density and heat of fusion of folded chain polyethylene crystals. The results were that the heat of fusion is proportional to the specific volume as long as the fold length stays constant. However, crystals with different fold lengths showed different specific volume - heat of fusion relationships. Wunderlich[53] concluded that the heat of fusion is affected by both the crystallinity and the lamellar fold length.

The melting phenomena of polyethylene as correlated with the lamellar thickness has been studied by Wunderlich, Harrison and their coworkers.[54-57] Wunderlich[54] observed the crystal melting on a microscope hot stage and found that melting temperature of the crystals was decreased as the heating rate increased. Harrison[55] observed a narrow, sharp melting for high molecular weight polyethylene single crystals in studies using DSC and differential thermal analysis, DTA. However, a broad, multiple melting endotherm for lower molecular weight specimens was reported recently.[56,57] An interpretation for this phenomena has been given in terms of the possibility of partially melting and recrystallization of the chain

folded crystals.

A number of scientists have studied the details of chain folding directly by chemical assay. Peterlin and Keller and their coworkers[58-60] studied polyethylene single crystals by degrading the amorphous portion with fuming nitric acid at high temperatures. The reactions were followed by analysis of the heat of fusion, density measurement and molecular weight distribution of the fragments as a function of reaction time. However, the results indicated that the strong degradative chemical reagent has very little selectivity between the amorphous regions and the crystalline interiors. Keller and several later workers[61-64] carried out the same experiment using a milder degrading reagent, ozone. The peak distribution studies from gel permeation chromatography showed that the undegraded fragments contained molecular lengths of single, double and higher multiple-chain traverses within the crystal layer. The results were interpreted in terms of adjacent reentry folds terminated via random chain scission by the ozone. However, once the chain folds have been cut, continuing reaction shortens the chains. The degradative method makes a quantitative study of the amorphous region difficult to carry out.

Recently Harrison and Juska[65] estimated the number of carbons of a tight-fold adjacent reentry fold of polyethylene using the CPK Precision space filling models. The fold was anchored with proper spacing and the volume occupied was measured to ±3Å. Visual inspection of the models indicated that the carbon number per chain is approximately from 9 to 11.

Based on the discussion above, it is clear that quantitative details concerning the fold surface are not readily forthcoming for a polymer such as polyethylene. However, trans 1,4-polybutadiene, TPBD, can be employed for such a quantitative analysis for the following reasons:

(1) TPBD contains one double bond in each monomer unit of the main chain. The reactivity of the double bond is advantageous in a study of the noncrystalline lamellar surfaces. As is expected the crystalline region is not penetrated by small molecules while the amorphous surface region is reactive. The amount of double bonds present at the crystal surfaces should be quantitatively accessible by nondegradative chemical methods and therefore will provide information concerning chain folding in polymer crystals. (2) TPBD is a flexible linear macromolecule and it can develop a high degree of crystallinity. (3) TPBD has two crystalline forms; the low temperature form, form I and the high temperature form, form II. The crystal-crystal transition temperature occurs between 55 to 75°C, which is relatively low compared with the final melting temperature (120 to 140°C). It is expected that in the crystal-crystal transition region less catastropic changes are taking place morphologically than in the melting region thereby making it easier to investigate the effect of various parameters, such as % crystallinity and molecular weight. A series of investigations on unfractionated TPBD single crystals grown from dilute solution were carried out previously by Woodward and coworkers.[66-75] An

investigation of the morphology and properties of TPBD samples with narrow molecular weight distribution prepared at various concentrations over a broad range can be an interesting and logical extension of the previous work.

Of the two crystalline forms known to exist in TPBD, form I is stable at room temperature and transforms to form II with the highest temperature of this being reported[76] as 76°C. The transformation between the two forms is a first-order crystal-crystal transition and is thermodynamically reversible. A typical DSC scan for TPBD single crystals is shown in Fig. 2a. The highest reported melting temperature for form II is 148°C.[78] It was revealed by X-ray structure analysis that form I crystals belong to the monoclinic system with the space group $P2/_1a$. The unit cell, with a = 8.63Å, b = 9.11Å, c = 4.83Å and β = 114°, includes four molecular repeat segments. The molecular packing, the arrangement of the center of mass of each chain projected on the a b plane, is hexagonal. After transformation of the crystal into high temperature form, Takayanaki[77] reported from the studies of X-ray diffraction patterns that form II crystals belong to a hexagonal lattice. The assignment of the space group is uncertain because the X-ray diffraction pattern consists of diffuse spots. The dimension of the unit cell are a = 4.95Å and c = 4.66Å. The diffuse spots were explained by the large degree of rotational motion of the chain segments around the molecular axis. The chain conformational differences of form I and form II are shown in Fig. 2b. The CH_2-CH_2 bonds in both form I and form II remain in the trans conformation but the internal rotation angles around two CH_2-CH

bonds in form II are decreased to 80 and -80 from 109 to -109 as present in form I. The molecular chains in form II are considerably distorted and this causes torsional oscillation of the $-CH_2CH_2-$ segments around the c-axis.

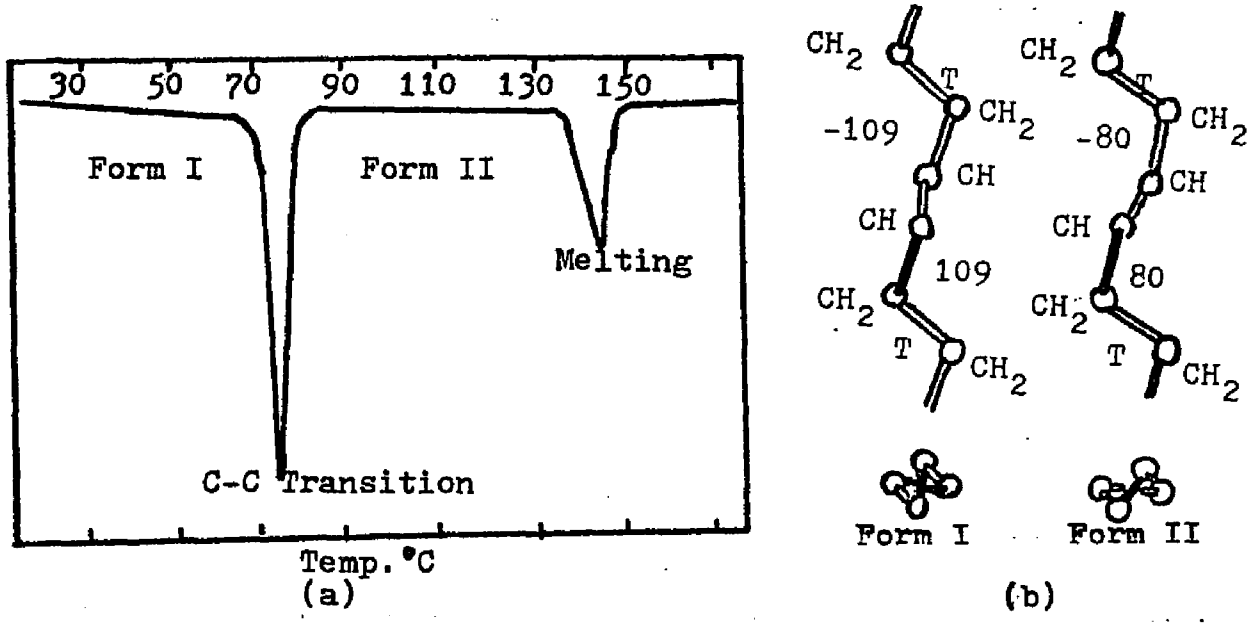

Fig. 2. (a) DSC Scan of TPBD Single Crystals (VH53) (b) Conformations of TPBD Form I and Form II Crystals as Taken From Reference 77.

Using a self-seeding method the technique of growing polymer single crystals requires: (1) a minimum disolution temperature, (2) a relatively high crystallization temperature and (3) low concentration. The nature of chain folding in TPBD crystals was first investigated by Tatsumi et al.[76] Single crystals were prepared from benzene solution at 18°C and studies of the crystal-crystal transition phenomena showed that the transition temperature changed from 55.5°C to 69.5°C after annealing of the single crystal

mats at 100°C for one hour. This phenomena was also studied using dilatometry. X-ray diffraction measurements following the heat treatment showed that the lamellar thickness changed to 155Å from 100Å. The result was explained in terms of rapid crystallization in the surface component at the annealing temperature . In particular, the loose loops at the fold surfaces of the crystal were dragged into the crystalline phase to form tight folds as a result of sliding diffusion of molecules along their axes. This was accompanied by the sudden thickening of the lamellae at the crystal transition temperature. After that time, more extensive studies concerned with the nature of chain folding of TPBD single crystals were carried out by Woodward and coworkers.[66-75]

Studies of chain folding were carried out by Stellman and Woodward[66,67] using a non-destructive method, an expoxidation reaction of m-chloroperbenzoic acid, MCℓPBA, with TPBD single crystals suspended in benzene at low temperature (6°C). The reaction between a peroxy group and a double bond to form an epoxy group in the polymer, was monitored from the loss of reactant, MCℓPBA, by iodometric titration. Kinetic studies using the iodometric titration results of the epoxidation reaction vs. reaction time showed that the surface epoxidation reaction was completed within 4 to 5 days. The quantitative chemical assay found that, depending on the crystal growth condition, from 14 to 27% of the double bonds are available for each reaction with MCℓPBA for crystals of approximately the same thickness (100Å). This leads to an average values of

monomer units per fold from 2.5 to 5 depending on the crystallization solvent (heptane or benzene). The number of double bonds necessary for the tightest reentry fold calculated from the crystal structure given by Iwayanagi[78] is between 1.5 to 2. Comparison of the value of double bonds per fold from the experiments of Stellman and Woodward[66,67] lead to a conclusion that reentry folding is highly probable, although some fold looseness can occur.

High resolution infrared spectra have been obtained in the 1000-1400 cm^{-1} region for TPBD crystal mats grown from six different solvents.[68,69] It was found that the ratio of the IR bands intensity at 1350 cm^{-1}, an amorphous band, to that at 1335 cm^{-1}, a regularity band, varied with the solvent used and thermal history. The ratio is larger for crystals grown at temperature well below the transition temperature than those grown near to the transition temperature. When the crystals were heated to 80°C and cooled down to room temperature, the infrared intensity ratio I_{1350}/I_{1335} decreased. It was concluded by Stellman and Woodward[69] that the internal order of the crystal increased upon annealing. Accompanying the heat treatment, the increase in crystal thickness would lead to a decrease in the number of folds but would not necessarily lead to fold tightening.

Comparison of epoxidation and IR results for several TPBD

crystals are given in Table 1. The relative agreement between

TABLE 1. COMPARISON OF EPOXIDATION AND IR RESULTS FOR TPBD Single Crystals. (Taken from reference 68)

Sample	Solvent	$\alpha/(1 - \alpha^{\ddagger})$	I_{1350}/I_{1335}
TPBD-K	MIBK*	0.28	0.2
$\bar{M}_n$ = 36000	Heptane	0.16	0.2
	Tolune	0.23	1
	Benzene	0.37	1
TPBD-U	Heptane	0.52	0.3
$\bar{M}_n$ = 5510			

*Methyl isobutyl ketone

$^{\ddagger}\alpha$ is the fraction of double bonds epoxidized

epoxidation and IR results for some of the preparations support the viewpoint that the amorphous regions can be predominantly on the crystal surfaces, where it is either associated with chain folds or with the presence of chain ends.

Ng, Stellman and Woodward[70] studied TPBD crystals by using differential scanning calorimetry. Assuming ΔH_{tr}, the heat of transition from form I to form II, to be in proportion to the crystallinity and taking the epoxidation value for TPBD-K, heptane grown crystals as a standard, it was found that toluene and benzene grown crystals have a greater amorphous content than

heptane grown crystals, in agreement with the epoxidation results.

Another method which was used to estimate the total amount of amorphous material in a solid is broad-line nuclear magnetic resonance. When the conditions are such that segmental motion is taking place in the amorphous component and the crystalline regions are effectively rigid, a two components nmr absorption will be found. The narrow component is associated with the mobile region. Eng and Woodward[71] reported the measurement of nmr intensity ratio for TPBD crystals grown from heptane and toluene. The crystals were wetted with a non-protonated solvent (CS_2) which served as a surface penetrant to increase the segmental mobility in the amorphous region of the crystals. The nmr determinations were carried out at low temperatures (-24°C to -90°C). Assuming that the narrow line accounts for all or most of the amorphous regions, toluene grown crystals have a greater amorphous content than heptane grown crystals. TPBD crystals annealed at 80°C in the dry state showed a lower amorphous content than unannealed single crystal mats.

Evans and Woodward[72] studied the Raman spectra of mats of TPBD crystals grown from dilute solution. The effect of crystal growth temperature, of solvent and of various thermal and mechanical treatments on the spectrum at 25°C were explored. The changes accompanying the form I to form II crystal-crystal transition were observed by obtaining Raman spectra at various temperatures in the 25-78°C range.

The spin-probe technique has been employed by Nagamura and Woodward[73] to study the nature of the surface region of TPBD crystals

grown from dilute heptane and toluene solutions. The spin probe method is based on the response of the line shape of the ESR spectrum of a paramagnetic probe, usually a nitroxide radical, embedded in a polymer matrix to molecular motion of the matrix. The probes are not chemically bonded but only weakly held by the polymer chains. The narrowing of the ESR spectrum of the nitroxide radical probe added to the TPBD crystals and the activation energy for the rotational motion of the probes were found to vary with crystallization solvent and annealing temperature. In every case heptane grown crystals showed a higher line narrowing temperature and activation energy than toluene grown crystals. Annealing at 80°C raised the narrowing temperature and activation energy for crystals prepared from both solvents. The results confirmed earlier work concerning the nature and location of the amorphous regions in TPBD crystals.

Recently Wichacheewa and Woodward[74] studied the kinetics of epoxidation of TPBD crystals in suspension at different temperatures. The % epoxidation was determined by obtaining the mole ratio of MCℓPBA, to products, m-chlorobenzoic acid (MCℓBA), in the solution using infrared spectroscopy. The IR absorbance ratio at 1700 and 1735 cm^{-1} which correspond to the carbonyl stretching band of MCℓPBA and MCℓBA, respectively, was calculated with a calibration curve obtained using known mixtures of the two reagents. Expoxidation conditions were investigated in 6-12°C range and IR measurements were carried out at room temperature. It was found that the reaction was completed within 3 to 5 days and the temperature dependence of the total number of double bonds available for reaction depend on the crystal preparation

conditions.

Wichacheewa and Woodward[74] also studied the bromination of TPBD crystals in suspension at low temperature (0°C) in the dark. The % bromination was measured with a visible light spectrometer using the absorption at 416 nm. An absorbance-concentration curve was obtained using known amount of Br_2 in the solvent (CCl_4). Enough Br_2 to react with the double bonds in the total polymer was added initially. It was found that the bromination reaction was completed within one hour.

Comparison of the disordered fraction of three TPBD crystals obtained using the various methods discussed above are given in Table 2. The % epoxidation for the three preparations is found to decrease with an increase in crystallization temperature and the polymer molecular weight. The change with molecular weight is caused at least in part by the increased presence of chain ends as the molecular weight is decreased.

TABLE 2. DISORDERED FRACTION IN TPBD SINGLE CRYSTALS (Taken from reference 74.)

Sample Preparation	$\bar{M}_n$	% Epoxidation				% Brominated	nmr	DSC	IR
		6C	12C	16C	21C				
K-H (78/70/63)	36000	0.14	...	...	0.13	0.13	0.13	...	0.14
K-T (50/45/23)		0.14	0.23	...	0.29	0.21	0.23	0.4±0.1	0.44
U-H (69/55/45)	5510	0.27	0.33	0.32	0.35	...	...	...	0.2

Brown, Jenkins and Park[79] studied the sorption and diffusion of small molecules into partially crystalline polybutadiene. The small molecules studied were methylene chloride, chloroform, benzene and 2,2,4-trimethylpentane. It was found that the diffusion coefficient at zero penetrant concentration decreases with increasing trans content and with increasing size of the diffusant. These changes were believed due to the inaccessibility of the crystalline regions with little change in basic mechanism of diffusion in the amorphous regions.

Oyama et al.[80] reported the conformations and the number of $-CH_2CH_2-$ units in the fold loop of TPBD single crystals from IR studies. Four conformation sensitive methylene scissor bands were assigned using the model compound 1,5-hexadiene. Two bands at 1458 cm^{-1} and 1449 cm^{-1} were assigned to amorphous conformations and the other two bands at 1451 cm^{-1} and 1438 cm^{-1} to crystalline conformations. The single crystal spectrum was resolved into four bands and the ratio between band intensities were obtained as a function of crystal annealing temperature. It was concluded that the average conformation in the noncrystalline part become gauch-rich. The total number of monomer units per fold was roughly estimated to be five for the as grown crystals (grown from benzene solution at 15°C) and to be three for the 80°C annealed sample.

Martuscelli et al.[81] reported on the selective bromination of TPBD single crystals in suspension. The selectivity of bromination at the fold surface was demonstrated by DSC, IR, small angle and wide angle X-ray diffraction. It was found that a larger

number of double bonds per fold are brominated as the thickness of the single crystal is increased. Martuscelli et al.[82] also investigated the morphology and thermal behavior of TPBD single crystals grown from heptane using the electron microscope, wide angle X-rang diffraction and differential scanning calorimetry. The thickness of crystals reported was much greater than those reported earlier by Woodward[66,67,74] and Takayanagi et al.[76] It was found that the equilibrium transition temperature of form I and form II is at 75°C and the melting temperature of form II is 139°C. The DSC thermograms of aggregated TPBD single crystals showed two endothermic peaks in the crystal-crystal transition region. The result was explained by the presence of crystalline blocks of form I with two different thermodynamic stabilities.

Recently Finter and Wegner[83] studied the SAXS and DSC for TPBD single crystals grown from heptane. Crystals with lamellar thickness varying from 83Å to 293Å were reported. The DSC thermograms showed that the crystal-crystal transition temperature increases as the thickness of the crystals increases. Multiple endotherms in the DSC scan for TPBD single crystals were also reported. This was explained as being caused by two different regimes of crystallization behavior, depending on whether nucleation occurred at high temperatures, form II, or at low temperature, form I. The two regimes of crystallization behavior determined the crystal thickness as well as the phase transition and annealing behavior of the crystals.

In the earlier studies of TPBD crystals little attention was paid to the effect, if any, of molecular weight distribution and

polymer concentration on the chain folding. Use of a nondegradative method, selective epoxidation, was considered as most appropriate for studying chain folding in TPBD crystals. However, rather than following the epoxidation by measuring the loss of the epoxidizing agent either by iodometric titration or IR absorbance it was believed of interest to develop methods that analyzed the polymer. Therefore, both ^{1}H and carbon 13, ^{13}C, nuclear magnetic resonance, nmr, were employed.

Statement of the problem

The major purposes for this project are:

(1) to obtain information about the amount and location of the non-crystalline portion in TPBD structures prepared by crystallization from solution as a function of molecular weight using relatively narrow fractions,

(2) to obtain information about the amount and location of the disordered portion in TPBD structures prepared at different concentrations, and

(3) to study in more detail the fold surfaces of these differently prepared TPBD crystals.

Approach to the problem

This investigation is divided into three parts:

(1) Fractionation of TPBD samples and determination of molecular weight and molecular weight distribution.

(2) The preparation and morphological characterization of TPBD structures which are obtained by crystallization from solution.

(3) The determination of the total crystalline and non-crystalline contents and the amount in the non-crystalline parts available to penetration by small molecule reactants for the TPBD structures prepared.

EXPERIMENTAL

Samples

Three trans 1,4-polybutadiene preparations were used in this study: TPBD-U supplied by Uniroyal Inc; TPBD-V supplied by Polysar Ltd. and TPBD-W obtained from Dr. C. E. Wilkes of B. F. Goodrich. The TPBD-U was purified by directly dissolving at elevated temperatures in heptane (1 gram per 100 cm^3 heptane) and precipitating at room temperature. Both the TPBD-V and -W polymers were placed in enough toluene to give a 1% solution with a sizable gel portion being separated. The soluble -V polymer was recovered by precipitating in methanol at room temperature. The -W polymer was directly precipitated from toluene solution at room temperature after separation of the insoluble materials. These will be refered to below as purified -U, -V and -W, respectively. Some preparation information and molecular weight data obtained on the purified materials using GPC are given in Table 3.

The fractionation method used in this research is temperature gradient fractional crystallization under nitrogen purge using heptane as solvent.

The samples used in the study of dilute solution grown crystals were fractionated from the purified -U, -V and -W polymers. For the -U polymer fractionation was carried out by preparing a 1% heptane solution and fractionally crystallizing at 56°C, 50°C, 48°C, 45°C, 40°C, 38°C and room temperature. The 56°C, 45°C and room temperature fractions were recrystallized at the same temperature from 0.05%

TABLE 3. CHARACTERISTICS OF TPBD SAMPLES

Sample	Polymer Preparation Condition	$\bar{M}_n \times 10^{-4}$	$\bar{M}_w/\bar{M}_n$
W	Urea Canal Complex	7.9	3.5
V		2.2	2.5
U	$RhCl_3$-Sodium Alkyl Benzene Sulfonate	.70	3.0

heptane solution yielding F1, F2 and F3 respectively. Another fraction also obtained from the -U polymer is designated UH45. It was prepared from the purified unfractionated -U polymer by isothermal crystallization in 0.01% heptane solution at 45°C. One fraction each were obtained from -V and -W polymers. They were prepared by isothermal crystallization of 0.01% purified -V and -W polymers in heptane solutions at 53°C and 62°C, respectively. These two fractions are designated as VH53 and WH62.

The fractions used in the study of concentrated solution grown crystals were obtained from purified -U polymer only. These were obtained by starting with a 1% heptane solution and fractionally crystallized at 56°C, 48°C, 45°C, 40°C and room temperature. The 56°C, 45°C and room temperature fractions were the ones used and are designated as F1b, F2b and F3b.

Sample Characterization

All of the fractions were subjected to ^{1}H nmr using a JEOLCO JNM MH 100. It was found that these samples did not contain 1,2-polymerized units or any other detectable chemical impurities. For two selective samples UH45 and VH53, the trans 1,4-contents were found to be 99.5% and greater than 99.7%, respectively, by ^{13}C nmr analysis as carried out by F. A. Bovey and F. C. Schilling at Bell Laboratories using a Varian XL-200 instrument.

Molecular weight and molecular weight distribution for the purified unfractionated polymers and for each fraction prepared were obtained using a Waters Associates 200 Analytical gel permeation chromatograph with toluene at 85°C as the solvent. The

optimum resolution was achieved by joining four columns of the pore size distribution in the packing material (styragel and paragel) together. Calibration was carried out with five polyisoprene standards in the 1.0×10^4 to 8.0×10^4 molecular weight ranges, two polybutadiene standards with weight average molecular weight of 1.0×10^3 and 2.7×10^3 and squalene (411 gm/mole).

For molecular weights above 8.0×10^4 an extrapolation of the results for the polybutadiene and polyisoprene standards was made paralleling a curve obtained from a series of polystyrene standards. The GPC scan for squalene yielded $\bar{M}_w/\bar{M}_n = 1.06$; therefore 0.06 was substracted from the $\bar{M}_w/\bar{M}_n$ values obtained with GPC for each of the TPBD preparations as a boundary spreading correction.

Crystal Preparation

Crystals were prepared from 0.02% (w/v) toluene or 0.01% (dilute) and 1, 5 and 10% (concentrate) heptane solutions by the following procedures: dissolution under nitrogen purge, precipitation at room temperature, redissolution at the minimum temperature, T_d, and quick transfer to a constant temperature water bath, T_c, regulated to ±0.1°C for isothermal crystallization. The crystallization temperature was varied in two ways: (1) by keeping the degree of undercooling, $T_d - T_c$, constant and equal to 12°C; (2) by keeping the crystallization temperature, T_c, constant for each fraction.

Crystallization usually started within 1 to 2 hours after reaching T_c for dilute solution grown crystals. For concentrated solution grown crystals the crystallization was detected within 5 to 10 minutes. To obtain complete crystallization all solutions

were kept in the constant temperature water bath for 12 to 16 hours.[74] The crystals were filtered, washed with fresh solvent at the crystallization temperature to remove any soluble materials, then air dried at low temperature.

Photomicroscope and Electron Microscope Observation

The crystals were observed using a Zeiss Photomicroscope with interference optics and a Phillips 300 Electron Micrsocope. The crystals in suspension were first diluted to avoid aggregation then deposited onto a microslide for photomicroscope observation. Pictures were taken with a 35 mm. camera contained inside the photomicroscope.

For electron microscope observation the crystals diluted from suspension, were deposited onto a carbon coated copper grid and shadowed with Pt-Pd vapor for better contrast. The crystals were usually observed at 2800 to 22000 magnification depending on the crystal dimensions. Pictures were taken directly with a plate camera attached to the electron microscope. At large magnification the shadow distance along shadowing direction on the crystal edges becomes measurable. The lamellar thickness of dilute solution grown crystals were those calculated by measuring the shadow distance along the shadowing direction, with knowledge of the shadowing angle. Magnification used for lamellar thickness measurement ranged from 35000 to 115000 times depending on the crystal thickness. Crystal shrinkage under the electron beam in this experiment was corrected for by carrying out electron microscopy on preparations studied by LAXS.

Low Angle X-ray Scattering (LAXS)

Lamellar thickness measurements by the LAXS method were carried out by B. A. Newman, Department of Mechanics and Material Science at Rutgers University using a Rigaku-Denki small angle goniometer. Samples prepared for this experiment were slowly filtered and completely dried. Lamellar thickness was calculated by measuring the spacing distance, h, and applying Bragg's equation:

$$n\lambda = d\sin 2\theta$$

where $\lambda = 1.54\text{Å}$, the wave length of the light source;

2θ = scattering angle

$= \sin^{-1} n/r$;

r = distance from sample to film;

n = diffraction order and

d = the lamellar thickness.

The lamellar thickness for crystals which are too brittle to form orientated dried mats, F3H29, F1H29, and F1T15, were measured by the electron microscope as mentioned above.

Density Measurement

The sample density was measured in a density gradient column. The column was prepared by gradually mixing a heavy liquid, water, and a light liquid, ethanol, at various portions so that the density in the column at constant temperature increases linearly from the top to the bottom. The linear gradient relationship of the column was confirmed by using glass beads of known density which are accurate to $\pm$ 0.0001 gm/cm^3 at 25°C. Fig. 3 and Fig. 4 are the column set up and a typical calibration curve for the density gradient, respectively.

Once the gradient is established, the column is usable for at least two to three days. Samples were pressed at 3.4×10^7 pa to eliminate air then dropped into the column and the floatation height measured accurately to ± 0.05 cm. A reproduced four-digit accuracy of density was achieved routinely.

For sample densities greater than one, a floatation method using ethylene glycol and water was employed. A known volume of water was titrated with ethylene glycol until the polymer sample floated freely. The sample density was determined by the densities of the known components of the solution mixture. Only one crystal preparation with a density greater than one was found in this research.

Differential Scanning Calorimetry (DSC) Measurement

Measurement were made with a Du Pont 990 Thermal Analyzer using sample weight of 2 mg. or less. Most of the scans were run at a heating rate of 20 degree per minute. It was found that a rate as low as 1 degree per minute did not cause any appreciable change in the four parameters measured - the apparent transition temperature, T_{tr}, the apparent melting temperature, T_m, the enthalpy of transition ΔH_{tr}, and the enthalpy of melting, ΔH_m.

The T_{tr} and T_m were read from the intersection of the base line extrapolation and the extrapolation of the low-temperature side of the endotherm, as shown in Fig. 5. The ΔH_{tr} and ΔH_m in calorie/gm. were calculated from the equation stated in the Instruction Manual:

$$\Delta H_{tr} \text{ (or } \Delta H_m) = \frac{A}{m} 60\ BE\Delta q_s$$

where $60\ BE\Delta q_s$ is a constant depending on a given set of DSC conditions

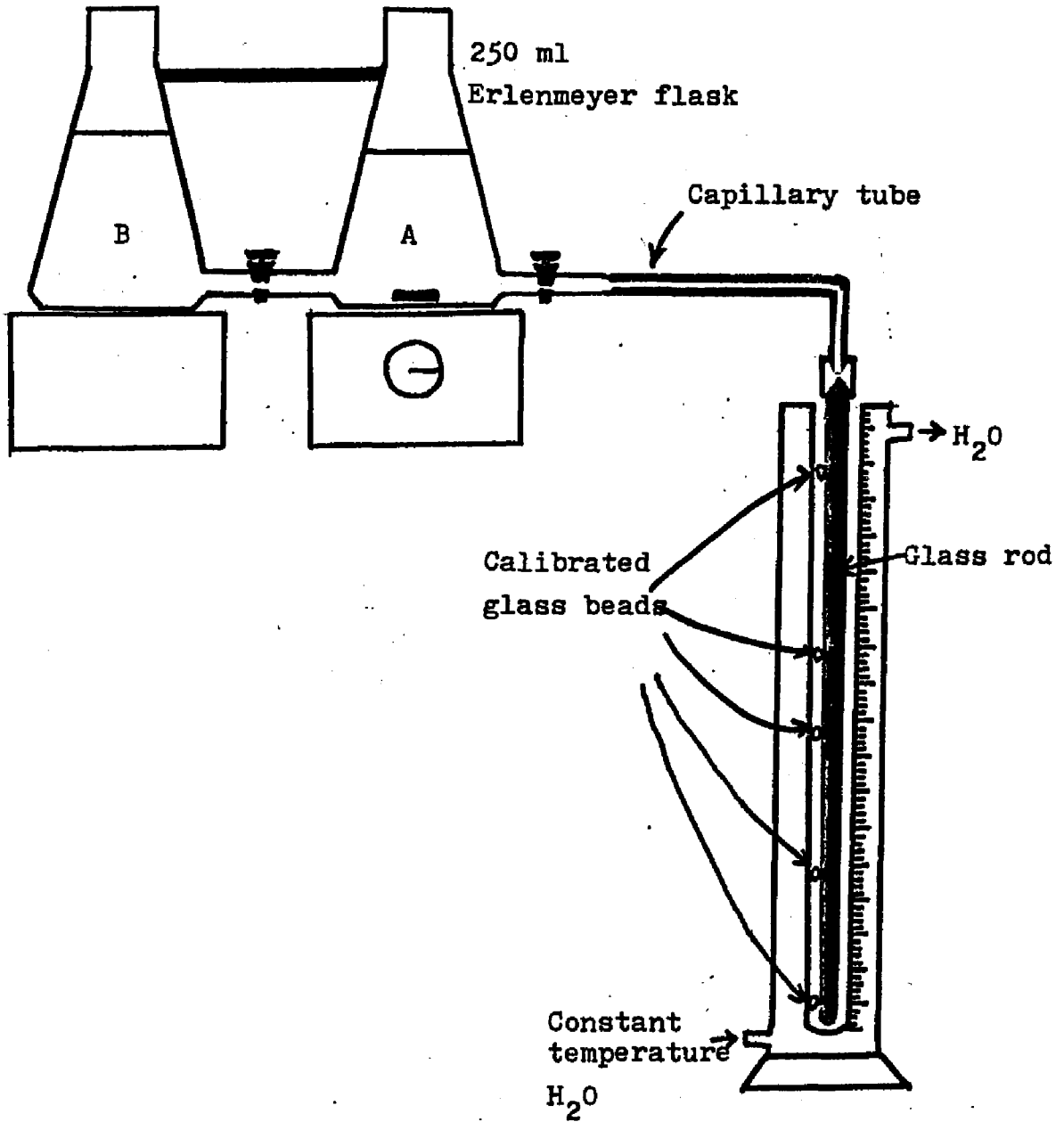

Fig. 3. Mixing Device for a Density Column Flask A contains the heavy liquid, H_2O, which is continuously diluted with the light liquid, C_2H_5OH, from flask B. The stirring must be rapid enough to keep the contents of flask A homogenous at all times. Column (2 x 25 in cm) with constant temperature H_2O thermojacket is used.

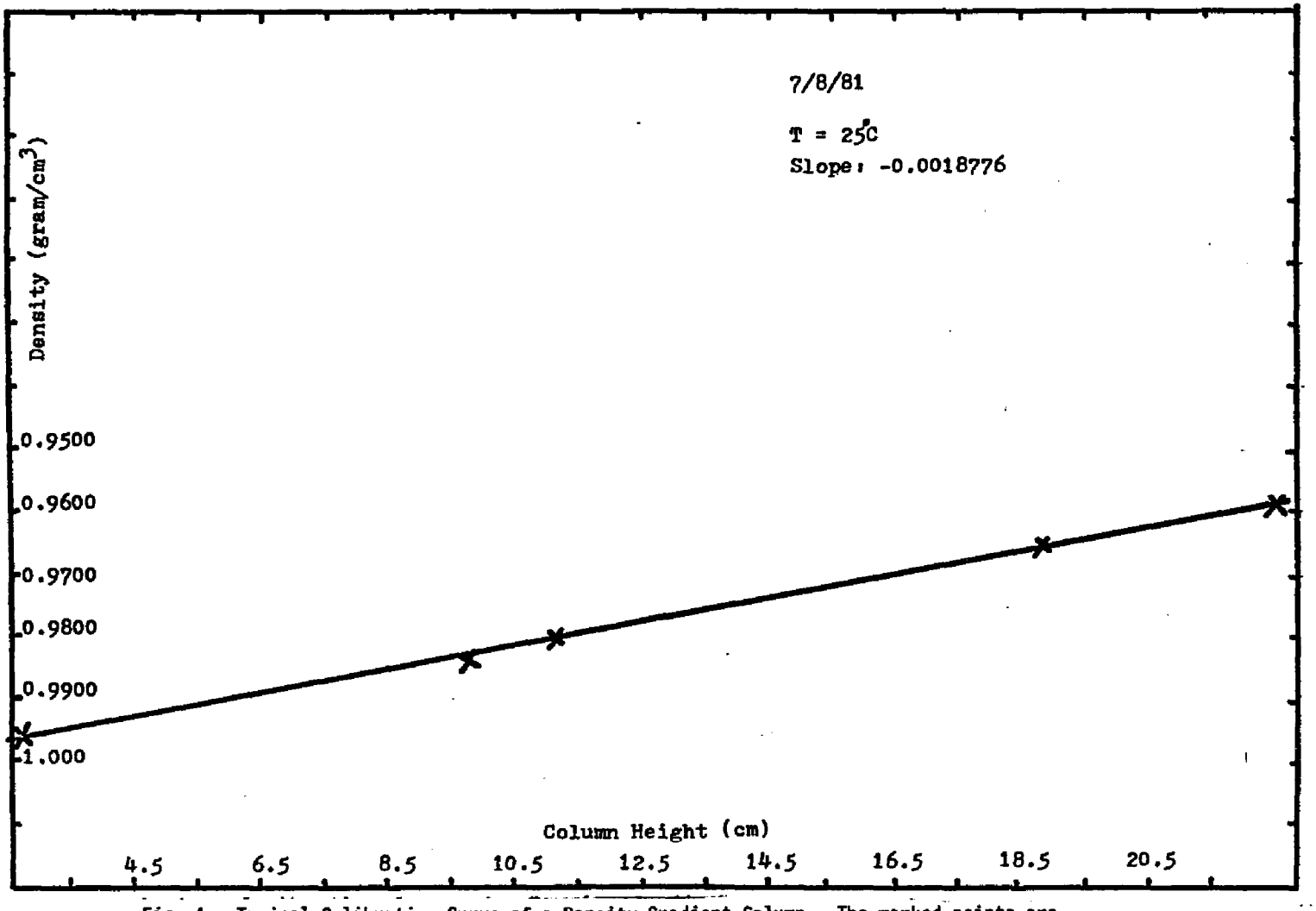

Fig. 4. Typical Calibration Curve of a Density Gradient Column. The marked points are the position of the calibrated glass beads.

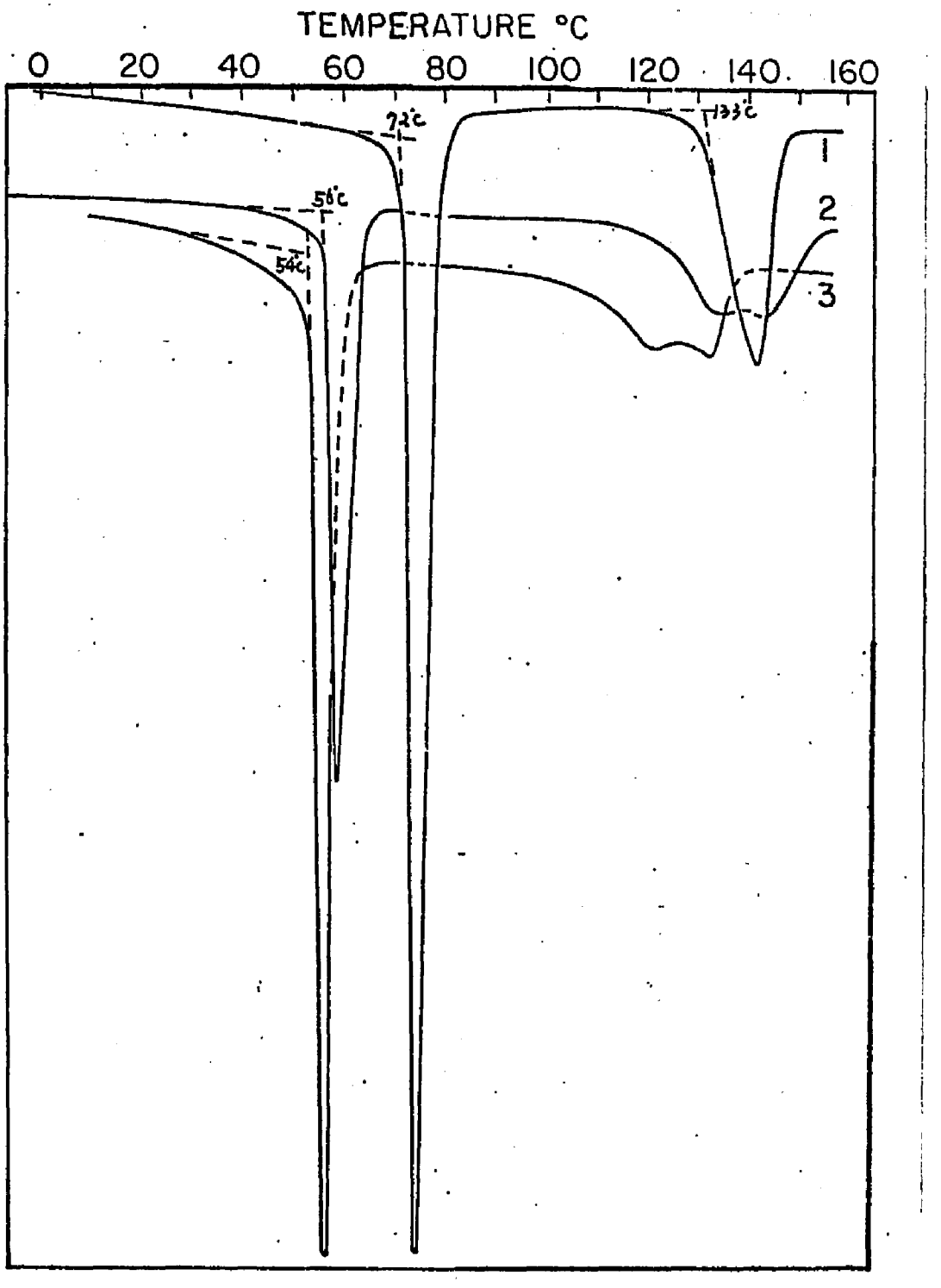

Fig. 5. Differential Scanning Calorimetry Scans for Dilute Solution Grown Crystals from Three TPBD Fractions: (1) F1H55 (2) F2H36 (3) F3H29

in each measurement:

B = Time base setting in min./cm;

E = Cell calibration coefficient in mw/mv (dimensionless);

Δq_s = Y-axis RANGE setting in mv/cm;

A = Peak area in cm^2;

m = Sample mass accurately weighed to ± 0.01 mg.

The endotherm peak area is measured by cutting out and weighing the paper under the peak. This weight is then compared with weight of a standard area of paper.

Epoxidation Reaction

The quantitative reaction of the double bonds at the crystal surfaces were carried out using an excess amount of m-chloroperbenzoic acid, MCℓPBA, reacted with crystals suspended in 1% toluene solution at 6°C:

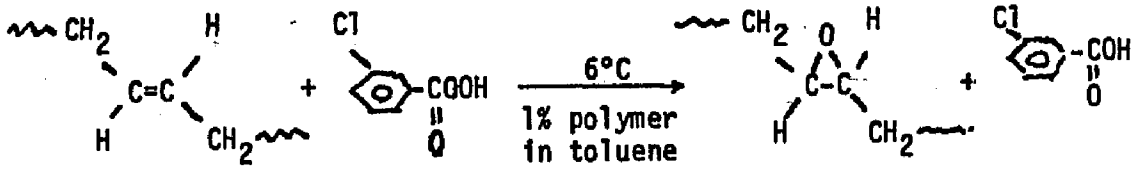

To check Stellman's[66,67] and Wichacheewa's[74] finding that the reaction was completed in 4 to 5 days, the epoxidation of crystals from one particular preparation, UH45, in the presence of an excess of MCℓPBA was carried out to various times. The % epoxidation obtained was constant over the reaction time of 5 to 14 days. Therefore, the reaction for all crystals were stopped after 5 to 10 days and the polymer recovered for determination of the extent of epoxidation.

In this recovery the epoxidized samples were washed with enough fresh toluene at 6°C to take out the excess peracid present, as detected by iodometric determination.

After freeze drying, this epoxidized sample was dissolved in deuterated chloroform, $CDCl_3$, and subjected to ^1H nmr using a JEOLCO JNM MH 100. A typical ^1H nmr scan for the partially epoxidized TPBD in $CDCl_3$ is shown in Fig. 6. Chemical shifts, as found from the literature,[86,89,90] are given in Table 4. The % double bonds available for the reaction was calculated by direct measurement from the nmr scan:

$$\% \text{ epoxidation} = \frac{\text{area of the epoxidized -CH- shift}}{\text{area of the non-epoxidized -CH- shift} + \text{area of the epoxidized -CH-shift}} \times 100$$

or

$$\% \text{ epoxidation} = \frac{\text{area of the epoxidized -CH}_2\text{-shift}}{\text{area of the non-epoxidized -CH}_2\text{- shift} + \text{area of the epoxidized -CH}_2\text{- shift}}$$

Using UH45, prepared the same as one of the samples studied previously by Wichacheewa,[74] two sets of experiments were carried out: (a) Epoxidation of crystals kept in suspension until reaction was completed. (b) Expoxidation of crystals obtained as dry mats and then resuspended in toluene. In method (a) a known weight of crystals grown from heptane was washed and suspended in toluene at 6°C. In method (b) a dry mat with a thickness around 30 to 100μ was swelled in toluene at 6°C. Enough MCℓPBA was added to react with 35-40% of

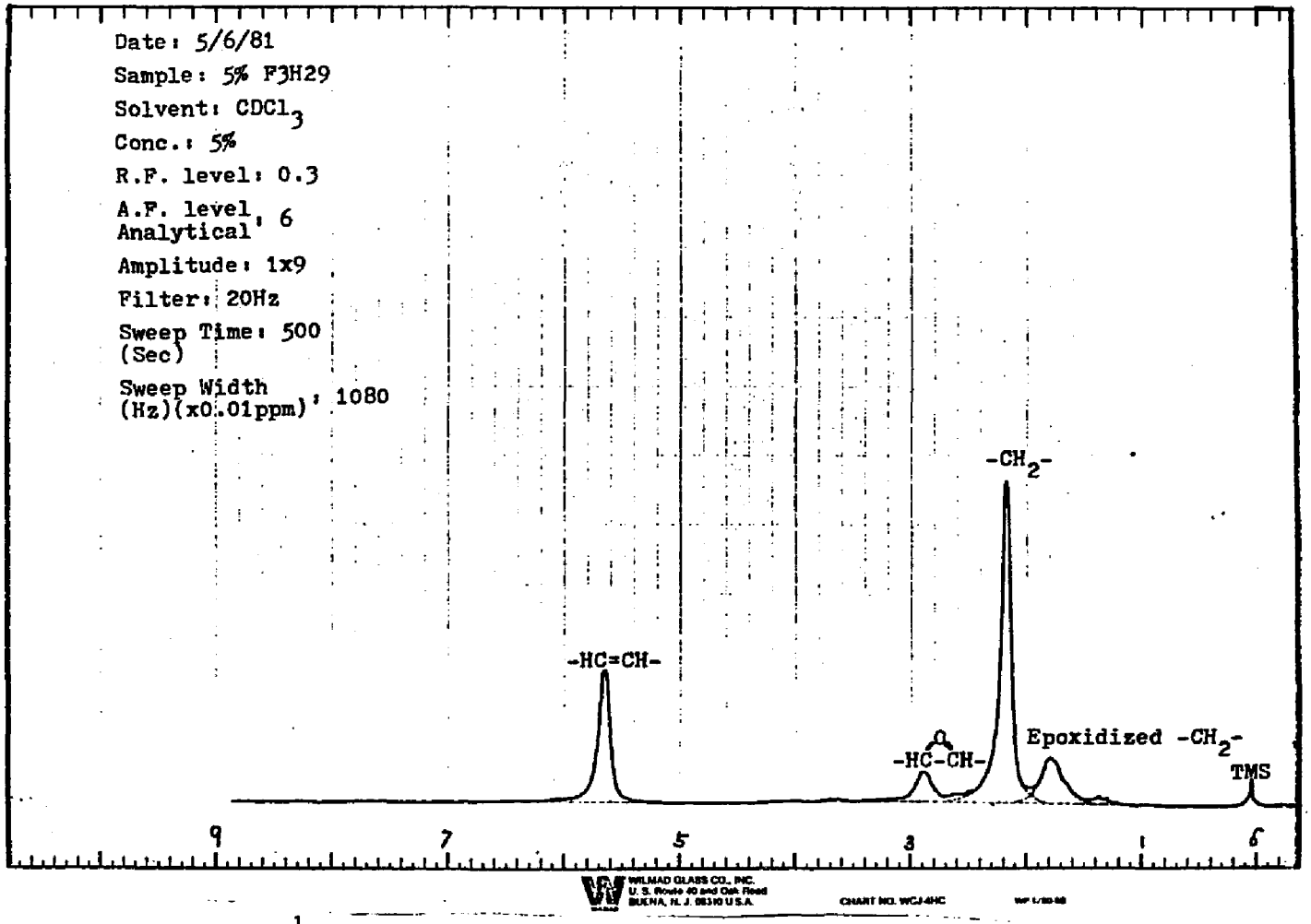

Fig. 6. 100 MHz ^1H NMR Spectrum of Partially Epoxidized TPBD Sample

TABLE 4. CHEMICAL SHIFTS OF POLYBUTADIENE AND EPOXYPOLYBUTADIENE

Type Proton	Chemical Shifts, ppm δ	Solvent Used
trans-HC=CH-	5.3	CCl_4
trans-CH_2CH_2-	2.0	CCl_4
trans-HC(O)-CH-	2.65	$CDCl_3$
trans-CH_2C(O)-CCH_2-	1.57	$CDCl_3$
cis -HC(O)-CH-	2.92	$CDCl_3$
cis -CH_2C(O)-CCH_2-	1.56	$CDCl_3$
$H_2C=C\overset{*}{H}$-	5.52	CCl_4
-HC=C$\overset{*}{H}_2$-	4.81	CCl_4
$H_2C=CH-C\overset{*}{H}$	5.35	CS_2
-CH_2-	1.28	CS_2

In reference 86,89,90

the double bonds present in each sample. The results of this experiment are given in Table 5.

In Table 5 it is found that the % epoxidation for wet crystals are comparable with the previous work where an IR method of detection[74] was used. The difference in % epoxidation for crystals kept in suspension vs. those from a resuspended dry mat are within ±2%. Since this difference is relatively small, epoxidation of dilute solution prepared crystals were carried out using resuspended dry mats. Epoxidation of concentrated solution grown crystals was carried out using crystals kept wet until reaction was completed.

A difficulty in the epoxidation reaction is that the epoxidized samples can very easily increase in molecular weight probably due to crosslinking during the drying process. Freeze air drying in the cold room was carried out as a precaution against crosslinking.

^{13}C nmr Measurements

A method for obtaining the number of monomer units in a chain fold is by using the ^{13}C nmr spectrum for the epoxidized crystals dissolved in a suitable solvent. The epoxidized sample is a block copolymer of chain units O and D, $..D(D)_mDO(O)_nO...$, where the butadiene blocks, D_{m+2}, correspond to the crystalline chain traverses and the epoxybutadiene blocks, O_{n+2}, correspond to the chain folds in the crystals. It is not expected that any ...DOD... sequence will be present in the sample. If the spectra resolution is good enough, the carbon atoms in the epoxidized units outside the epoxy sequence should have a different position than those inside the epoxy sequence and from the relative intensities of these, the number of monomer units

TABLE 5. EPOXIDATION DATA FOR WET AND DRY SINGLE CRYSTALS

UH45. (Reaction medium: 1% Polymer in Toluene at 6°C)

Sample	Double Bonds $\times 10^3$ Moles	MCℓPBA $\times 10^3$ Moles	Mole % MCℓPBA/D.B	% D.B. Reacted Calc. From =CH-/-CH_2-	Average
	19.389	6.743	35	22.5/21.5	
	0.797	0.282	35	27.5/27.2	
UH45 in Suspension	1.227	0.448	36	27.1/23.0	
	3.259	1.144	35	23.5/23.0	24±2
	2.058	0.728	35	20.3/22.5	
	1.014	0.357	35	27.3/26.3	
	0.711	0.259	36	27.1/23.0	
	0.779	0.274	35	25.7/22.9	
UH45 Dry Mats	1.008	0.354	35	21.1/21.2	22.5±2
	1.811	0.649	36	19.1/20.1	
	1.224	0.435	36		

in the epoxy sequence can be calculated.

Two samples were used in the ^{13}C nmr experiments, UH45 and F1H55. Peak assignments were made from spectra for the two epoxidized crystal samples and the following four other samples:

(a) 35% solution epoxidized TPBD,

(b) 75% solution epoxidized TPBD,

(c) 50% epoxidized 3,7-decadiene and

(d) 100% epoxidized 3,7-decadiene.

In the preparation of solution epoxidized TPBD samples around 0.6 gram of polymer was dissolved in 100 ml chloroform, $CHCl_3$. Enough MCℓPBA to react with the prescribed amount of double bonds was predissolved in 20 ml of $CHCl_3$ and then this solution was added to the original polymer solution. The reaction was allowed to proceed at room temperature in the dark for over 24 hours. After the reaction the random epoxidized samples were recovered from ethanol. The samples were filtered and washed several times with methanol/ether to wash out the MCℓBA residue. After freeze drying the samples were redissolved in 17% $CDCl_3$ for spectral analysis.

The procedures for the epoxidation of 3,7-decadiene was modified from the procedures for the epoxidation fo squalene[84] and cyclohexene.[85] Around 3 ml of 3,7-decadiene was diluted with $CHCl_3$ in a 100 ml round bottom flask. Enough MCℓPBA to react with 50%/or 100% of the double bonds of the sample was dissolved in 50 ml of $CHCl_3$. Using a dropping funnel the predissolved MCℓPBA solution was added dropwise within 20 minutes to the 3,7-decadiene solution. The reaction flask was stirred at room temperature overnight. After reaction

the solution was extracted with 50 ml of 5% NaOH solution several times until the solution became basic. About 4 to 5 grams of anhydrous sodium sulfate was added to the flask and the solution was swirled occasionally until dry and clear. The $CHCl_3$ solvent was removed using vacuum distillation at room temperature. This epoxidized sample was then diluted with $CDCl_3$ and subjected to ^{13}C nmr analysis using a Varian XL-200. The ^{13}C nmr spectra and the detailed spectrum analysis and peak assignment was carried out by F. C. Schilling and F. A. Bovey at Bell Telephone Laboratories.

RESULTS

Eight dilute solution preparations (0.01% and 0.02%) and ten concentrated solution preparations (1%, 5% and 10%) of crystals were studied. The crystal preparation conditions are given in Table 6. The sample designation used indicates the parent polymer, W, V, U or fractions, F1, F2, F3, F1b, F2b, F3b; the solvent, H (heptane), T (toluene); and the crystallization temperature, T_c. Holding the degree of undercooling, T_d-T_c, constant, generally necessitates the use of a crystallization temperature which decreases with either decreasing $\bar{M}_n$ or decreasing concentration. The minimum dissolution temperature, T_d, increases with both molecular weight and concentration.

Gel Permeation Chromatography

The molecular weight distribution curves from GPC for all samples used are given in Fig. 7 and Fig. 8. Fractions F1, F2 and F3 obtained from the U-polymer, are precursors for four dilute solution crystal preparations - F1T15, F1H29, F2H36 and F3H29. When the F1H55 crystals are obtained from F1 further fractionation takes place as suggested by the smaller $\bar{M}_w/\bar{M}_n$ value found from curve number 5 as compared to number 1 of Figure 7. Although the percentage recovery as given in Table 6, shows that appreciable amounts of material were washed out, there is no further fractionation taking place in the crystal preparation of 5% F1bH60, 5% F1bH55 and 1% F1bH55. It can be seen that the sample with the highest molecular weight, WH62, has the broadest distribution. Comparison of the distribution curves for F1, F2, and F3 given in Fig. 7 with those for F1b, F2b, and F3b as shown in Fig. 8, indicates that the latter give the higher number average molecular weights and

TABLE 6. PREPARATION OF TPBD CRYSTALS

Sample Design.	$\bar{M}_n$	$\bar{M}_w/\bar{M}_n$	Conc. (w/v)	T_d	T_c	% Recovd.
WH62	12×10^4	2.7	0.01	74	62	60±5
VH53	6.9×10^4	1.4	0.01	65	53	10±5
F1H55	4.4×10^4	1.5	0.01	67	53	35
F1H29	2.7×10^4	1.6	0.01	67	29	(100)
F1T15	2.7×10^4	1.6	0.02	27	15	(100)
UH45	1.7×10^4	1.7	0.01	55	45	45±5
F2H26	1.2×10^4	1.4	0.01	48	36	(100)
F3H29	0.47×10^4	1.3	0.01	41	29	(100)
F1bH55	2.8×10^4	1.9	1	70	55	61
F1bH60	2.8×10^4	1.9	5	72	60	70±10
F1bH55	2.8×10^4	1.9	5	72	55	88
F1bH29	2.8×10^4	1.9	5	72	29	(100)
F2bH42	1.7×10^4	1.8	5	54	42	(100)
F1bH36	1.7×10^4	1.8	5	54	36	(100)
F3bH40	0.59×10^4	1.6	5	52	40	(100)
F3bH29	0.59×10^4	1.6	5	52	29	(100)
F3bH42	0.59×10^4	1.6	10	54	42	(100)
F3bH29	0.59×10^4	1.6	10	54	29	(100)

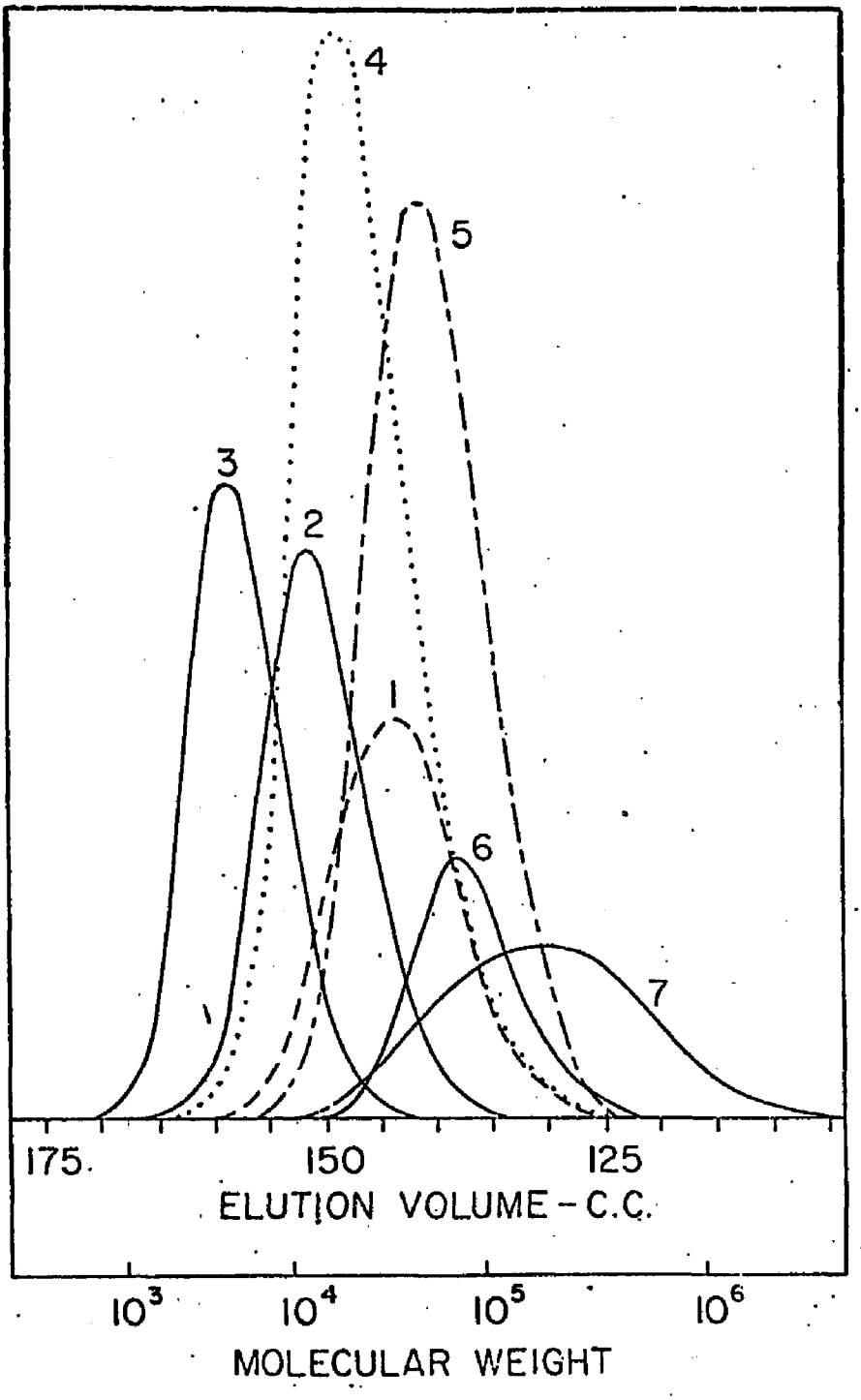

Fig. 7. Gel Permeation Chromatograms for TPBD Fractions: (1) F1; (2) F2; (3) F3; (4) UH45; (5) F1H55; (6) VH53; (7) WH62.

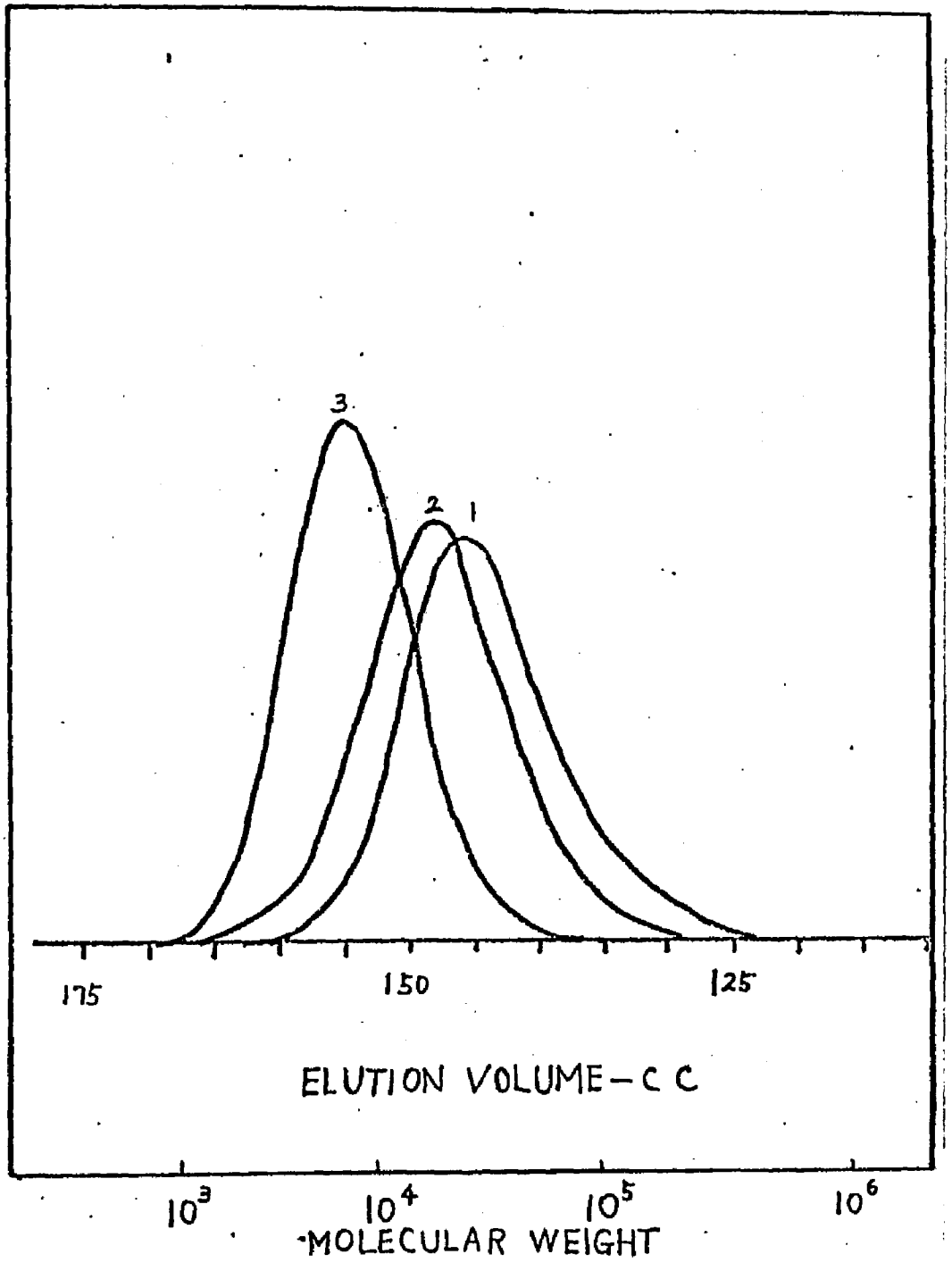

Fig. 8. Gel Permeation Chromatograms for TPBD Fractions: (1) F1b; (2) F2b; (3) F3b.

larger $\bar{M}_w/\bar{M}_n$ values. A comparison of the number average molecular weight and $\bar{M}_w/\bar{M}_n$ values of the crystal preparations UH45, VH53 and WH62 given in Table 6 with prepurified non-fractionated U, V and W polymers as given in Table 3 indicates that fractionation is taking place during the crystallization process of dilute solution grown crystals at relatively high temperatures.

Photomicroscope and Electron Microscope Observation

Fig. 9 through Fig. 16 are representative transmission electron micrographs for each fraction of TPBD crystals grown from dilute solution by self-seeding using the minimum dissolution temperature technique. As can be seen, this growth technique produces a lamellar habit with some screw dislocation overgrowths. The crystal shape changes from elongated hexagonal to rounded hexagonal as the crystallization temperature changes from 29°C to 62°C in heptane solvent. As mentioned before, the crystallization temperature and the molecular weight are interrelated when T_d-T_c, the degree of undercooling, is fixed. The crystal dimensions vary by 1 to 5μ. An exception is WH62 where the crystal dimension is in the range of 30 to 40μ, around 100 times larger in size than the other crystals.

The lamellar thickness, L in nm, determined from the distance of the crystal shadow in the electron micrograph, and from small angle X-ray scattering, are given in the next to last column of Table 7.

Fig. 17, showing a group of lamellae, is an optical micrograph of 5% F1bH60. Optical microscope investigation of F1b crystals grown at 55°C and 60°C at high concentration was found to contain single lamellas with and without screw dislocation overgrowth, as well as

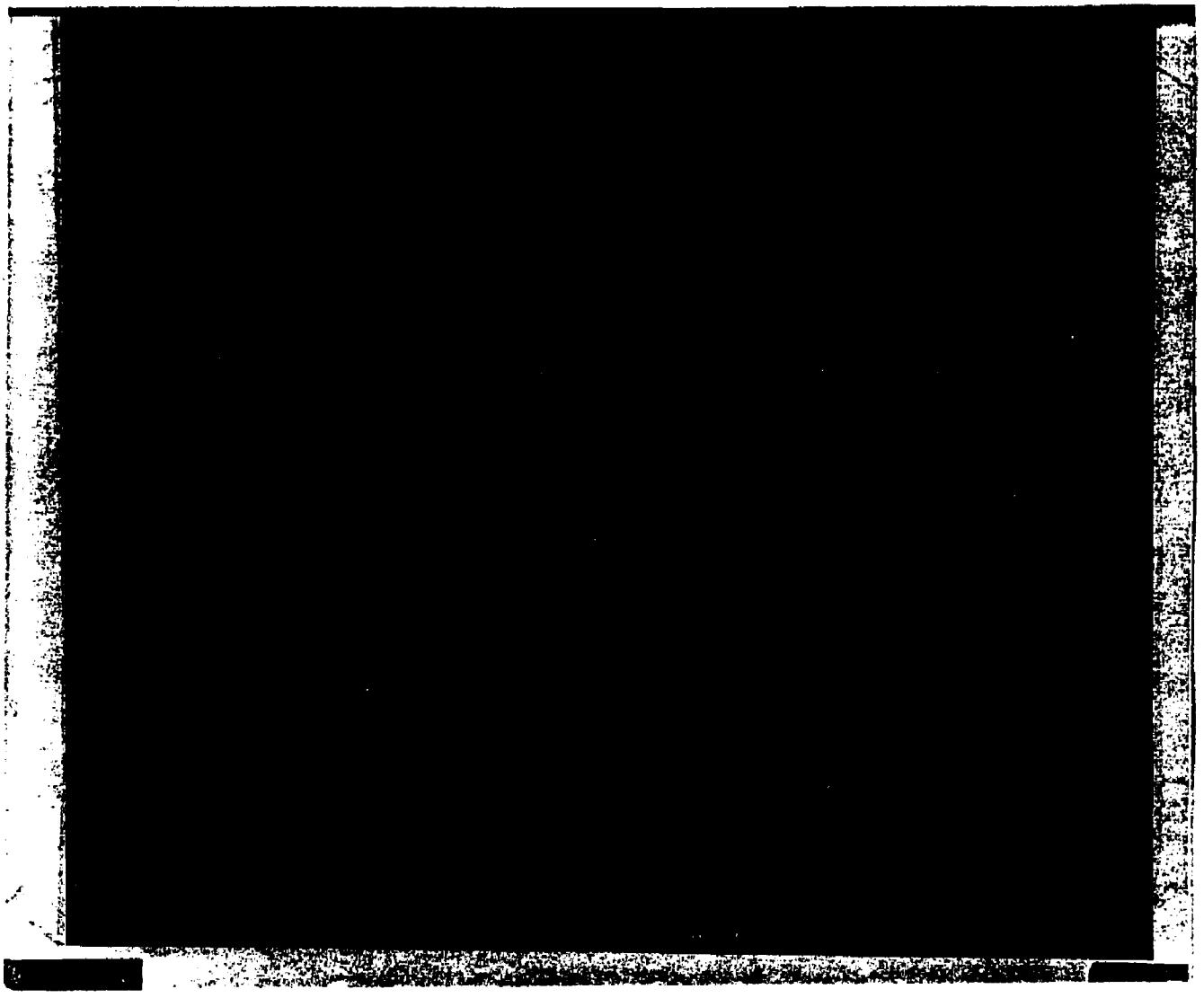

Fig. 9. Electron Micrograph of TPBD Crystals, F3H29.
(Mag. 1.8 x 1.4 x 6000)

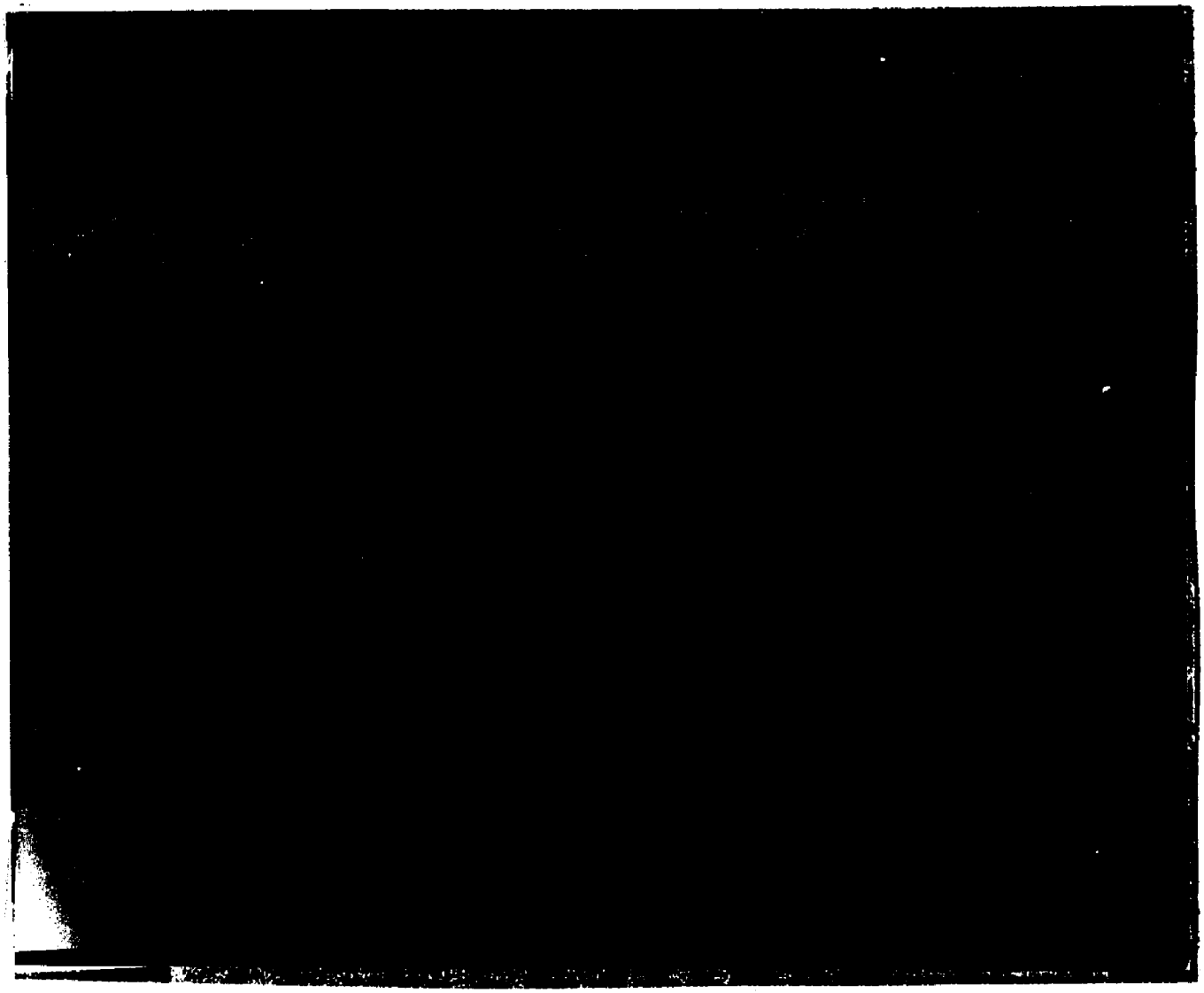

Fig. 10. Electron Micrograph of TPBD Crystals, F2H36.
(Mag. 1.8 x 1.4 x 18000)

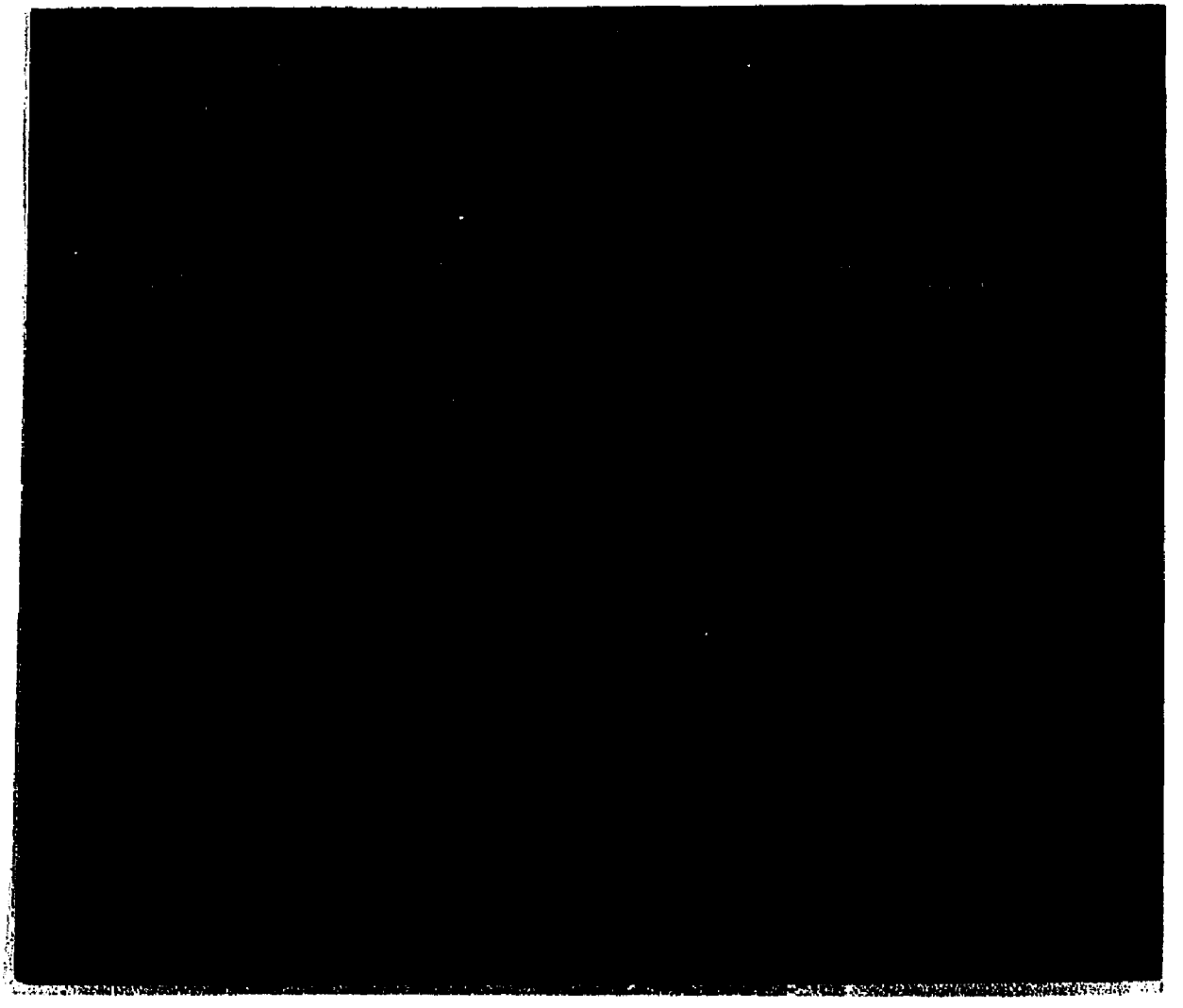

1 μ

Fig. 11. Electron Micrograph of TPBD Crystals, F1H55

(Mag. 1.8 x 1.14 x 22000)

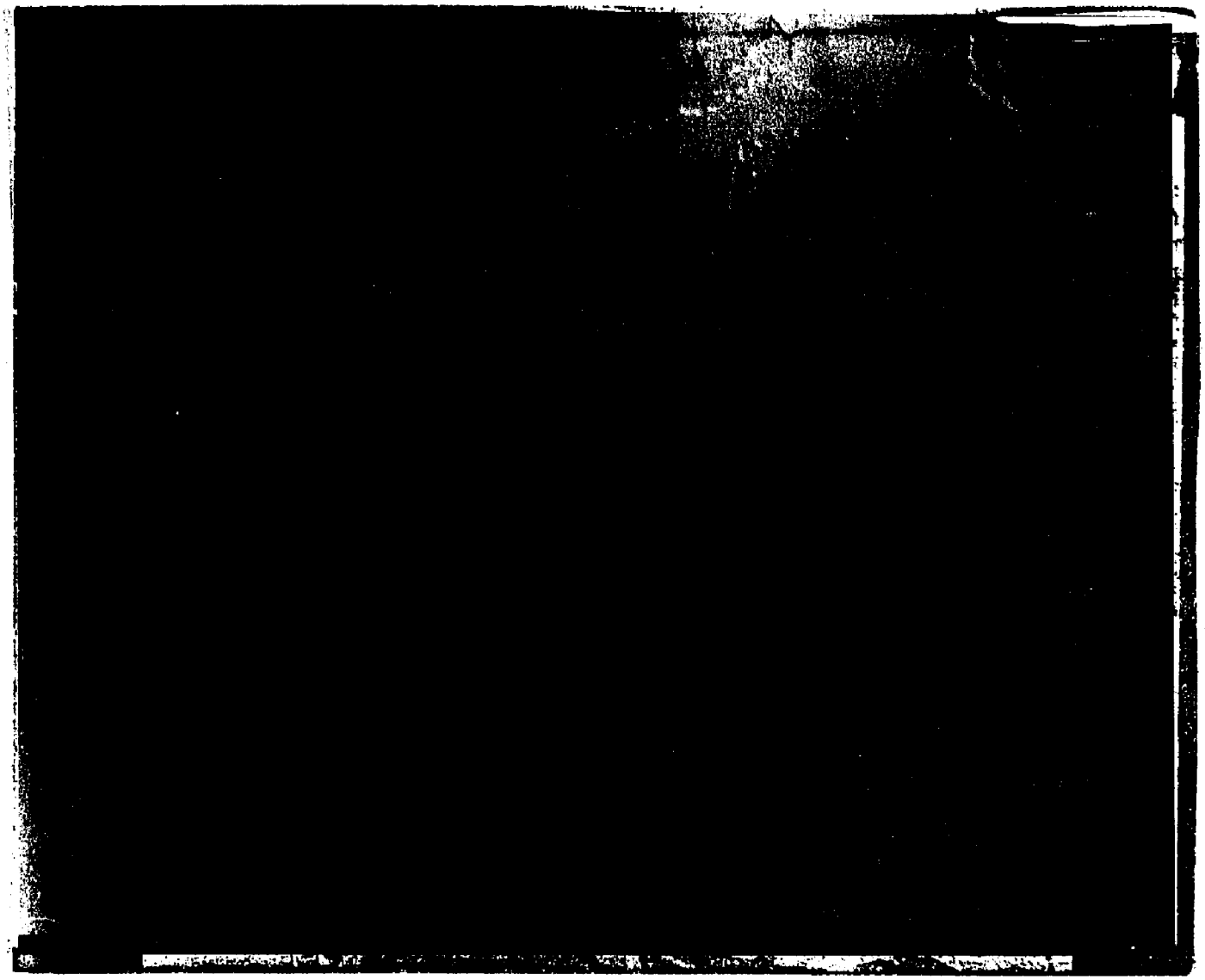

Fig. 12. Electron Micrograph of TPBD Crystals, VH53.

(Mag. 1.8 x 1.14 x 18000)

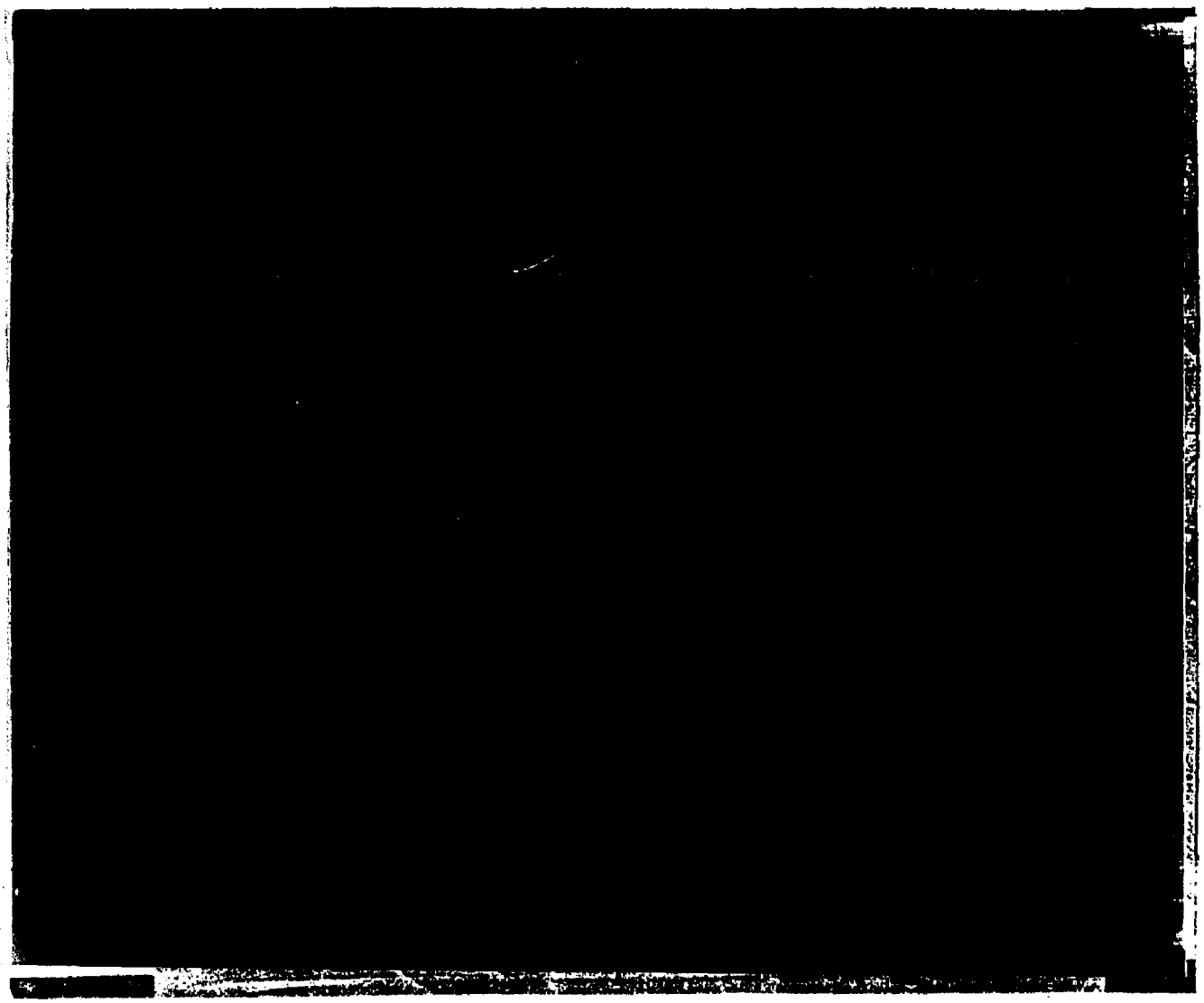

Fig. 13. Electron Micrograph of TPBD Crystals, WH62
(Mag. 1.8 x 1.14 x 2800)

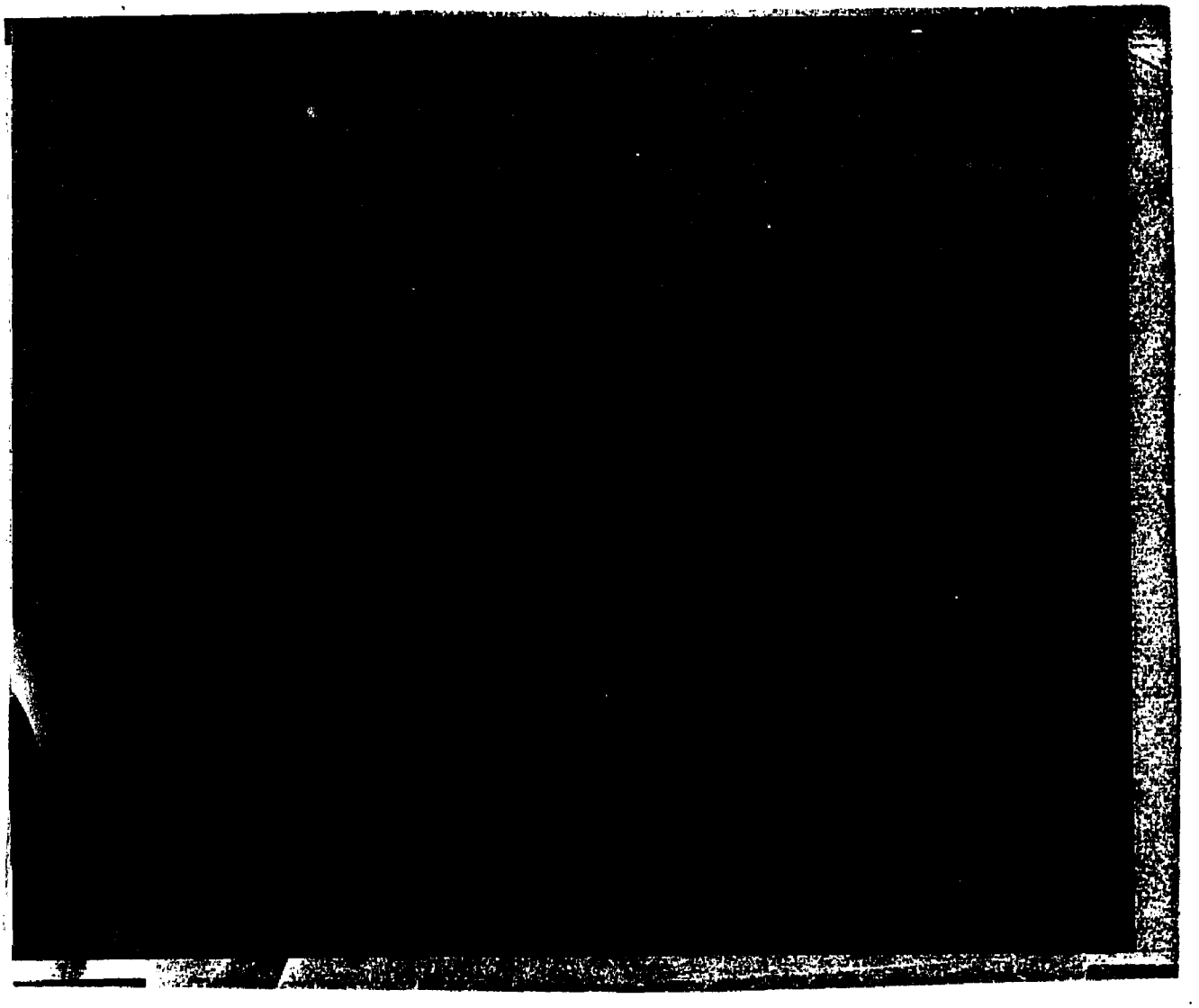

Fig. 14. Electron Micrograph of TPBD Crystals, F1H29.
(Mag. 1.8 x 1.14 x 14000)

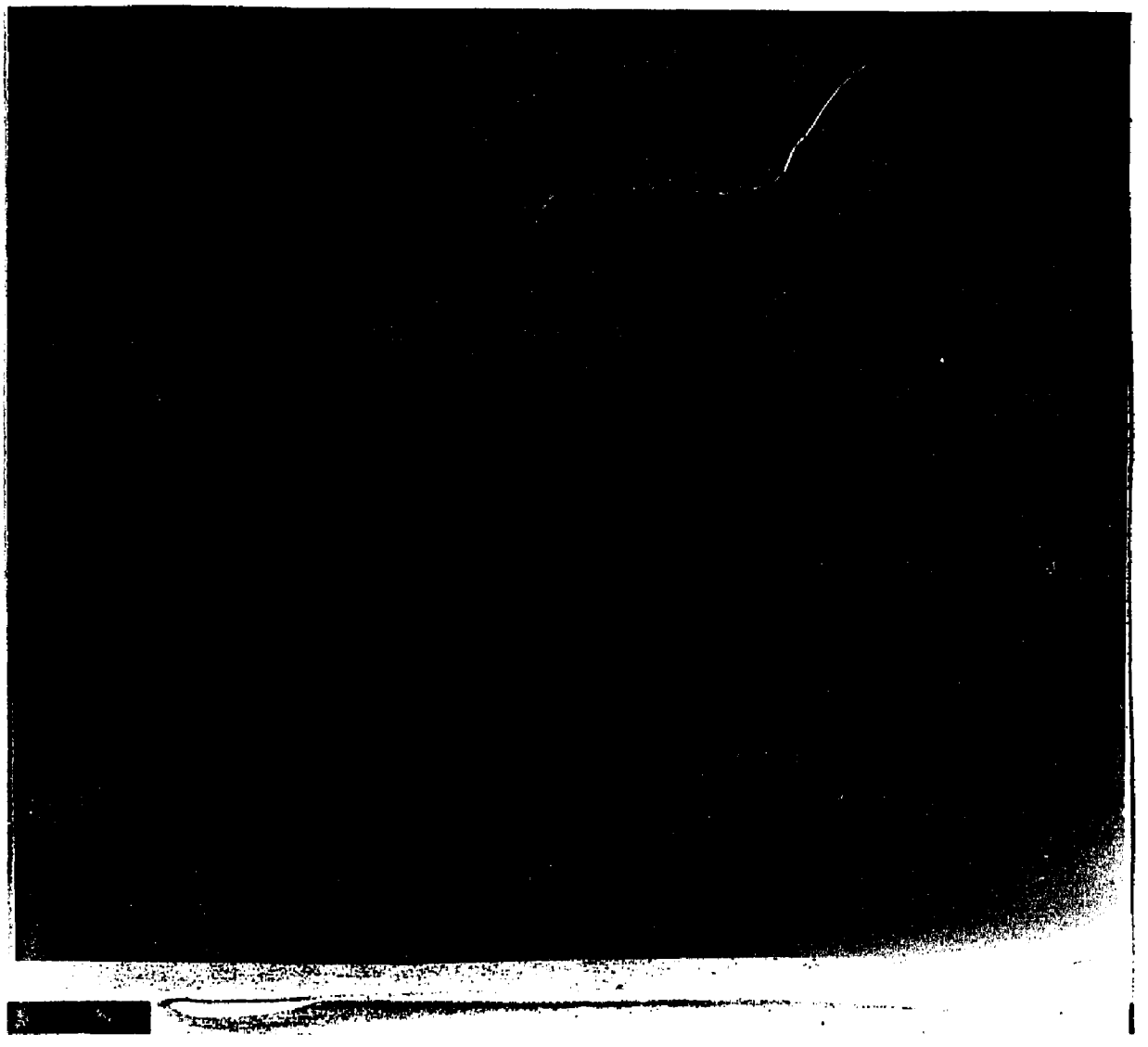

Fig. 15. Electron Micrograph of TPBD Crystals, F1T15.

(Mag. 1.8 x 1.14 x 11000)

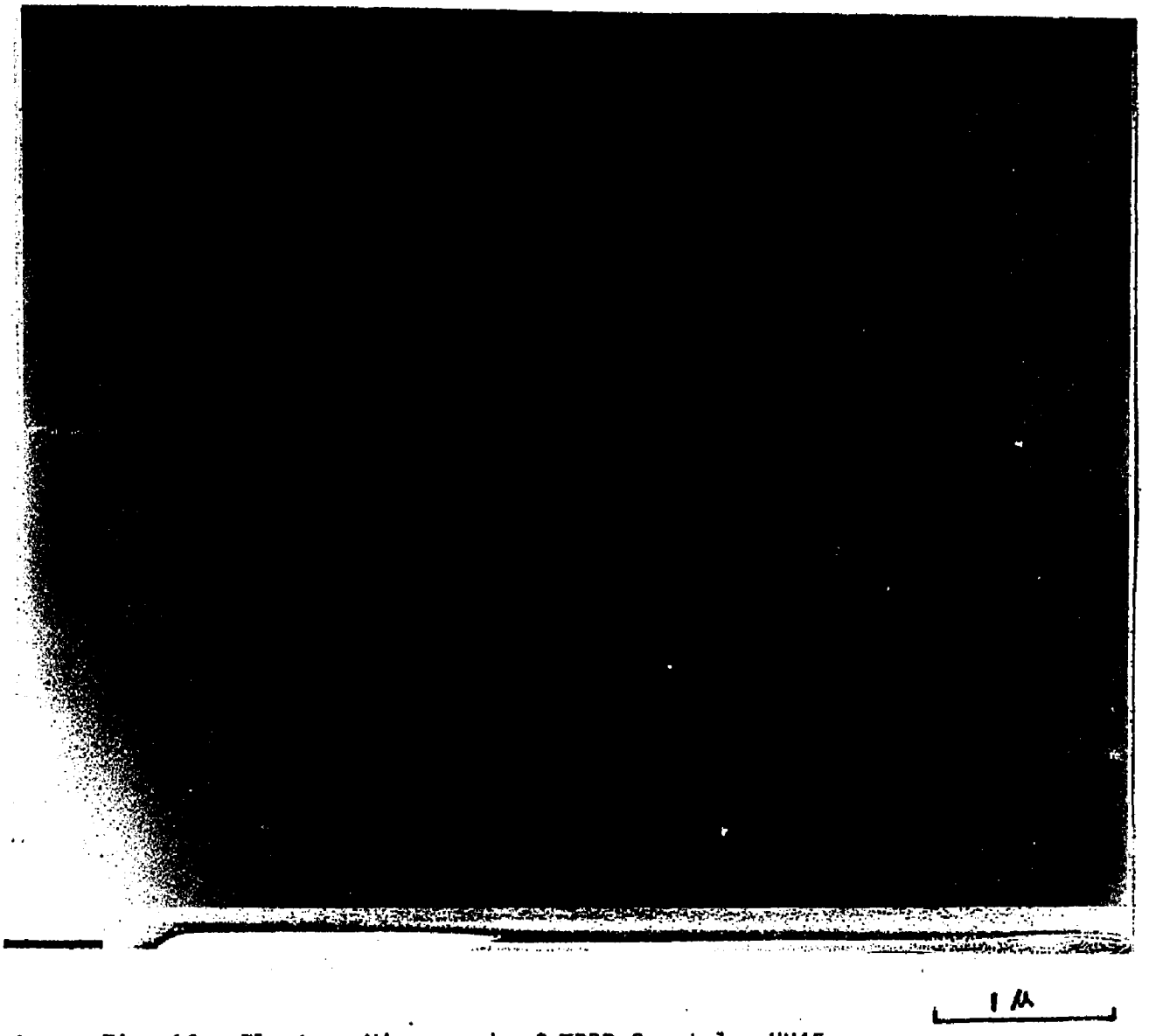

Fig. 16. Electron Micrograph of TPBD Crystals, UH45.
(Mag. 1.8 x 1.14 x 14000)

TABLE 7. CALORIMETRIC, DENSITY EPOXIDATION AND LAMELLAR THICKNESS RESULTS FOR DILUTE SOLUTION-GROWN TPBD CRYSTALS

Sample	$\bar{M}_n \times 10^{-4}$	$\bar{M}_w/\bar{M}_n$	T_{tr} C	ΔH_{tr} cal/mol.	T_m	ΔH_m cal/mol	ρ g/cm^3	$1-w_c$	F_s	L nm	L_c nm
WH62	12	2.7	74	30.1	142	19.9	0.998	.20	.14	27	23
VH53	6.9	1.4	72	23.9	129	14.2	0.996	.21	.19	11.8	9.2
F1H55	4.4	1.5	72	26.1	133	15.1	1.005	.16	.15	24	19.5
F1H29	2.7	1.6	54	18.6	136	15.9	0.986	.27	.24	8.3	6.0
F1T15	2.7	1.6	54	19.1	135	15.9	0.988	.26	.22	9.0	6.8
UH45	1.7	1.7	60	19.5	132	14.6	0.987	.26	.24	11.0	8.0
F2H36	1.2	1.4	56	18.6	-	13.7	0.984	.28	.26	10.3 (25.8)	7.3
F3H29	0.47	1.3	54	17.7	-	11.1	0.984	.28	.27	9.1	6.3

Fig. 17. Photomicrograph of TPBD Crystal, 5% F1bH6O.
(Mig. 6.3 x 40 x 2 x 3.2)

multilamellar objects. Since the multilamellar objects for these preparations vary considerably in thickness, it is possible to obtain electron micrographs of some of the thinner ones. Fig. 18 is a picture of the thinner part of the multilamellar objects for 5% F1bH60 observed by electron microscopy. For the other preparations, F2b and F3b, the crystal dimensions are too small to allow observation with the optical microscope. Under the electron microscope thick multilamellar objects were observed for these prepartions.

Differential Scanning Calorimetry

DSC results for three of the eight TPBD crystal samples prepared from dilute solution are given in Fig. 5. All eight samples show only one endotherm in the crystal-crystal transition region and the transition temperature varies from 54°C to 74°C. It was found that the presence of small amounts of water in the DSC pan along with a TPBD sample would cause the appearance of a second smaller endotherm on the low temperature side of the transition. The melting endotherm, as can be seen in Fig. 5, broadens and displays more than one component as the molecular weight is decreased. The results of the calorimetric measurement for dilute solution grown crystals are given in Table 7 in terms of T_{tr}, ΔH_{tr}, T_m and ΔH_m. Melting temperature are not listed for F2H36 and F3H29 due to the presence of broadened multiple endotherms. The values given in Table 7 are averages of three to six determinations for T_{tr} and T_m; a variation of ±2 cal./gm. for ΔH_{tr} and ΔH_m was found.

The T_{tr} and ΔH_{tr} values show a more regular relationship to T_c than to molecular weight. The enthalpy of transition, ΔH_{tr}, is found to be proportional to the specific volume, as shown in Fig. 19, with

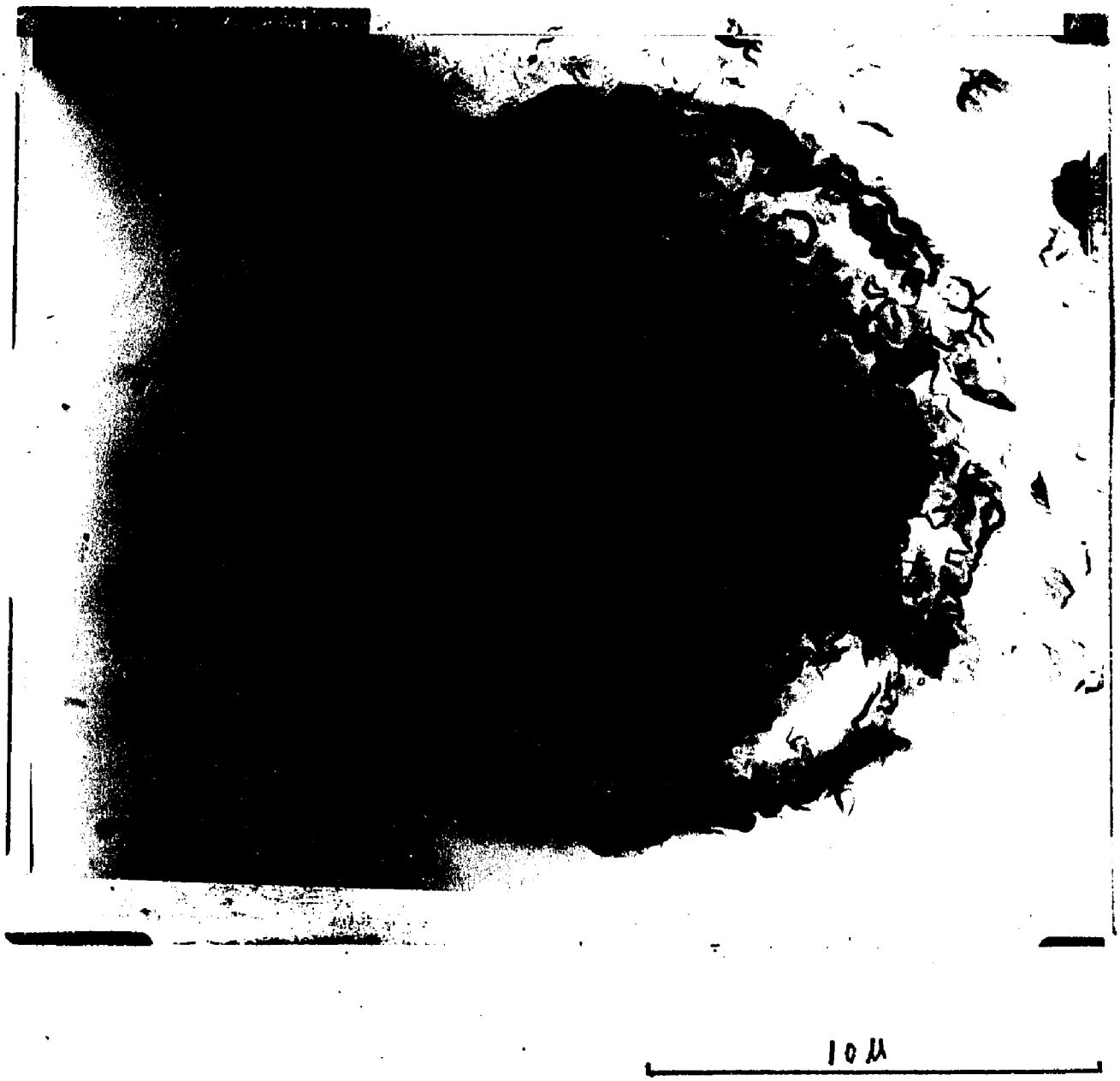

Fig. 18. Electron Micrograph of TPBD Crystals, 5% F1bH60.
(Mig. 1.8 x 1.14 x 3300)

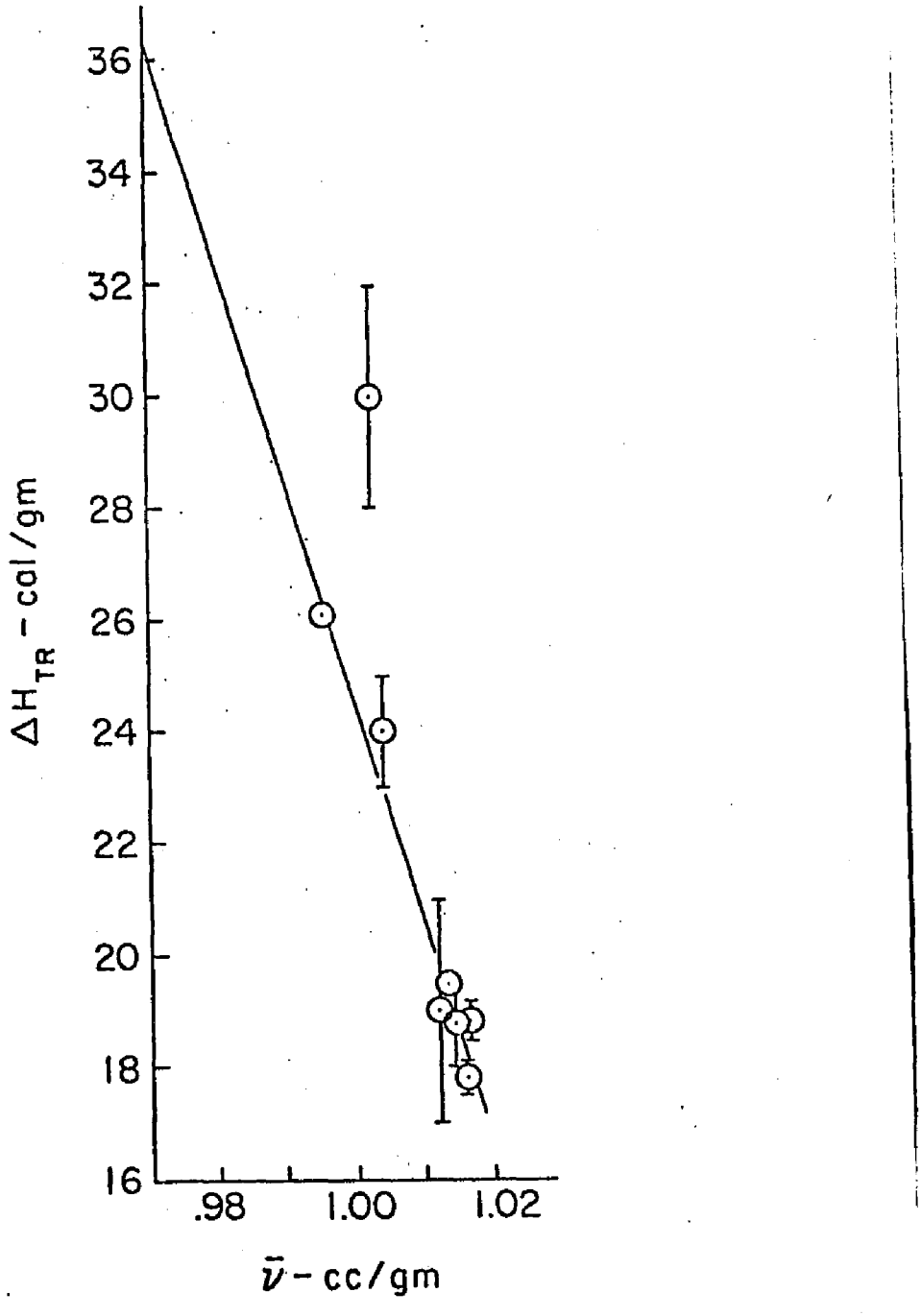

Fig. 19. Enthalpy of Crystal-Crystal Transition vs. Specific Volume for Dilute Solution-Grown TPBD Crystals.

only one sample (WH62) having a substantial deviation. Extrapolation of the straight line in Fig. 19 to a $\bar{v}$ value corresponding to 100% crystallinity yields a ΔH_{tr} of 36.2 cal./gm. A literature value[83] for this quantity is 34.6 cal./gm.

DSC scans for concentrated solution grown crystals are given in Fig. 20. In the crystal-crystal transition region (54°C-74°C) the preparations from F2b and F3b show one endotherm at the temperature position similar to the preparation of dilute solution grown crystals. For F1b, on the other hand, an additional one or two endotherms are apparent. For F1b crystallized at 60°C, 5% F1bH60, the small low temperature endotherm is only about 2% of the total. For F1b crystallized at 55°C, 5% F1bH55 and 1% F1bH55, the additional endotherm varies in size relative to the principal one. In two repeated preparations of 5% F1bH55 the endotherm peak height ratio were 1:2.4 for one preparation and 1:6.4 for the other. In the case of F1b crystallized at 29°C, 5% F1bH29, the secondary endotherm is at a higher temperature than the primary one. And again, the relative size of this additional endotherm to the principal one is not reproducible; the peak height ratio being 1:4.7 and 1:2.3 for two repeated preparations.

For DSC time base scans the enthalpy of crystal-crystal transition, ΔH_{tr}, taking all pertinent endotherms into account were obtained as given in Table 8. For duplicate preparations, ΔH_{tr} showed a maximum average deviation of ±2 cal/gm and the T_{tr} was reproduced, the same reproducibility as gotten from the dilute solution grown crystals. Comparison of the ΔH_{tr} data for concentrated solution grown crystals with that obtained for dilute solution grown crystals under similar conditions, it shows a decrease in ΔH_{tr} with an increase

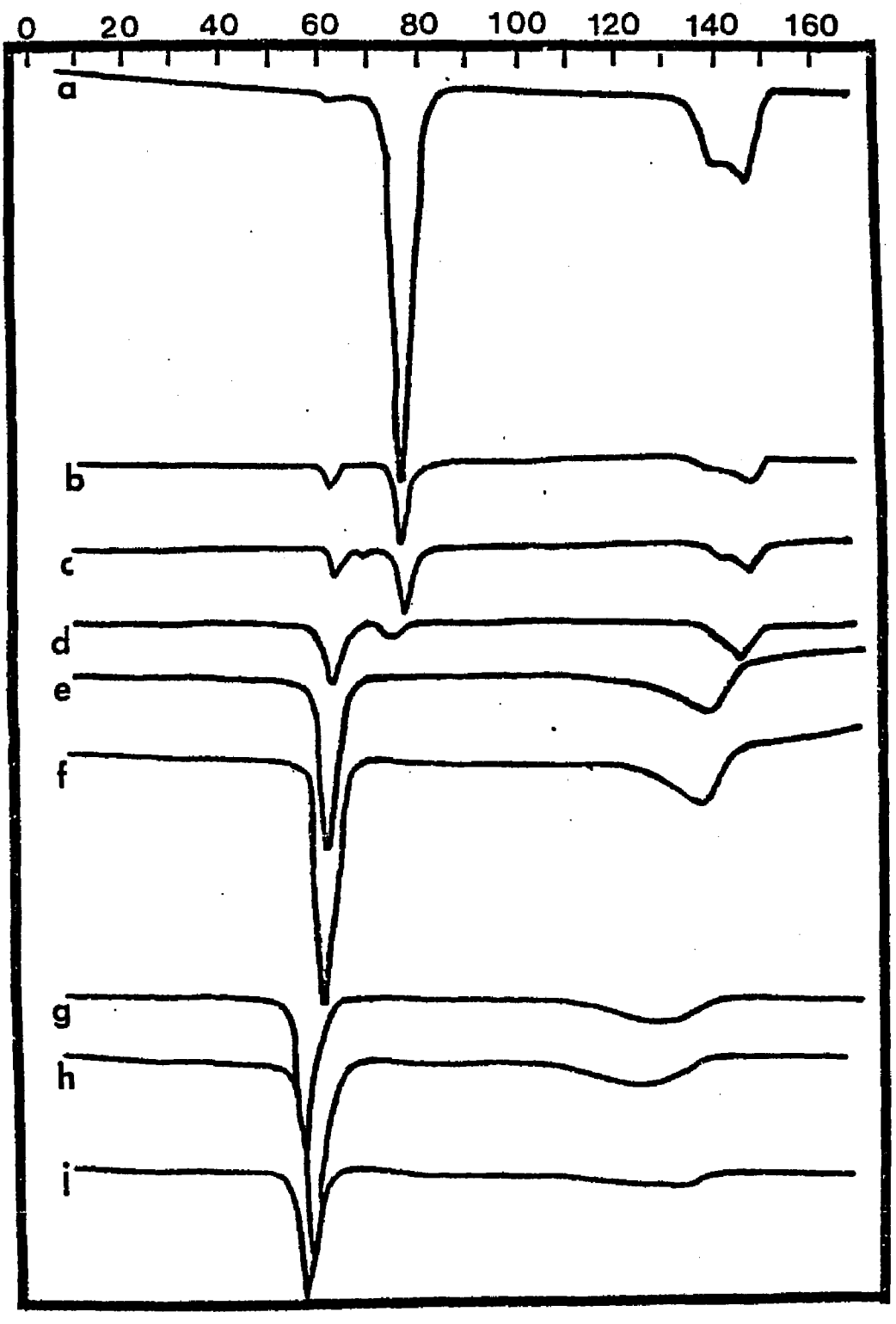

Fig. 20 DSC Scans for TPBD Crystals Grown from Concentrated Solution: (a) 5% F1bH60; (b) 5% F1bH55; (c) 1% F1bH55; (d) 5% F1bH29; (e) 5% F2bH36; (f) 5% F2bH42; (g) 5% F3bH29; (h) 5% F3bH40; (i) 10% F3bH29

TABLE 8. THE TRANSITION TEMPERATURE HEAT OF TRANSITION AND THE NON-CRYSTALLINE FRACTION FOR TPBD GROWN FROM SOLUTION AT VARIOUS CONCENTRATION

Sample	$\bar{M}_n x10^{-4}$	Conc. %(w/v)	T_{tr}	ΔH_{tr} (cal/gm)		$1-w_c$	F_s
F1H55	4.4	0.01	72	26.1	1.005	.16	.15 .12*
F1bH55	2.8	1	74/60**	23.0	0.995	.22	.21
		5	74/60**	24.0	0.994	.22	.19
F1bH60	2.8	5	74/60**	25.7	0.995	.22	.24
F1H29	2.7	0.01	54	18.6	0.986	.27	.24
F1bH29	2.8	5	56/72**	16.8	0.984	.28	.26
F2H36	1.2	0.01	56	18.6	0.984	.28	.26
F3bH36	1.7	5	57	15.9	0.985	.27	.29
F2bH42	1.7	5	58	15.9	0.986	.27	.29
F3H29	0.47	0.01	54	17.7	0.984	.28	.27
F3bH29	0.59	5	54	16.4	0.980	.30	.29
F3bH40	0.59	5	55	15.5	0.982	.29	.30
F3bH29	0.59	10	54	15.9	0.983	.29	.29
F3bH42	0.59	10	58	16.4	0.984	.28	.26

*Data from ^{13}C NMR.

** Secondary Endotherm From DSC

in concentration.

Density Measurement

The density, ρ, of each sample is given in the eighth column in Table 7 and fifth column in Table 8. From the measured density, ρ, assuming a two phase system the weight fraction crystallinity, w_c, for each crystal was calculated:

$$w_c = \frac{\rho_c}{\rho} v_c = \frac{\rho_c}{\rho} \left(\frac{\rho - \rho_a}{\rho_c - \rho_a}\right) \quad (1)$$

where v_c = volume fraction crystallinity;

ρ_a = density for 100% amorphous TPBD[80,91]

= 0.874 gm/cm^3 and

ρ_c = density for 100% crystallinity TPBD[78,80]

= 1.03 gm/cc at 25°C

The value of $1-w_c$ of each sample as obtained from density are also given in Table 7 and 8. The quantity $1-w_c$ is the total noncrystalline portion of each sample. This value will be used to compare with F_s, the noncrystalline portion in each sample available by an epoxidation reaction. The precision of the $1-w_c$ values is ±0.01.

Epoxidation Reaction

The fraction of monomer units at the crystal surfaces, F_s, as determined by epoxidation of crystals with MCPBA in toluene suspension at 6°C are given in the third from the last and the last column of Table 7 and 8, respectively. These values are obtained from averages of areas under -CH- and -CH$_2$- ^{1}H nmr peaks. Other than UH45, the results given are for duplicate preparations with a maximum

average deviation of ±0.03.

Comparison of each F_s value with the corresponding value of $1-w_c$ from density shows the latter to be consistently larger. However, the difference between $1-w_c$ and F_s is only 2 to 4% which is within the experimental precision, except for the sample with the highest molecular weight, WH62. For this sample, use of a higher epoxidation temperature, 12°C led to no significant change in the double bonds epoxidized.

Low Angle X-Ray Scattering

As mentioned before, experimental values for the lamellar thickness, L, gotten from LAXS and electron microscopy for dilute solution grown crystals are given in the next to last column of Table 7. Values of L for F2H36, UH45, VH53, F1H55 and WH62 were obtained from LAXS. Two L values are listed for F2H36, the larger one having a much lower X-ray intensity. This sample showed two order of reflection for the more prominent line. The LAXS pattern for UH45, VH53, F1H55 and WH62 exhibited one, one, two and four order of reflection, respectively. The lamellar thickness of F1H29, F1T15 and F3H29 were measured from electron microscopy using the LAXS spacing for F2H36 to correct for sample shrinkage or inaccuracies in the shadowing procedure.

In order to calculate the average number of monomer units per chain fold, the values for the crystalline thickness, L_c, are necessary. The crystalline thickness along the chain direction, L_c, was calculated from L assuming that the crystalline part of the lamella is sandwiched between two noncrystalline portions with total

thickness $L-L_c$ as shown in Fig. 21. Therefore, L_c is directly proportional to the fraction of crystalline material present ($F_c = 1 - F_s$) and inversely proportional to ρ_c:

$$L_c A = \frac{mF_c}{\rho_c} \qquad (2)$$

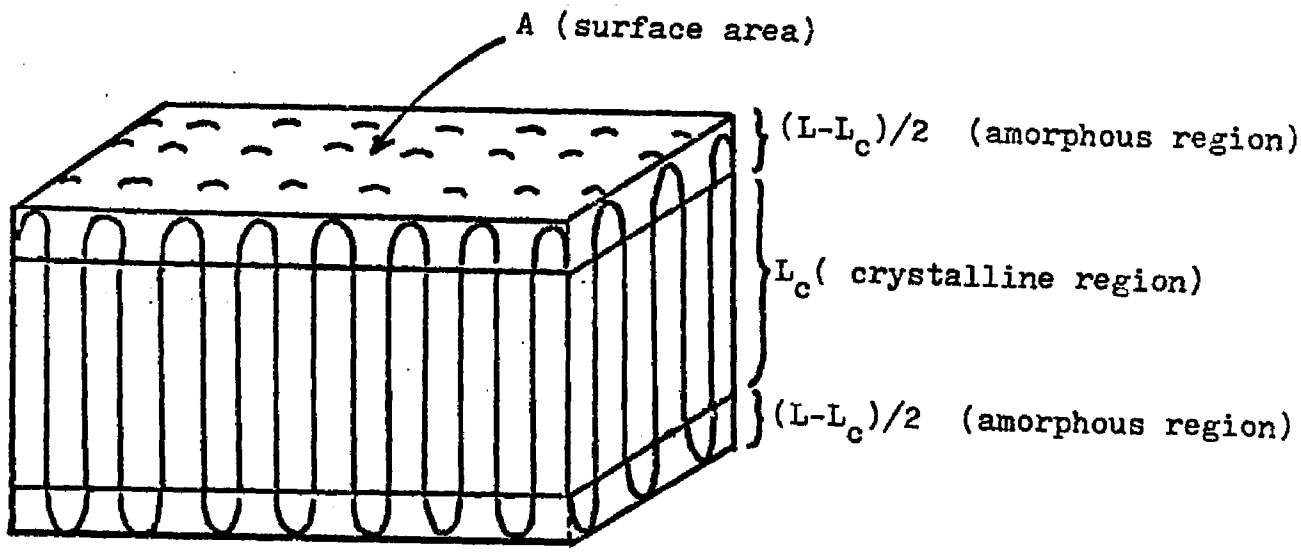

Fig. 21 Schematic Representation of Crystalline and Associated Noncrystalline Region.

And $L-L_c$ is directly proportional to F_s and inversely proportional to ρ_a:

$$(L - L_c)A = \frac{mF_s}{\rho_a} \qquad (3)$$

where L = the lamellar thickness;

L_c = the crystalline thickness;

F_c = the fraction of crystalline material,

= $1-F_s$;

F_s = the fraction of noncrystalline material,

= the % epoxidation;

ρ_c = crystalline density;

ρ_a = amorphous density;

A = the surface area of one crystal and

m = the total mass of one crystal.

Combination of equation (2) and equation (3) with elimination of A and m yield:

$$L_c = \frac{(1 - F_s)\rho_a L}{\rho_a(1 - F_s) + \rho_c F_s} \qquad (4)$$

The values of L_c given in Table 7 and Table 8 were calculated from the above equation

^{13}C nmr Measurement

The ^{13}C nmr spectra for TPBD crystals epoxidized in suspension, for TPBD epoxidized in solution and for the epoxidized model compound, 3,7-decadiene as obtained by F. A. Bovey and F. C. Schilling are given in Appendix I. Detailed peak assignments for the four model samples and the two crystal epoxidized samples are also given in Appendix I. It was found that the resolution for the solution epoxidized TPBD was much higher than that previously reported for partially epoxidized TPBD in solution by Golub et al.[86] and Hayashi,

Takahashi, Kurihara and Ueno;[87] difficulties of the peak assignment were solved by analyzing the epoxidized small molecule, 3,7-decadiene. ^{13}C nmr showed that rather than 100% pure trans,trans,3,7-decadiene, the small molecule sample contains small amount of cis,trans,3,7-decadiene. It was found that due to the presence of the d, ℓ isomers of the asymetric group, -HC(O)CH-, a further splitting in several regions of the spectrum was obtained.

The F_s values obtained from the ^{13}C nmr measurements on UH45 and F1H55 are compared in Table 9 with ^{1}H nmr obtained at both 100 and 200 MHz in the first case and 100 MHz for the second. The F_s values from ^{13}C nmr at least in one case are lower than the ^{1}H nmr result. The values given for F_s in Table 7 and 8 may be somewhat high, although the general trends are believed to be correct.

TABLE 9. ^{13}C NMR Measurement for Epoxidized TPBD Crystals

Sample	% Epoxidation
Epoxidized UH45	16.2
	19*
	22**
Epoxidized F1H55	12
	15**

*% epoxidation obtained from ^{1}H nmr VXL-200.

**% epoxidation obtained from ^{1}H nmr JEOL-100.

DISCUSSION

Temperature Gradient Fractionation

It was found in this investigation that the temperature gradient fractionation method for TPBD in the 5 x 10^3 to 10^5 molecular weight range is a temperature, concentration and molecular weight dependent technique. It was found to be less effective for high molecular weight fractions. Presumably for extremely high molecular weight polymer, most of the material will precipitate out and very little fractionation will take place. It was also shown that the more concentrated the solution the less effective the fractionation. However, for extremely dilute solutions, the $\bar{M}_w/\bar{M}_n$ reached a limiting value. A principal limitation of this method is the time necessary to carry it out on a practical scale. In order to obtain around 10 grams of each fraction for carrying out this research, it is necessary to fractionate around 250 grams of the original polymer. Thus, using a 6 liter flask and 6 grams of original polymer (starting with 0.1% solution) each time, the separation process must be repeated approximately 40 times.

It was also found that the preparation of crystals from 0.01% heptane solution leads to considerable narrowing of the molecular weight distribution, depending on the degree of undercooling used. In fact, fractionation was found to occur in dilute solution for samples UH45, VH53, F1H55 and WH62. In the case of F1H55, crystallization at 0.01% led to a change of $\bar{M}_n$ from 2.7 x 10^4 to 4.4 x 10^4 and of $\bar{M}_w/\bar{M}_n$ from 1.6 to 1.5. Therefore, unless the degree of undercooling and molecular weight are large, in the preparation of dilute

solution grown crystals of TPBD, a considerable fraction of the lower molecular weight components remains in the solution portion.

In dilute solution grown TPBD crystals the total noncrystalline fraction as calculated from density measurement, $1-w_c$, is larger than the fraction available for epoxidation at the crystal surfaces, F_s. Similar results were also observed for concentrated solution grown TPBD crystals. Considering the differences to be precise, one possible explanation for the results are that some of the double bonds present in the amorphous region are not reached by the peracid penetrants. This unreactive amorphous component could possibly be due to hidden folds or other interior crystal defects as suggested by Keller,[64] Wunderlich[100] and Wichacheewa and Woodward.[74] Keller suggested a model of crystal lamella based on an adjacent reentry fold which includes hidden folds, as illustrated in Fig. 22a. Other possible crystal defects suggested as shown in Fig. 22b, c,d; it is not expected that any of these crystal imperfections could be detected by a chemical reagent.

Crystallinity and Crystal Defects

Hoffman and Davis[88] proposed a model of adjacent reentry folding with an amorphous phase that consists of polymer molecules that are physically adsorbed on the fold surface as shown in Fig. 23. It is conceivable that the amorphous layer on the fold surface could be further crystallized under appropriate conditions, could be removed by long extraction in a proper solvent or could be subjected to chemical attack such as by an epoxidation reaction.

Another possible reason for a difference in $1-w_c$ and F_s is that

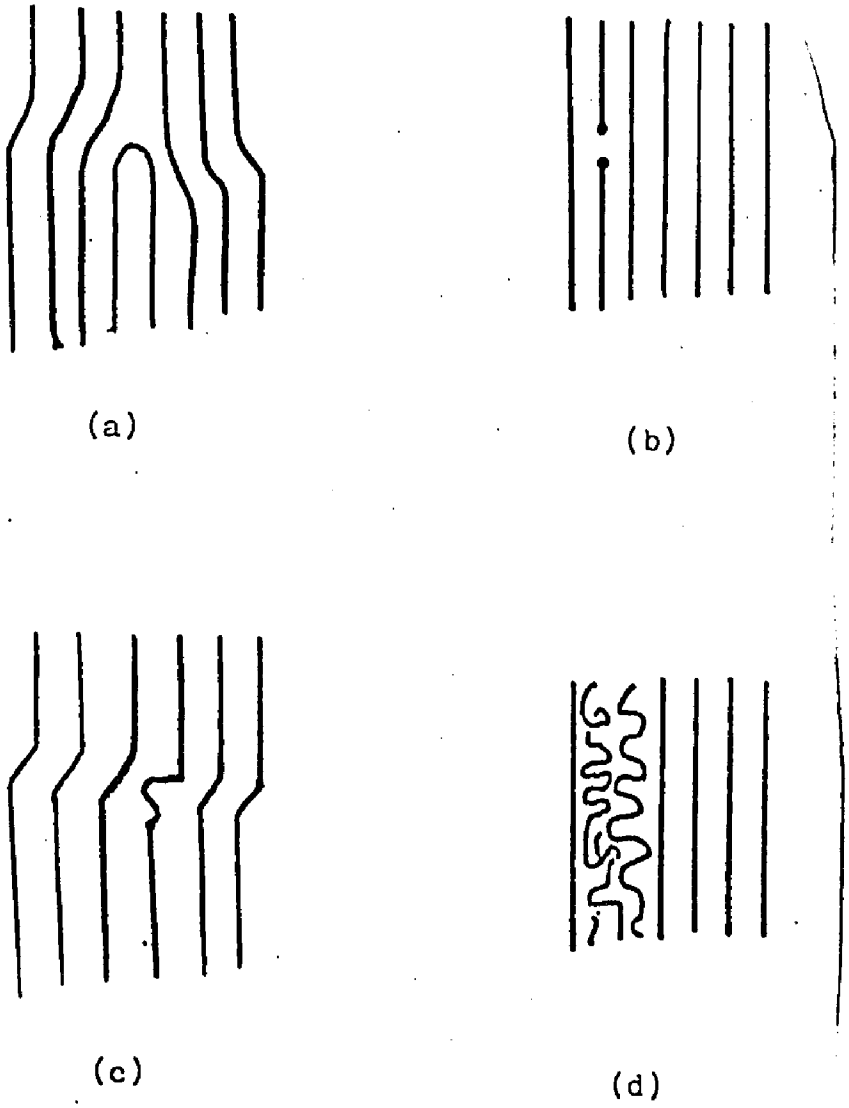

Fig. 22. Different Kinds of Defects in the Crystalline Region, (a) fold buried deep inside the crystal, (b) chain ends inside the crystal, (c) kink chain defect, (d) mosaic block

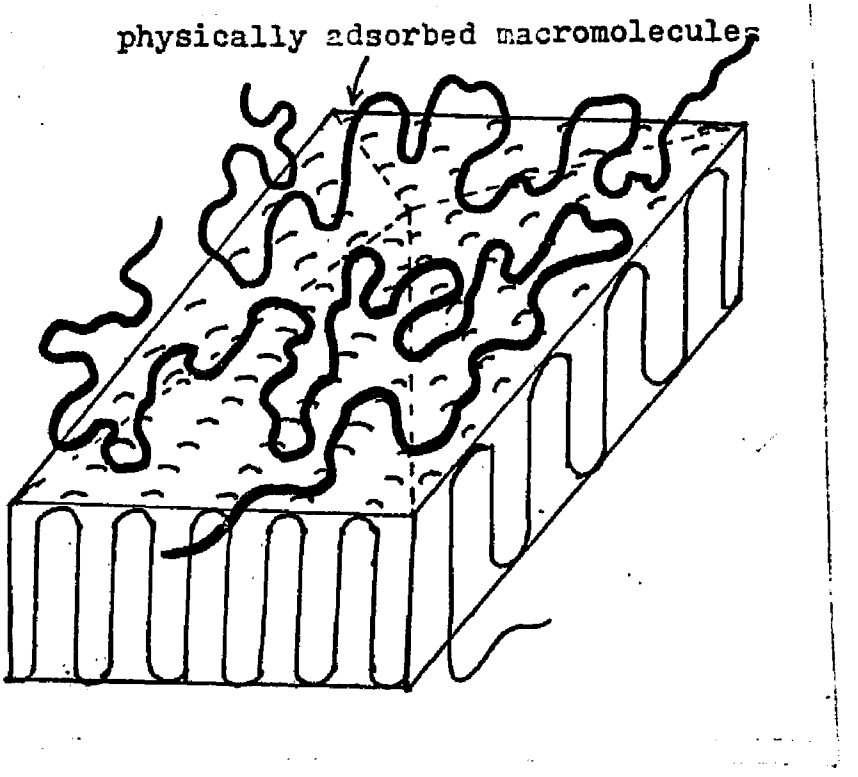

Fig. 23 Proposed model of adjacent reentry fold with an amorphous phase that consists of polymer molecules that are physically adsorbed on the fold surface. (Taken from reference 88).

observed from the polymer melt. In order to give a smaller value of $1-w_c$, ρ_a would have to be smaller than that used. If the crystallinity, w_c, is given by $1-F_s$, ρ_a values for dilute solution grown crystals are calculated as follows:

Sample	WH62	VH53	F1H55	F1H29	FIT15	UH45	F2H36	F3H29
			(0.85)			(0.81)		
ρ_a g/cc^3	0.84	0.87	0.88	0.87	0.86	0.86	0.87	0.88

where the two numbers in the brackets for F1H55 and UH45 are calculated using the F_s values obtained from ^{13}C nmr measurement. Since ^{13}C nmr has better resolution than ^{1}H nmr, the ρ_a values calculated from ^{13}C nmr results for F1H55 and UH45 are believed to be more accurate than those calculated from ^{1}H nmr results. In general, the ρ_a values given above are smaller than the density extrapolated from that for the polymer melt, 0.874 g/cc^3; the lowest ρ_a value is calculated to be 0.81 g/cc^3. A value of ρ_a lower than that extrapolated from the melt is in agreement with the calculation of the density for thefold region in polyethylene as given by Harrison and Juska.[65] Assuming a tight adjacent reentry fold, the calculations made on space-filling models indicated that the density at the polyethylene fold surface is on the order of 0.75 g/cc^3 as compared to an extrapolated melt density of 0.86 g/cc^3. However, the difference between $1-w_c$ and F_s given in Table 7 and 8 can be as small as 1 to 3% which is within the experimental precision. Three fractions, F1T15, WH62 and UH45 (^{13}C nmr) show an absolute deviation of 4% or larger (around 15 to 30% on a relative scale).

Sample F1T15 is the only preparation of crystals grown from toluene solvent. Assuming that the ρ_a used is correct, the relatively large deviation between $1-w_c$ and F_s confirms the earlier suggestion that crystalline defects exist in crystals grown from a better solvent. In a study of the dynamic behavior of TPBD crystal mats Tatsumi[76] postulated that crystals from a "good" solvent, such as benzene, should have looser folds than crystals from a "poor" solvent, such as n-heptane. A "good" solvent was defined as one in which the particular polymer

dissolves at a relatively low temperature. An estimate of the number of monomer units in a chain fold in TPBD crystals grown from various solvents, heptane, toluene and benzene was reported by Stellman.[67,69] From results of epoxidation and low angle X-ray diffraction, it was concluded that crystals grown from the better solvent had a higher % epoxidation and larger number of monomer units per chain fold. In a kinetic study of crystal epoxidation Wichacheewa[74] reported an increase of % epoxidation with temperature in the range of 6 - 21°C for TPBD toluene grown crystals. This temperature dependence of % epoxidation was not found for heptane-grown crystals. It was concluded that for toluene grown crystals, at lower temperature some of the double bond in amorphous parts of the lamellar are completely excluded from reaction with epoxidizing reagent. The postulated models of regular folds and irregular folds (combination of loose folds and tight folds) for crystals grown from heptane and toluene, as given by Wichacheewa[101] as shown in Fig. 24.

Sample WH62 shows a significant positive deviation from the straight-line plot of the enthalpy of transition vs. specific volume given in Fig. 19. The extensive data for the change of the heat of fusion of polyethylene as a function of specific volume[42,52-54] leads to the conclusion that the heat of fusion is not proportional to % crystallinity. Using the heat of fusion, difficulties in finding the % crystallinity arise when (1) the crystal perfection, as roughly indicated by the crystallinity or specific volume and the effects of surface are varied separately; (2) the separation of the heat capacity of the sample from the heat of fusion - the

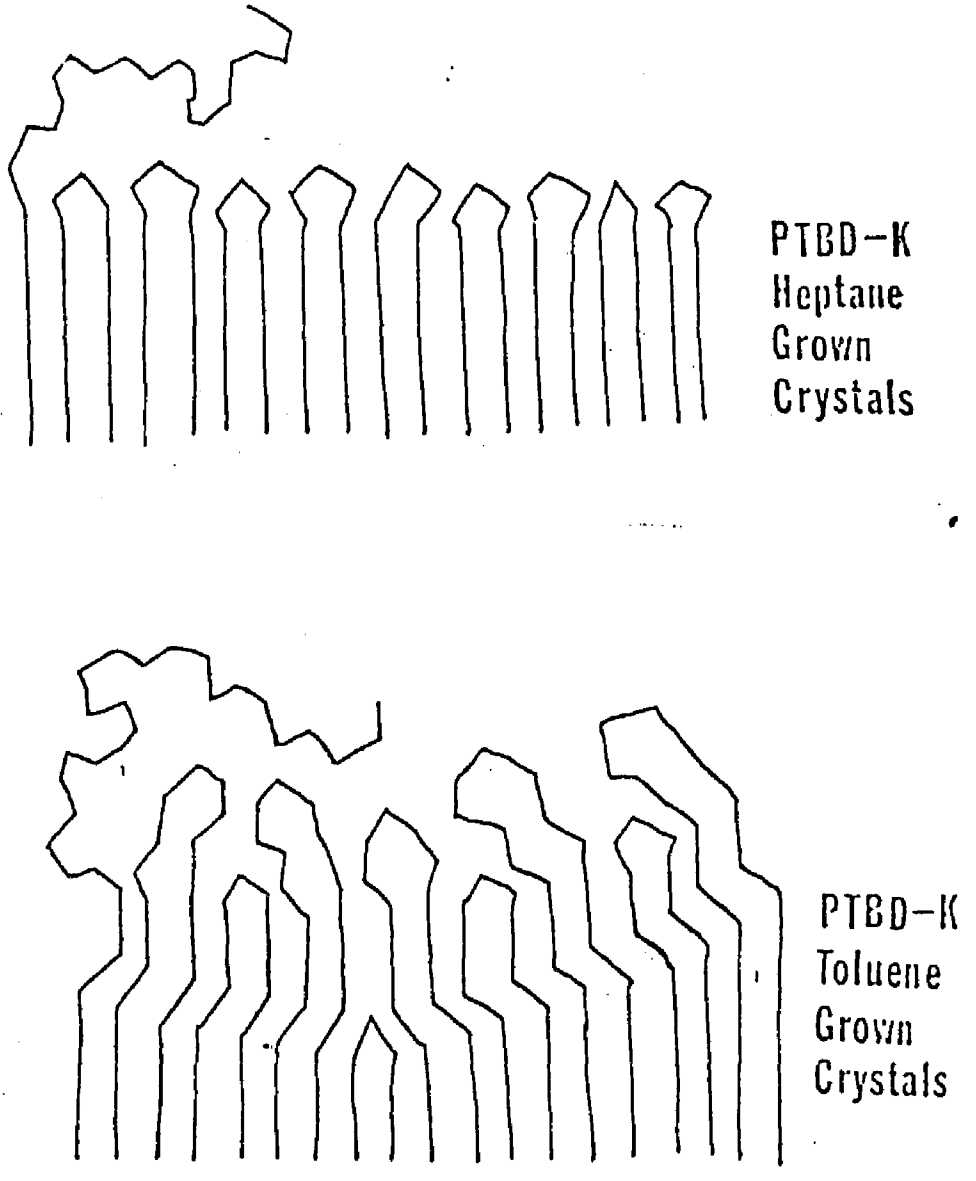

Fig. 24. Models of the fold region for TPBD crystals grown from two different preparations. (a) heptane grown crystals (b) toluene grown crystals (taken from reference 101).

baseline problem and (3) the amorphous portion of the sample is strained which usually happens in melt-grown crystals where the stress relief in the amorphous polymer may cause an exothermic contribution.

The WH62 fraction has the highest molecular weight and the highest molecular weight distribution. These crystals gave the highest transition temperature from the DSC scan. They also had the largest lateral dimensions, being approximately 100 times larger than crystals from the other preparations, the largest crystal thickness and few screw dislocation growths. It is expected that the DSC measurement of the enthalpy of transition will take the crystal perfection as well as crystal size into account. Apparently, for this preparation crystal perfection is the dominating factor and results in the higher value of ΔH_{tr} from the DSC measurement. Besides, the larger dimensions for the crystals from WH62 could lead to the absorption of polymer molecules at the crystal surfaces. The large deviation of % crystallinity as measured from the density method and by the chemical assay (epoxidation) method could be possible if desorption of the absorbed layer happened during epoxidation in toluene.

Multiple Endotherms in the Crystal-Crystal Transition Region

For the dilute solution-grown crystals single crystal-crystal transition endotherms were observed. The crystal-crystal transition position shifted to lower temperature with decreasing crystallization temperature, T_c. For crystals grown from concentrated solution using fractions with $\bar{M}_n$'s of 1.7×10^4 and 5900, one transition

endotherm was observed at about the same temperature position as for crystals from dilute solutions at the same T_c. However, multiple peaks in the crystal-crystal transition region were observed for a fraction with $\bar{M}_n = 2.8 \times 10^4$ crystallized at high concentration. The major endotherm was found in the same temperature region as for lamellas grown from dilute solution at a similar temperature. Therefore, the crystal-crystal transition endotherm behavior for TPBD crystallized from solution is dependent on molecular weight and polymer concentration as well as on crystallization temperature.

Multiple endotherms in the transition region were also reported by Marchetti and Martuscelli[81,82] and recently by Finter and Wegner[83] in their studies of dilute solution grown TPBD crystals. Using the self-seeding technique, Marchetti and Martuscelli[81] varied the crystallization temperature, T_c, (from 16°C - 64°C in 0.1% heptane) and observed a large and increasing lamellar thickness from SAXS (from 200 to 480Å) with an increase in crystallization temperature. Bromination of these crystals showed that as the thickness of the single crystals was increased, a larger number of repeat units become accessible.[81] However, regardless of the crystallization temperature difference, DSC thermograms showed two endothermic peaks in the crystal-crystal transition region. Using wide-angle X-ray diffraction measurement Marchetti and Martuscelli[82] attributed the two solid-solid transitions to the presence of "crystalline blocks" in the single crystals with the crystallographic structure of form I but with different thermodynamic stability.

In contrast to the large long spacing observed by Marchetti and

Martuscelli, Finter and Wegner[83] observed the lamellar thickness in the two regimes of crystallization behavior depending on the degree of undercooling (namely, $\Delta T > 27°C$ and $\Delta T < 27°C$). The lamellar thickness for regime I varied from 83Å to 102Å and for regime II from 204Å to 293Å. In both regimes a decrease of the long spacing with increasing ΔT, the degree of undercooling, was observed. There was, however, a sudden jump of lamellar thickness between regimes I and II. Crystals obtained in regime II showed a particularly simple DSC behavior, and crystals obtained in regime I showed two endotherms in the phase transition region. Finter and Wegner[83] believed that the two peaks in the crystal-crystal transition region are not due to the presence of different modifications but due to the precipitation of crystals of different crystallite thickness for the following three reasons:

(1) All samples showed the same wide-angle X-ray diffraction pattern at room temperature independent of the growth history.

(2) DSC scans of two mixed samples of crystals from regime II with different lamellar thickness also showed two crystal-crystal transition peaks.

(3) The relative enthalpies of the two transition peaks depend on the polymer concentration in the crystallization process.

The larger portion of the higher temperature endotherm was found in the more concentrated solution (0.05% vs. 0.01% in heptane solution). The third reason implies that the larger lamellar thickness is produced by nonisothermal crystal growth in the crystallization process.

A comparison of the lamellar thicknesses observed by Marchetti and Martuscelli,[81,82] Woodward and coworkers[67-69,74] and Finter and Wegner,[83] was given by the latter authors; only part of the data of Marchetti and Martuscelli, that for samples crystallized at relatively high T_c, fit approximately the extrapolation of Finter and Wegner's curve describing the crystallization behavior in regime II; the lamellar thickness for crystals obtained at T_c's in regime I are too large. The data observed previously by Woodward and coworkers fit Finter and Wegner's curve in regime I. The results obtained in the present work fall in both regime I and regime II depending on T_c as described by Finter and Wegner.[83] The large difference in the results as observed by Marchetti and Martuscelli[81] and Finter and Wegner[83] for samples crystallized at large ΔT (low T_c) are believed to be caused by nonisothermal crystallization taking place in the former study. Nonisothermal crystallization also occurs to a small extent in the present study on dilute solution grown crystals (0.01%) when preparing them in large quantity. When the container is quickly removed from temperature T_d to the constant temperature bath at T_c, the system takes a relatively long time to reach the isothermal crystallization temperature, T_c, due to the large volume, and crystallization could start before the whole system is equilibrated. The sample F2H36 (dilute solution grown crystals) prepared for SAXS shows two periodicities; the one corresponding to a large lamellar thickness has a much lower intensity. This is evidence of nonisothermal crystal growth, in agreement with the assignment by Finter and Wegner.[83]

Since the crystal-crystal transition temperature is related to the lamellar thickness, the presence of a significant secondary endotherm in the transition region for 5% F1bH29, for 5% and 1% F1bH55, and for 5% F1bH60 is evidence that the final dried products of these samples contain crystalline components with more than one lamellar thickness; however, the secondary components might appear either during the crystallization process by nonisothermal means or during the recovery of the principal component.

In the case of F1bH29, it is reasonable to attribute the secondary endotherm to the occurrence of some nonisothermal crystallization at a temperature higher than T_c. Because of the high concentration and relatively low crystallization temperature, crystal growth starts earlier before the whole system reaches the isothermal crystallization temperature, T_c. Some of the material nucleates and crystallizes at a higher temperature with a larger lamellar thickness and therefore, contributes a higher temperature seondary endotherm in the DSC scan.

In the case of 5% F1bH55, 5% F1bH60 and 1% F1bH55, the secondary endotherms occur at temperatures expected for samples crystallizing near to or somewhat above room temperature. As mentioned earlier, these three preparations have a considerable fraction of soluble material remaining in solution after crystallization is completed. Therefore, a possible explanation for the presence of the secondary endotherm in these preparations is that part of the noncrystalline material is adsorbed on the crystal surfaces and it is not entirely desorbed upon washing. However, upon cooling from T_c to room temperature, these adsorbed polymer molecules crystallize to form

thinner lamellas, thereby, contributing a lower transition temperature endotherm. It is expected that a more rapid desorption occurs during the washing process at higher temperature due to the increased solvent power; therefore, the second component in F1bH60 is almost negligible. Since these adsorbed polymer molecules have already crystallized, removal of the adsorbed layer would not happen during epoxidation in toluene solution. The data obtained from epoxidation and density measurement on these samples are consistent with this explanation.

Chain Folding

(A) Calculation of the Monomer Units Per Chain Fold and Chain End

For dilute solution grown crystals the surface fractions, F_s, will consist of three components,[67] one due to the folds, another due to the noncrystallizing chain ends, and the third due to the lateral crystal surfaces. For the crystals investigated the lateral surface area did not exceed 4% of the total surface area, so that only the first two components are considered. As shown in Fig. 25, each chain of degree of polymerization, N, will have $F_s N$ monomer units at the two surfaces. This can be written in terms of the number of monomer units per fold, U, the number of folds in each chain, F, and the number of monomer units in two noncrystalline chain ends, c. For a polydisperse system it can be shown that the number average degree of polymerization, $\bar{N}_n$, should be used (see Appendix C). The total number of monomer units in the noncrystalline region per chain equals the total in the chain folds plus the total in the two chain

ends per chain:

$$\bar{N}_n F_s = \bar{M}_n F_s / M_o = UF + c \qquad (5)$$

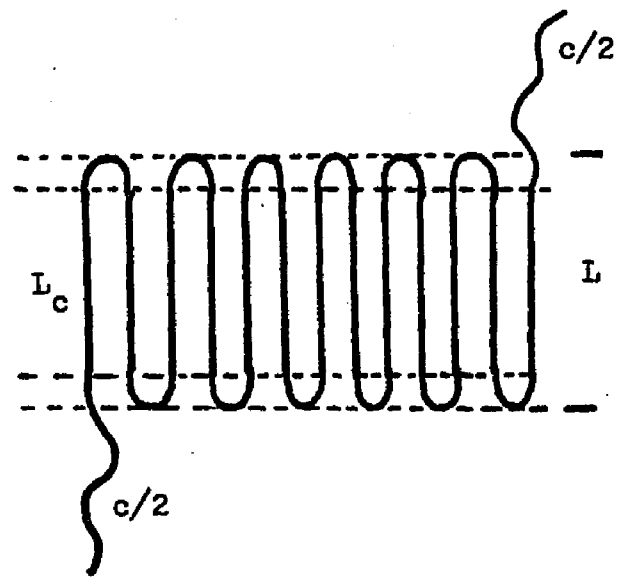

Fig. 25 Schematic representation of chain folds, chain ends and crystal stems of a polymer molecule.

where $\bar{M}_n$ is the number average molecular weight of the polymer, and M_o is the molecular weight of a monomer unit in the chain, 54 gm/mole. It is assumed that the remaining monomer units in the chain, $\bar{M}_n (1 - F_s)$ are in the crystalline core, the following equation relates the total number of monomer units in the crystalline regions to the crystalline thickness and the number of crystalline traverses

as well as the repeat distance per chain unit along the chain direction, R, as follows:

$$\bar{N}_n(1 - F_s) = L_c(F + 1)/R \qquad (6)$$

where L_c is the crystalline thickness, R is the repeat distance of the monomer unit in the chain direction, 4.83Å, and F + 1 is the number of chain traverses per chain. Combination of equation (5) and (6) with elimination of F yields:[102]

$$U = \frac{L_c}{R}\left\{\frac{F_s\bar{M}_n}{M_o} - c\right\} \Big/ \left\{\frac{\bar{M}_n(1 - F_s)}{M_o} - \frac{L_c}{R}\right\} \qquad (7)$$

(see Appendix C)

For large $\bar{M}_n$, chain ends can be neglected, and equation (7) becomes:

$$U = \frac{L_c F_s}{R(1 - F_s)} \qquad (8)$$

When the part of the polymer chain next to the end group is not long enough to traverse the crystal lamella, it should remain outside of the crystallite. It is therefore, reasonable to assume that the number of monomer units associated with a chain end, c, is a function of lamellar thickness, L/R without specifying the proportionality constant. Therefore, c can be given by aL/R. Substitution for c in equation (7) and rearranging yields:[102]

$$\frac{F_s\bar{M}_n R}{LM_o} = \frac{UR}{L}\left\{\frac{R\bar{M}_n(1 - F_s)}{L_c M_o} - 1\right\} + a \qquad (9)$$

An equation similar to equation (7) was given earlier by Wichacheewa and Woodward.[74] It was assumed in previous work on TPBD that the average length of a chain end is half of the lamellar thickness, L, and therefore was given by L/R. Equation (7) is thought to be more exact than the equation given earlier. Nevertheless, it leads to similar results. If U and a are independent of molecular weight and other parameters such as the crystallization temperature, T_c, the degree of undercooling, T_d-T_c, and the crystallization solvent, a plot of the above equation of $F_s\bar{M}_nR/LM_o$ vs. (R/L) $[R\bar{M}_n(1-F_s)/L_cM_o-1]$ should yield a straight line with the slope equal to U and an intercept equal to a.

A plot of the results for the dilute solution grown crystals is given in Fig. 26 using the F_s and L_c values found in Table 7. With the exception of WH62, the points define a straight line within a ±10% error limit with an intercept of 0.79 and a slope of 3.8, i.e. U = 3.8 monomer units per fold and c = 0.79 L/R. The two numbers obtained from Fig. 26 suggest that chain folding in the crystals is independent of many other factors. However, taking c = 0.79 L/R and calculating the value of U for each crystal preparation using equation (7) yields a number of monomer units per fold chaning from 2½ to 6½, as follows:

Sample	F3H29	F2H36	UH45	F1T15	F1H29	F1H55	VH53	WH62
U	2½	4	4	3½	3½	5	4	6½

Independent studies of U for sample UH45 and F1H55 using ^{13}C nmr

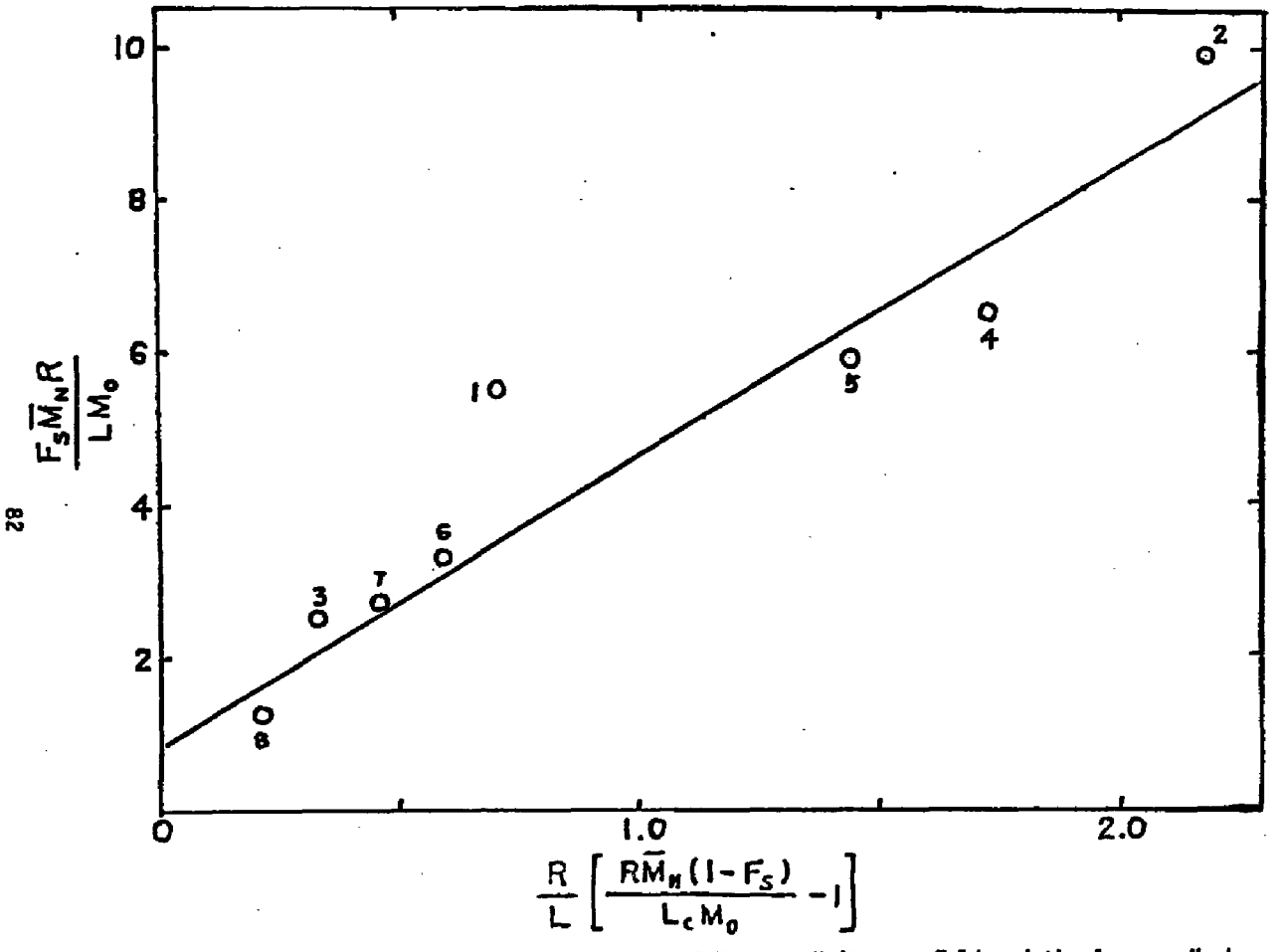

Fig. 26. Determination of the Average Number of Monomer Units per Fold and the Average Number of Monomer Units Per Chain End for Dilute Solution-Grown TPBD Crystals: (1) WH62; (2) VH53; (3) F1H55; (4) F1H29; (5) F1T15; (6) UH45; (7) F2H36; (8) F3H29.

spectrum analysis, which will be discussed in the last section, give 2½ and 3. The U and c from the present study are dependent upon the determination of a number of parameters: F_s, $\bar{M}_n$, L, ρ_a, the amorphous density and ρ_c, the crystalline density and therefore only approximate agreement between the two methods is found.

Using equation (7) and doing the same calculation for concentrated solution grown crystals yields the results given in Table 10. Values for lamellar thickness, L, and the number of monomer units per fold, U, for dilute solution grown crystals (0.01%), as presented above, are given in Table 10 for comparison. For concentrated solution grown crystals L is calculated by assuming a linear relationship vs. T_c between any two measured L values obtained for dilute solution grown crystals. The c values in Table 10 are calculated using the relationship found in Fig. 26, 0.79 L/R; L_c values are calculated with equation (4).

In this calculations the L_c values used were not corrected for chain tilt in the crystals. Since the angle is given as 114°[78] for TPBD crystals, the correction of chain tilt would lead to about 10% increase in U (see Appendix B). In analyzing the changes taking place in U for the series of samples studied, one needs to consider two effects: that caused by changing molecular weight and that caused by changing crystallization temperature. Comparison of the results for F1H29 and F3H29 shows a decrease in U with decreasing molecular weight at the same T_c. Although the amount of this change is small, it is obvious that U is molecular weight dependent. The low molecular weight fraction does not crystallize at high

TABLE 10. CALCULATION OF NUMBER OF MONOMER UNITS PER FOLD FOR TPBD CRYSTALS

Sample	Conc. (w/v)	L(nm)	c	L_c(nm)	U
F1H55	0.01%	24	39	20	5
F1bH60	5%	26	43	20	6
F2H36	0.01%	10	17	7.3	4
F2bH36	5%	10	17	7.0	5
F2bH42	5%	11	18	7.3	5.5
F3H29	.01%	9.1	15	6.3	2.5
F3bH29	5%	9.1	15	6.1	3.5
F3bH40	5%	11	18	7.3	3.5
F3bH29	10%	9.1	15	6.1	3.5
F3bH42	10%	11	18	7.6	2.5

temperature. When crystallized at high temperature the high molecular weight fraction undergoes further fractionation and a smaller $\bar{M}_w/\bar{M}_n$ value is observed. Apparently U is also crystallization temperature dependent in which a decrease of U accompanies the decrease of T_c, e.g. compare F1bH60 and F1H29. This result is in agreement with the earlier study reported by Marchetti and Martuscelli using the chemical assay bromination method.[81]

In addition to chain folds and chain ends, the multilamellar structures crystallized from concentrated solution might contain an interzonal component linking the lamellas. As increase in U, the average of the various fold and interlamellar chain lengths, with a change in concentration from 0.01% to 5% is seen in Table 10 for F2H36 and F3H29. However, this effect is not large suggesting that only a small number of traverses from one lamella to others are present. The increase in U with an increase in T_c and $\bar{M}_n$ as obtained from dilute solution grown crystals, also occurs for crystals grown from concentrated solution.

In Table 11 is given a collection of data for the disordered fraction reported previously by Woodward and coworkers: Stellman[67,69] Hendrix and Whiting,[68] Eng[71] and Wichacheewa.[74] The results for sample F1H55, F1H29, F1T15and UH45 prepared in this study are also listed for comparison. U values were calculated from the % epoxidation data using equation (7) from this study.

The TPBD-K heptane grown crystals has similar F_s and $\bar{M}_n$ values to F1H55. However, its U value is smaller than the ^{13}C nmr derived U value for F1H55 due mainly to about a two fold difference in

TABLE 11. DISORDERED FRACTION AND U VALUES FOR TPBD CRYSTALS

Sample	Solvent	T_d	T_c	% Epoxidation	% Bromination[d]	IR[b]	NMR[c]	U
F1H55		67	55	15				5
				12[h]				3½
F1H29		67	29	25				3½
TPBD-K	Heptane	78	63.5	14[a]	13	14	13	2½
TPBD-K	Toluene	50	23	18[a]		19	23	3
F1T15		27	15	22				3½
TPBD-K	Toluene	45	23	14-29[d]	21			2½-5
TPBD-U	Heptane	55	45	27[d]				5
UH45		55	45	22[e]				4
				19[f]				3
				16.2[h]			17[g]	2½

a. See Refs. 67,69; $\bar{M}_n$ of Toluene Grown K-Crystals Taken as Same as Heptane Grown (36000). b. See Ref. 68. c. See Ref. 71. d. See Ref. 74; $\bar{M}_n$ Taken as 1.7×10^4 and L as 11.0 nm as Obtained in This work. e. Obtained From ^1H NMR JEOLOCO-100. f. Obtained From ^{H}NMR Varian-200. g. From Solid State ^{13}C NMR By F. A. Bovey and F. C. Schilling, h. Obtained From ^{13}C NMR in $CDCl_3$ Solution by F. A. Bovey and F. C. Schilling.

lamellar thickness, L. The F1H29 preparation has a lamellar thickness similar to K-H but ΔT is larger.

Comparison of the calculated U values for TPBD-K toluene grown crystals with that for F1T15, shows close agreement. However, the solvent effect noted earlier -[69,74] an increase in U as crystallization solvent is changed from heptane to toluene - is not found in the present work when ΔT was held constant.

The U values for UH45 are smaller than those calculated for TPBD-U crystals. This is due to the lower F_s values obtained for UH45, the larger F_s value for TPBD-U could have been due to the indirect method of assaying it in the earlier work.[74]

For heptane grown crystals, K crystals and UH45, the disordered fraction found by other methods: bromination, IR and nmr, are in good agreement with the disordered fraction found by epoxidation. These results suggest that for crystals prepared under these conditions disorered fraction/mobile fraction is present on the crystal surfaces.

For K crystals grown from toluene solution, the disordered fraction shows a lack of agreement between the three surface penetration methods, epoxidation, bromination and nmr. Woodward and Wichicheewa[74] explained this discrepancy and the temperature dependence of the % epoxidation for K-toluene crystals as due to the size of the penetrant molecules as well as the temperature. Smaller size molecules such as CS_2 and Br_2 can penetrate to a greater degree at lower temperature than MCℓPBA.

(B) Independent Calculations of The Monomer Units Per Chain Fold From ^{13}C nmr Spectrum

In analyzing the ^{13}C nmr spectrum for $-CH_2-$ or -CH- on epoxidized butadiene units in a partially reacted polymer, Bovey and Schilling have found (see Appendix A) that there are two types of carbons which show different chemical shifts. One is inside the epoxidized sequence and one is outside the epoxidized sequence, shown as follows:

$-CH_2$ region:

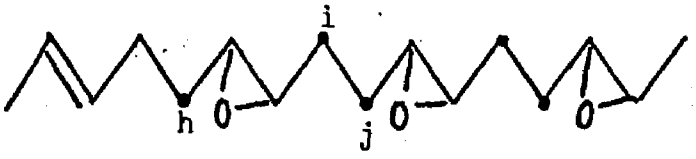

-CH- region:

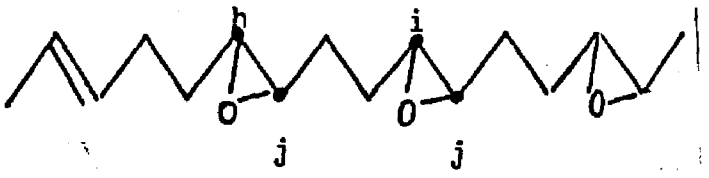

where carbon i and j with spectrum intensity A are inside the epoxidized sequence and carbon h with spectrum intensity B are outside the sequence. A direct measurement of the number of monomer uits per chain fold, $U_{uncor.}$, can be obtained from the spectrum intensity:

$$\frac{2(U_{uncor.} - 1)}{2} = \frac{A}{B} \qquad (10)$$

At the degree of resolution obtained to date, ^{13}C nmr can not distinguish a difference in an epoxidation sequence for a chain fold

versus that for a chain end. Therefore, the value obtained from equation (10) is uncorrected for chain ends, and is related to the actual U by the equation:

$$U_{uncor.} = (UF + c^{-2})/(F + 1) \qquad (11)$$

where F is the number of folds per chain gotten from equation (6) and the number of monomer units per two chain ends in each molecule, c, is taken as 0.79 L/R. The results of this direct analysis using ^{13}C nmr to obtained U for UH45 and F1H55 are given in Table 12.

In Table 12, three U values are given for each sample; two of these are calculated from equation (7) with F_s values measured by ^{1}H nmr (JEOLCO-100) and ^{13}C nmr and the third was obtained from application of equations (10) and (11). It was estimated earlier[78] that the tightest reentry fold possible from the TPBD crystal structure contained from 1.5 to 2 monomer units. The relatively small U values obtained from ^{13}C nmr leads to two possibilities:

(i) essentially reentry chain folding occurs for TPBD dilute solution grown crystals using relatively low molecular weight polymer;

(ii) or incomplete epoxidation of the surface double bonds is taking place.

However, the latter explanation is not supported by the results from spectroscopy on unreacted crystals (see Table 11). The tightness of the chain fold in TPBD crystals is apparently affected by molecular weight and/or crystallization temperature.

TABLE 12. ^{13}C NMR MEASUREMENT FOR EPOXIDIZED TPBD CRYSTALS

Sample	% Epoxidation		U		
	^{1}H nmr	^{13}C nmr	$F_s(^{1}H$ nmr)	$F_s(^{13}C$ nmr)	Direct(^{13}C nmr)
UH45	22	16	4	2½	2½
F1H55	15	12	5	3½	3

CONCLUSIONS

The following conclusions can be drawn from this investigation:

(1) For TPBD crystals grown from heptane and toluene solution, the noncrystalline fraction as obtained from density measurement is found to be larger than the fraction at the crystal surfaces available for a chemical reaction.

(2) The change of heat of transition of TPBD single crystals measured from DSC is proportional to the specific volume at room temperature, as long as the crystal size/fold length are similar.

(3) A more complicated multilamellar morphorlogy for TPBD crystals was obtained in concentrated heptane solution as compared with dilute solution grown lamellas.

(4) Two lamellar components were found in crystals grown at small undercoolings from concentrated solutions indicating that an adsorbed layer can exist at high growth temperatures.

(5) The number average monomer units per chain fold, U, is molecular weight and crystallization temperature dependent, with U increasing with an increase of molecular weight and T_c. At low molecular weight ($\lesssim 2 \times 10^4$) a tight reentrant fold apparently occurs.

(6) The number of monomer units per noncrystallizing chain end is proportional to the lamellar thickness, L, and is given by 0.4 L/R where R is the crystal repeat distance.

(7) Any interzonal component linking the lamellas is considered to be made up of relatively short tie chains in TPBD multilamellar

crystals prepared from concentrated solution.

Suggestions For Further Work

The following projects are extensions of the present work:

(1) A study of the nature of chain folding for TPBD fractions with number average molecular weights greater than 1.2×10^5, the highest molecular weight fraction studied in this research.

(2) An examination of the ^{13}C nmr spectra for a series of epoxidized TPBD crystals over a wide range of molecular weight and crystallization conditions.

(3) Measurement of the mobile and rigid fraction in TPBD crystals and epoxidized TPBD crystals using solid state ^{13}C nmr.

(4) Study of solution grown TPBD crystals using various crystal growth techniques such as growing the crystals at large degrees of undercooling, i.e., quenching the solution to low T_c.

APPENDIX A

^{13}C nm Spectroscopic Study of Epoxidized TPBD Crystals and Model Compounds

The ^{13}C nmr spectrum in solution of TPBD crystals epoxidized in suspension, UH45 and F1H55, are shown in Fig. A1 and A2. Spectra for TPBD epoxidized in solution to 35% and 75% are shown in Fig. A3 and A4. Resonances corresponding to solvents toluene, methanol and ether which remain in the samples after epoxidation and washing also appear. A triplet weak resonance is also found for the solvent $CDCl_3$ used for the nmr sample preparation.

From the ^{13}C nmr peak intensities for the carbon atoms in the olefinic CH and CH_2 and the epoxidized olefinic CH and CH_2 groups, the % epoxidation for these four samples are found to be 16.2%, 12%, 30% and 78% individually.

A spectrum for the model compound, 3,7-decadiene, is given in Fig. A5. It is found that this sample contains the trans-trans and small amount of the trans-cis 3,7-decadiene isomers. The spectrum of 50% epoxidized 3,7-decadiene is given in Fig. A6; this spectrum is fairly complicated due to the presence of seven possible molecular structures. Fig. A7 is the spectrum for 100% epoxidized 3,7-decadiene where t and c correspond to the epoxy group of the trans and cis double bond after epoxidation. From Fig. A7 it is shown that in addition to the effect of the geometric isomers, t & c on the resonances for C_1, C_2, and C_3, the resonances of carbon C_4 and C_5 are sensitive to the stereoisomers of the d and 1 epoxy group.

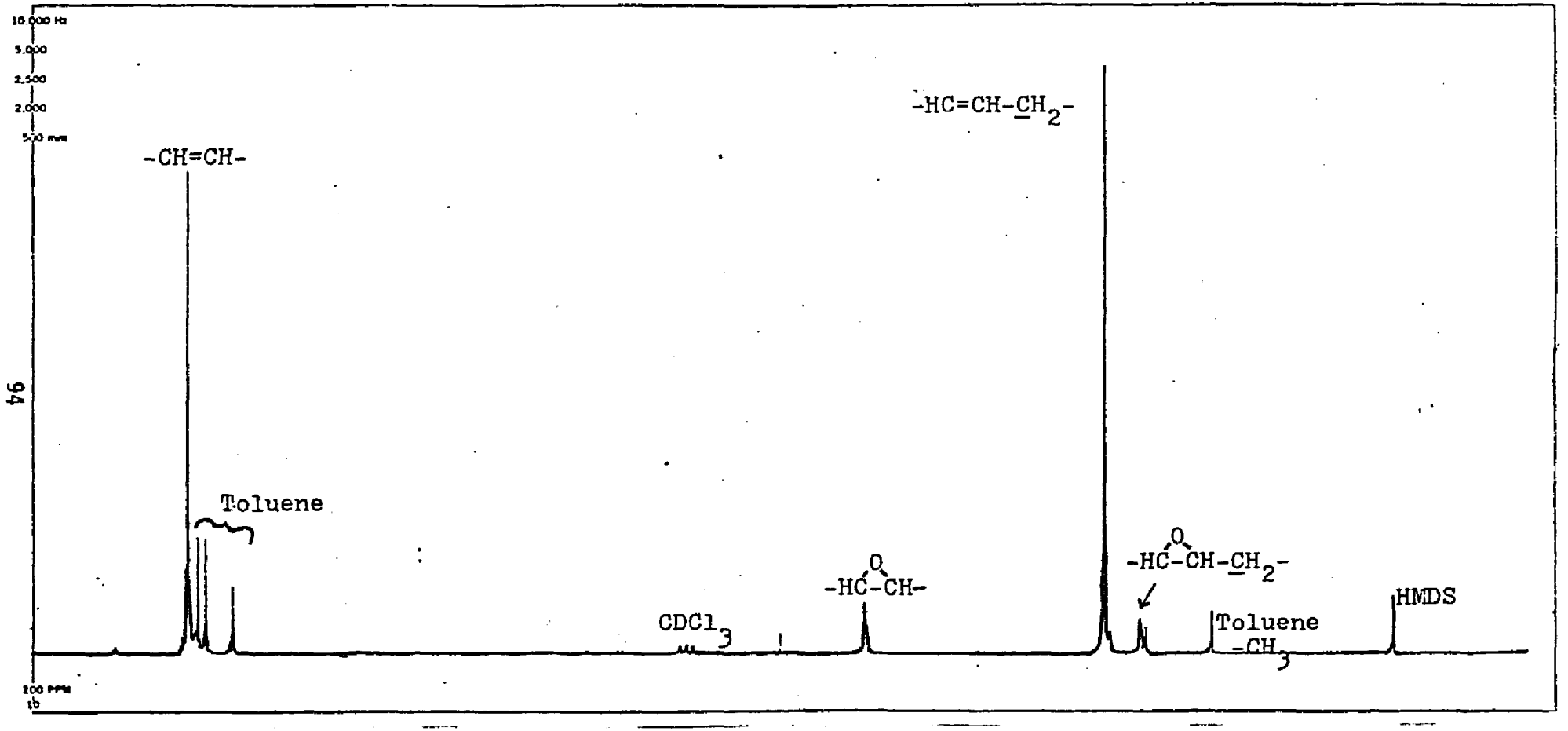

Fig. A1 Proton Noise Decoupled ^{13}C nmr Spectrum at 50 MHz of Epoxidized TPBD Crystals UH45.

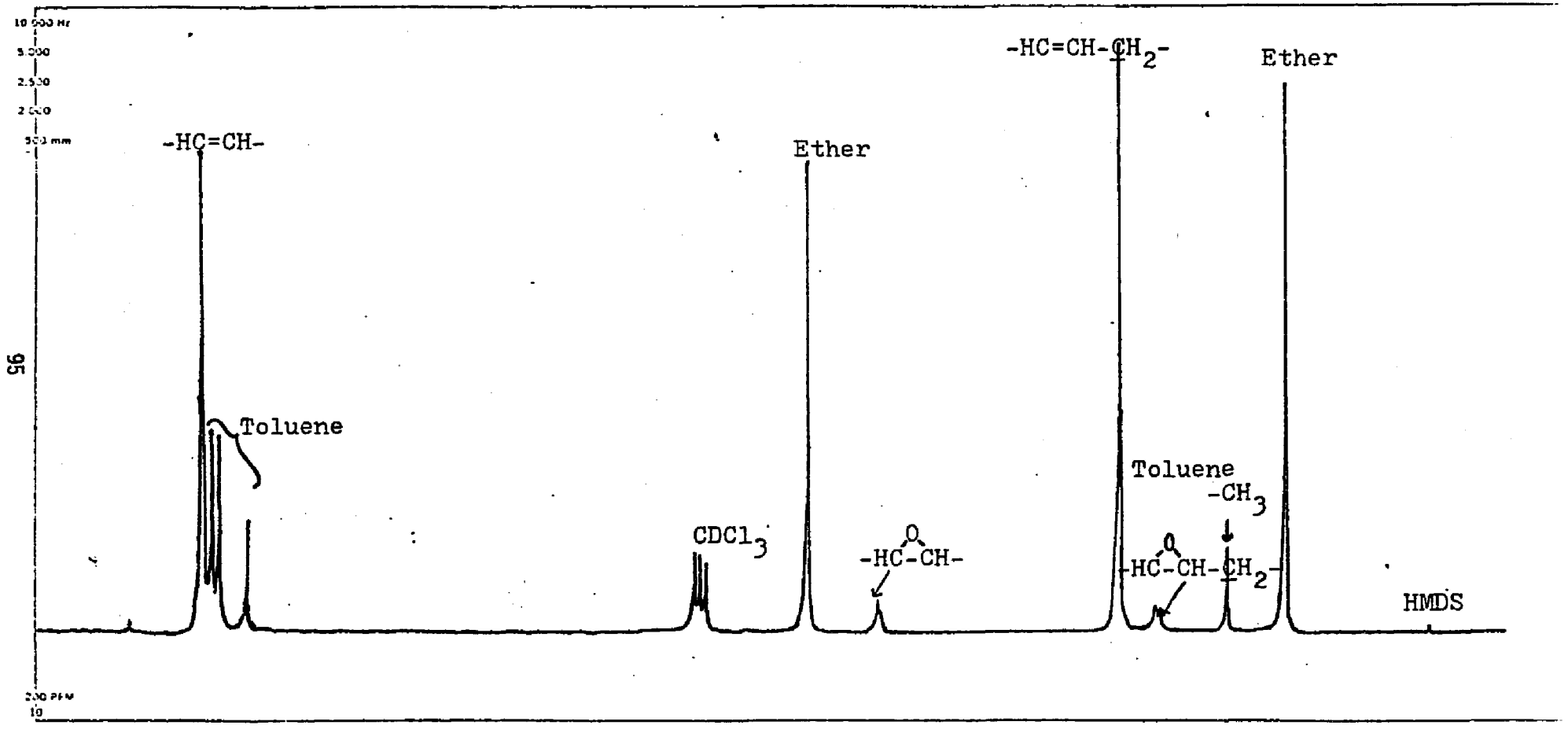

Fig. A2. Proton Noise Decoupled ^{13}C nmr Spectrum at 50 MHz of Epoxidized TPBD Crystals F1H55.

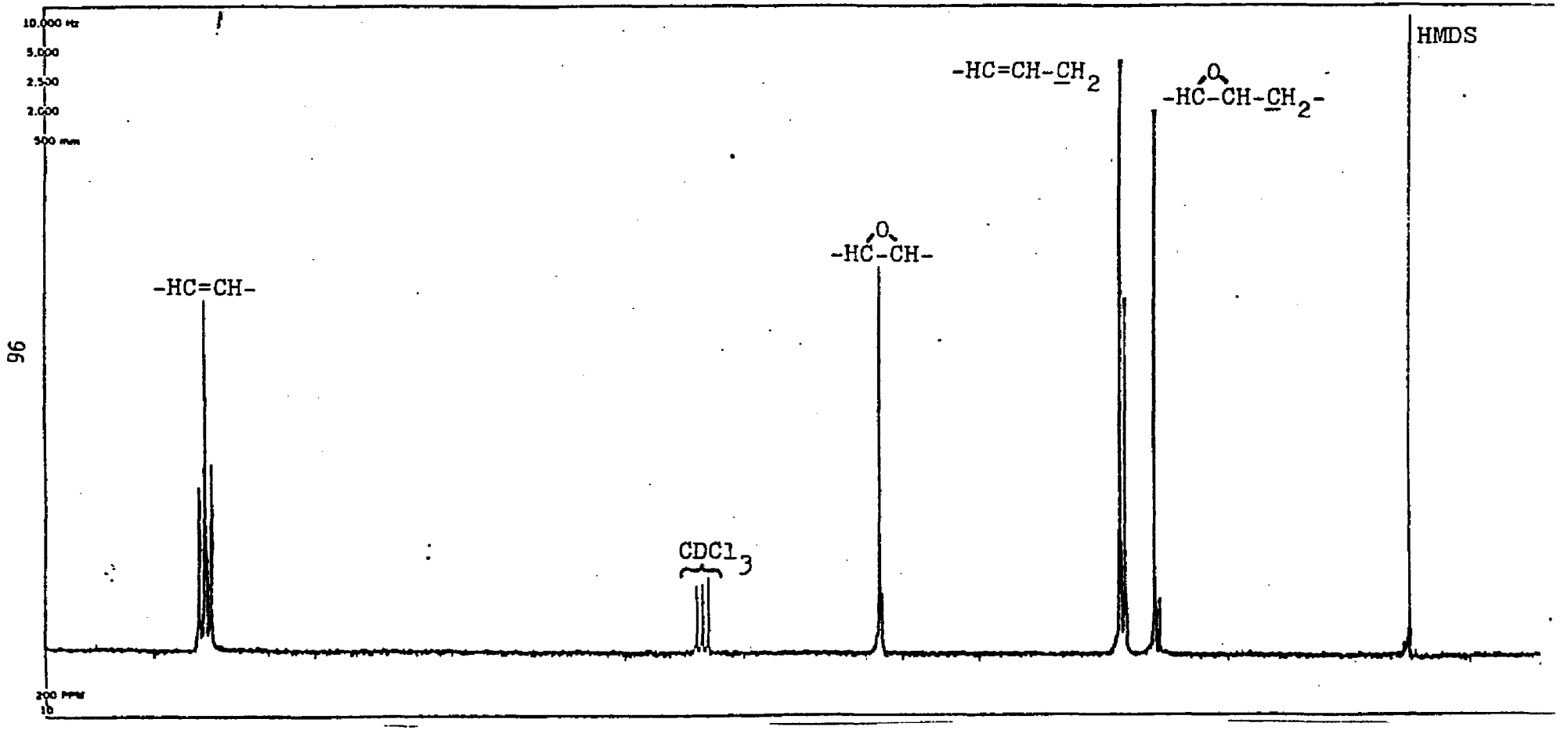

Fig. A3. Proton Noise Decoupled ^{13}C nmr Spectrum at 50 MHz for TPBD Epoxidized in $CHCl_3$ Solution to 30%.

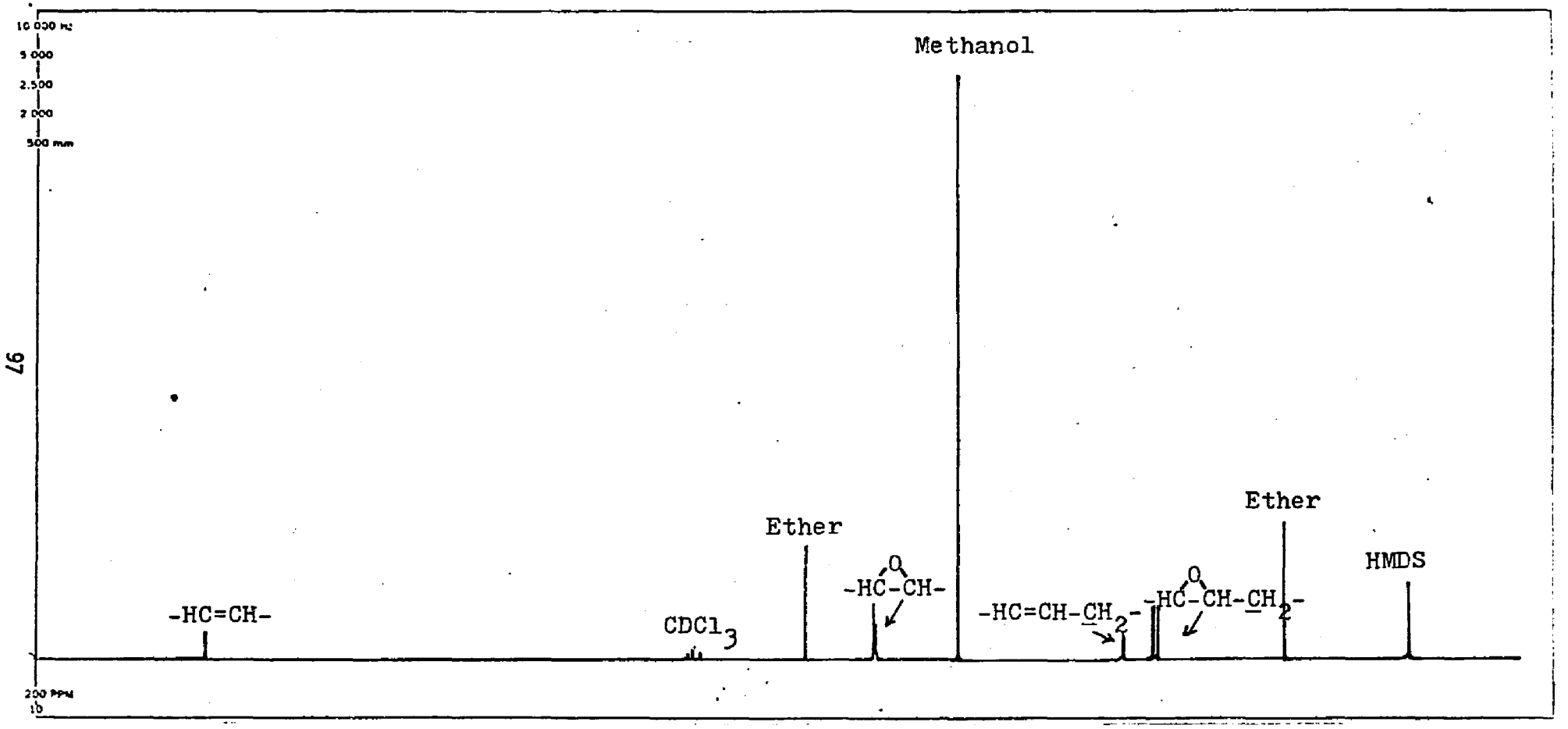

Fig. 4A Proton Noise Deocupled ^{13}C nmr Spectrum at 50 MHz for TPBD Epoxidized in $CHCl_3$ Solution to 78%.

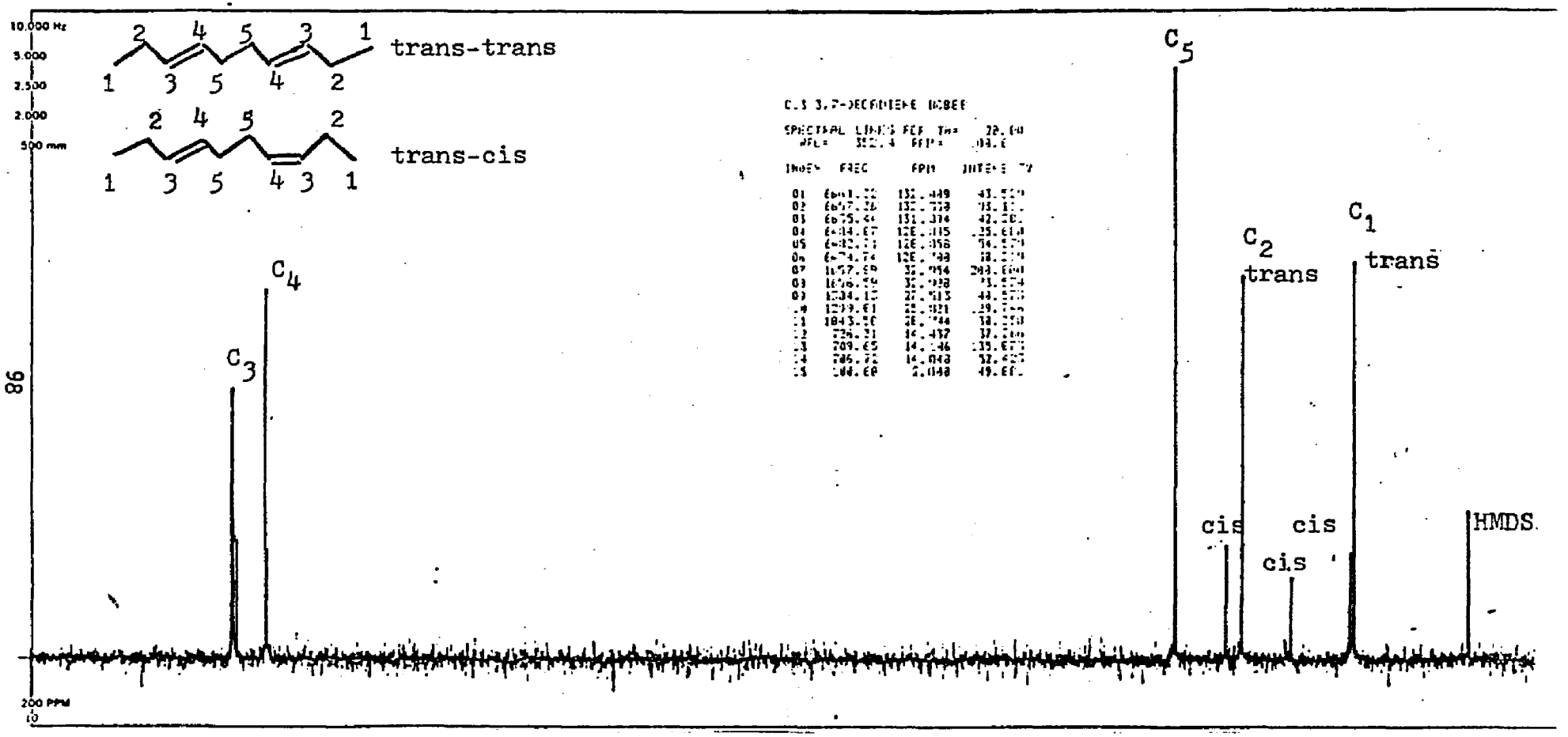

Fig. A5. Proton Noise Decoupled ^{13}C nmr Spectrum at 50 MHz of 3,7-Decadiene in $CHCl_3$/HMDS

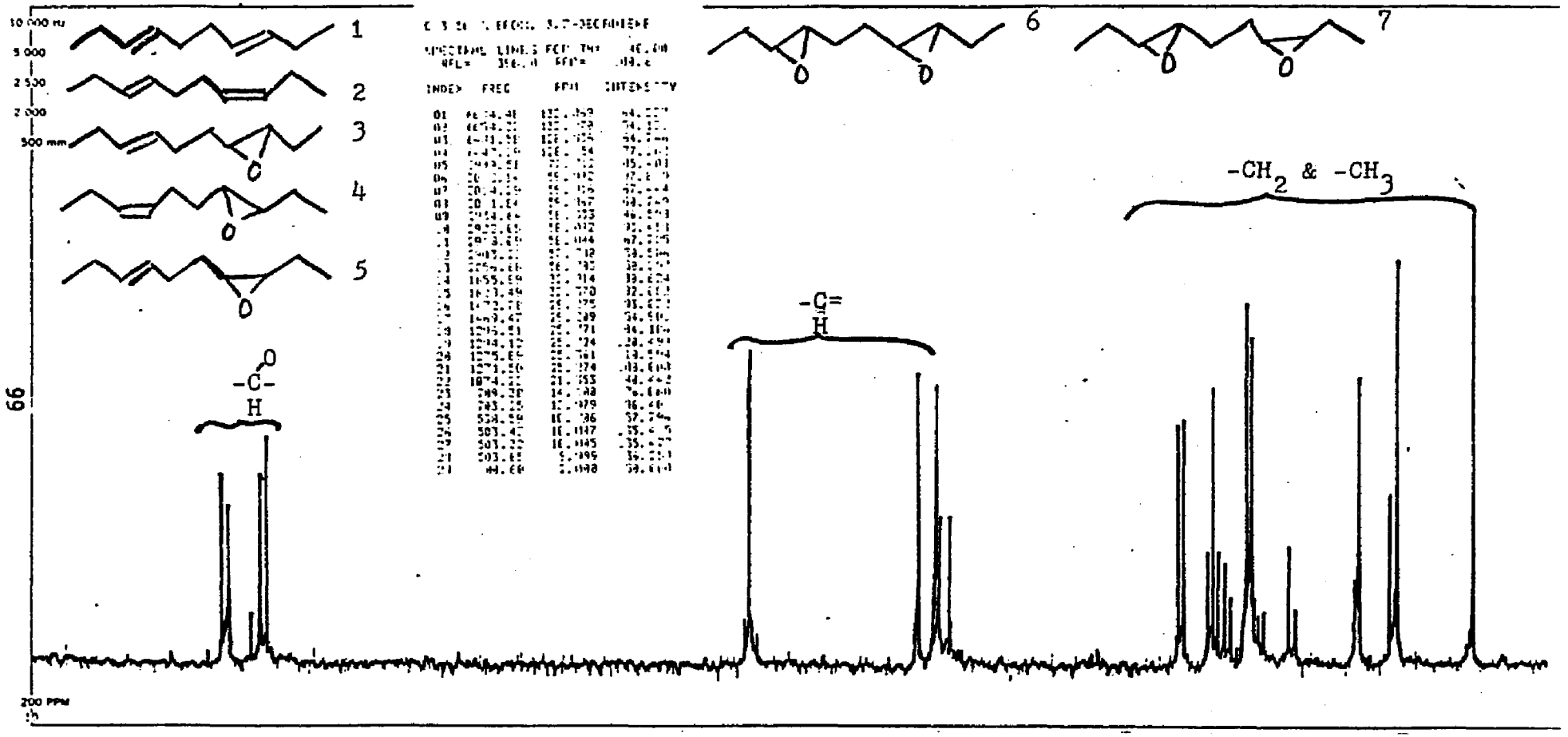

Fig. A6. Proton Noise Decoupled ^{13}C nmr Spectrum at 50 MHz of 50% Epoxidized 3,7-Decadiene.

7 possible isomers are designated as 1.DD-EE 2. DD-ZE 3. OD-tE 4. OD-tZ 5. OD-cE

6. OO-tt 7. OO-ct.

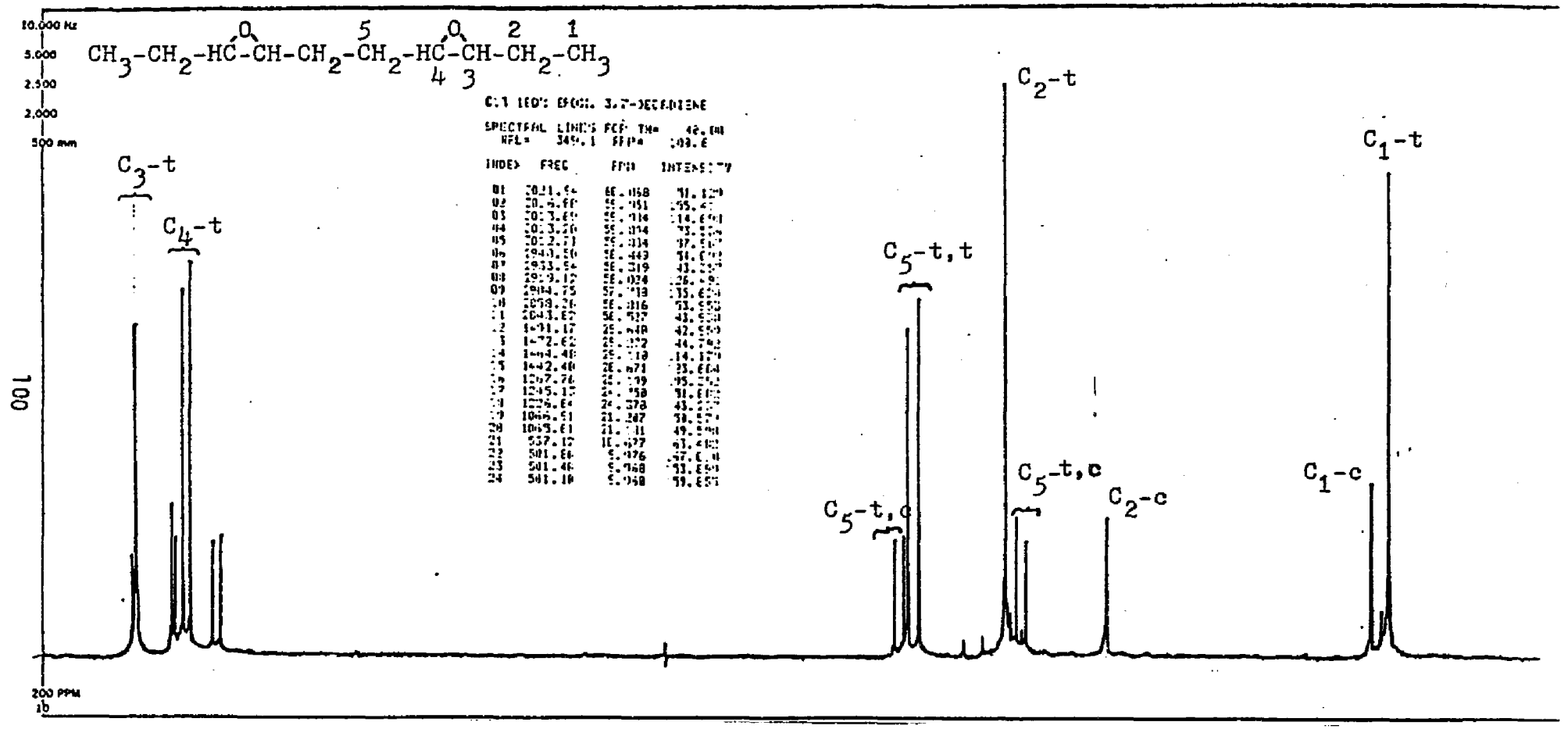

Fig. A7. Proton Noise Decoupled ^{13}C nmr Spectrum at 50 MHz of 100% Epoxidized 3,7-Decadiene. The two geometric isomers of the epoxy group are designated as t and c.

The sensitivity of resonances to the d ℓ isomers will be seen more clearly below where the scale is expanded.

The seven possible molecular structures for the model compound are given in Fig. A8 where E and Z correspond to the geometric isomers, trans and cis of the carbon-carbon double bond, and D & O correspond to the double bond and the epoxy cyclic ring. For convenience the ten carbons in the five molecular structures, DD-ZE, OD-tE, OD-tZ, OD-cE and OO-ct, are labeled with letters α-K, while the molecular structures of DD-EE and OO-tt composed of five equivalent carbon pairs are labeled with letters α-ε.

The $-CH_2-$ and $-CH_3$ region spectrum on an expanded scale is given in Fig. 9 with the detailed spectrum assignment shown in Table A1. Fig. A10 and A11 and Table A2 and A3 give the expanded scale spectrum for the -CH=CH- and $-HC\overset{O}{-}CH-$ region and their detailed peak assignments respectively. As can be seen from these spectrum, some carbons in the molecular structures are sensitive to the stereoisomers dd/ℓℓ and dℓ/ℓd. In the trans double bond molecular structures are sensitive to the stereoisomers dd/ℓℓ and dℓ/ℓd. In the trans double bond molecules the possible stereoisomers after the epoxidation are RR and SS, shown as follows:

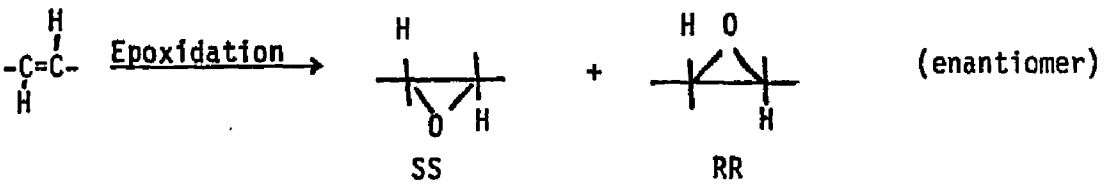

SS RR

While the cis double bond molecules may produce RS and SR isomers after epoxidation, shown as follows:

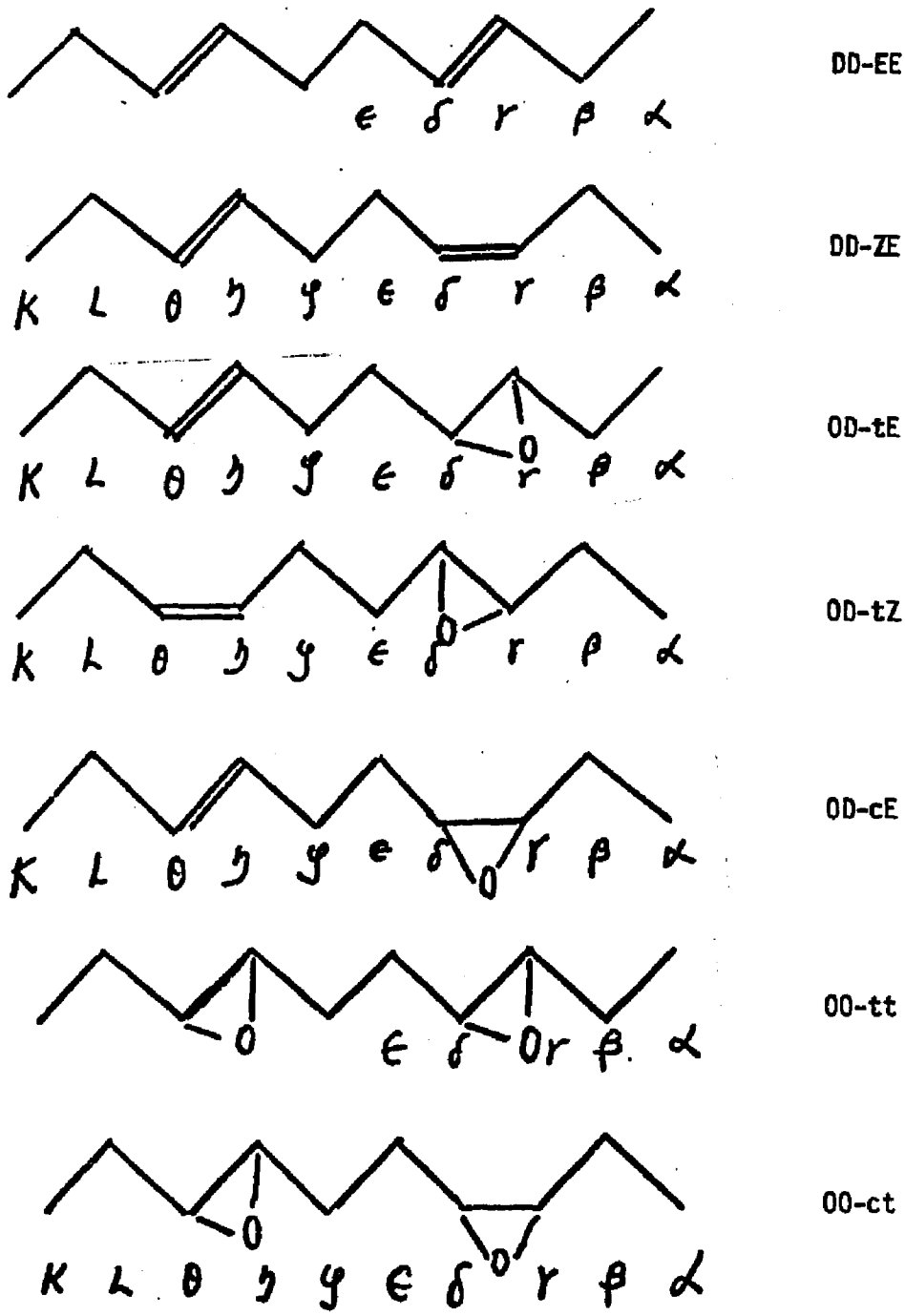

Fig. A8. The Seven Possible Compounds Presented in 50% Epoxidized 3,7-Decadiene and Their Designations.

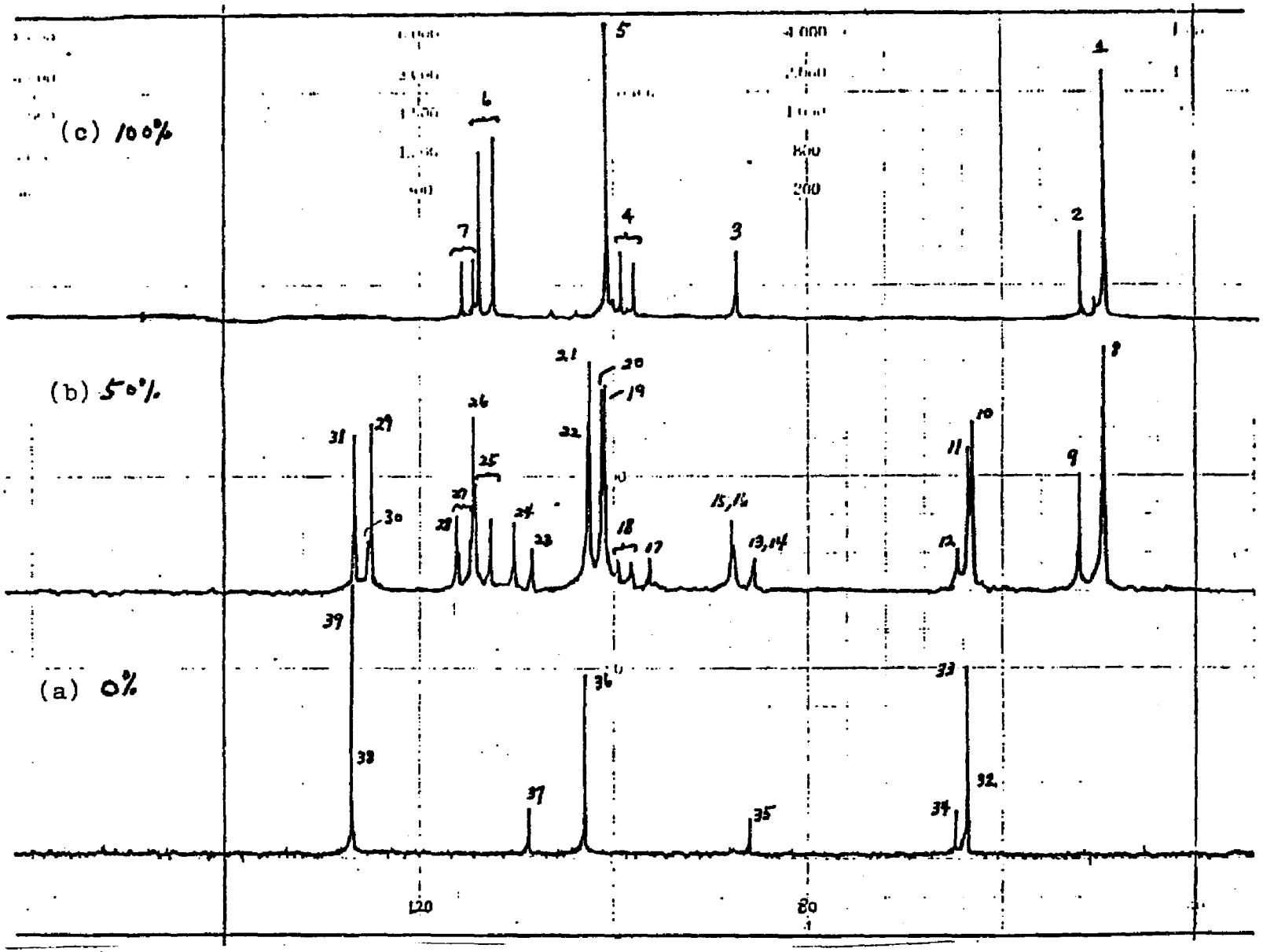

Fig. A9. The $-CH_2-$ and $-CH_3$ Regions of Proton Noise Decoupled ^{13}C NMR Spectrum at 50 MHz of (a) 3,7-Decadiene, (b) 50% Epoxidized and (c) 100% Epoxidized 3,7-Decadiene.

TABLE A1

SPECTRUM ASSIGNMENT FOR FIG. A9

Peak Designation	Assignment	Chemical Shift	Peak Designation	Assignment	Chemical Shift
1.	OO.tt-α	9.97	17.	OD.cE-ε	23.88
	OO.ct-K	9.97	18.*	OO.ct-ε	24.44
2.	OO.ct-α	10.68			24.83
3.*	OO.ct-β	21.18	19.	OO.tt-β	25.27
		21.21		OO.ct-L	25.27
4.*	OO.ct-ε	24.37	20.	OD.tE-β	25.36
		24.75		OD.tZ-β	25.36
5.	OO.tt-β	25.20	21.	OD.tE-L	25.72
	OO.ct-L	25.20		OD.cE-L	25.72
6.*	OO.tt-ε	28.67	22.	DD.EE-β	25.77
		29.11		DD.ZE-L	25.77
7.*	OO.ct-ϒ	29.27	23.	DD.ZE-ε	27.45
		29.64	24.	OD.tZ-ϒ	27.99
8.	OD.tE-α	10.00	25.*	OO.tt-ε	28.70
	OD.tZ-α	10.00			29.21
	OO.tt-α	10.00	26.	OD.tE-ε	29.28
	OO.ct-K	10.00	27.*	OO.ct-ϒ	29.38
9.	OD.cE-α	10.71			29.81
	OO.ct-α	10.71	28.	OD.tZ-ε	29.81
10.	OD.tE-K	13.98	29.	OD.tE-ϒ	32.37
	OD.cE-K	13.98	30.	OD.cE-ϒ	32.47
	DD.ZE-K	13.98	31.	DD.EE-ε	32.91
11.	DD.EE-α	14.10		DD.ZE-ϒ	32.91
12.	OD.tz-K	14.46	32.	DD.ZE-K	14.05
	DD.ZE-α	14.46	33.	DD.EE-α	14.11
13.	OD.tZ-L	20.66	34.	DD.ZE-α	14.44
14.	DD.ZE-β	20.70	35.	DD.ZE-β	20.74
15.	OD.cE-β	21.25	36.	DD.EE-β	25.82
16.*	OO.ct-β	21.35		DD.ZE-L	25.82

TABLE A1 (Continued)

Peak Designation	Assignment	Chemical Shift	Peak Designation	Assignment	Chemical Shift
37.	DD.ZE-ε	27.51			
38.	DD.ZE-ζ	32.93			
39.	DD.EE-ε	32.95			

*Diastereoisomeric Sequences

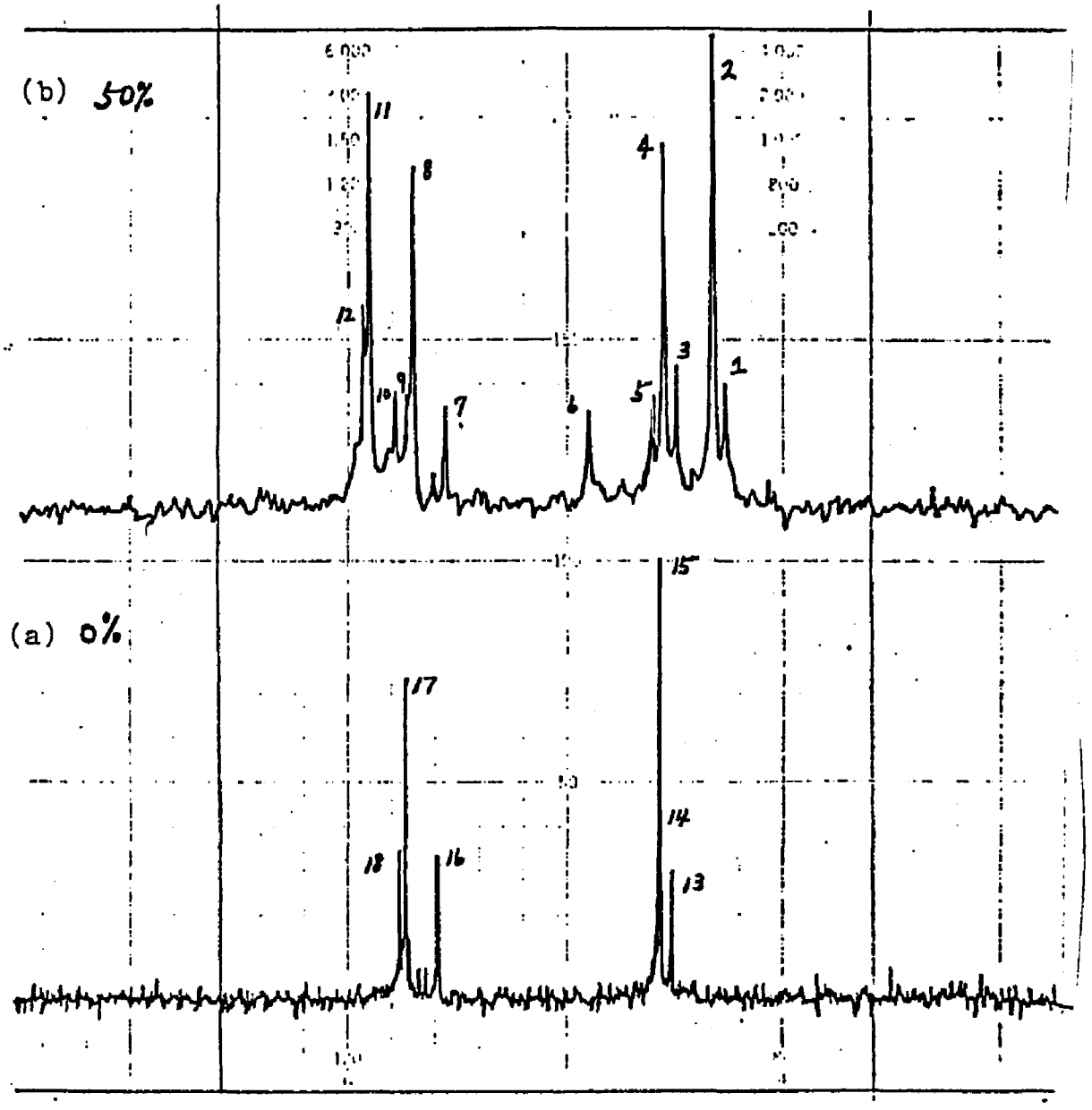

Fig. A10. The -HC=CH- Region of Proton Noise Decoupled ^{13}C NMR Spectrum at 50 MHz of (a) 3,7-Decadiene and (b) 50% Epoxidized 3,7-Decadiene.

TABLE A2

SPECTRUM ASSIGNMENT FOR FIG. A10

Peak Designation	Assignment	Chemical Shift
1.	OD.cE-η	127.99
2.	OD.tE-η	128.15
3.	DD.ZE-δ	128.66
4.	DD.EE-δ	128.84
5.	DD.ZE-η	128.98
6.	OD.tZ-η	129.86
7.	DD.ZE-γ	131.83
8.	DD.EE-γ	132.27
9.	DD.ZE-θ	132.36
10.	OD.tZ-θ	132.51
11.	OD.tE-θ	132.87
12.	OD.cE-θ	132.95
13.	DD.ZE-δ	128.70
14.	DD.ZE-η	128.86
15.	DD.EE-δ	128.89
16.	DD.ZE-γ	131.89
17.	DD.EE-γ	132.33
18.	DD.ZE-θ	132.41

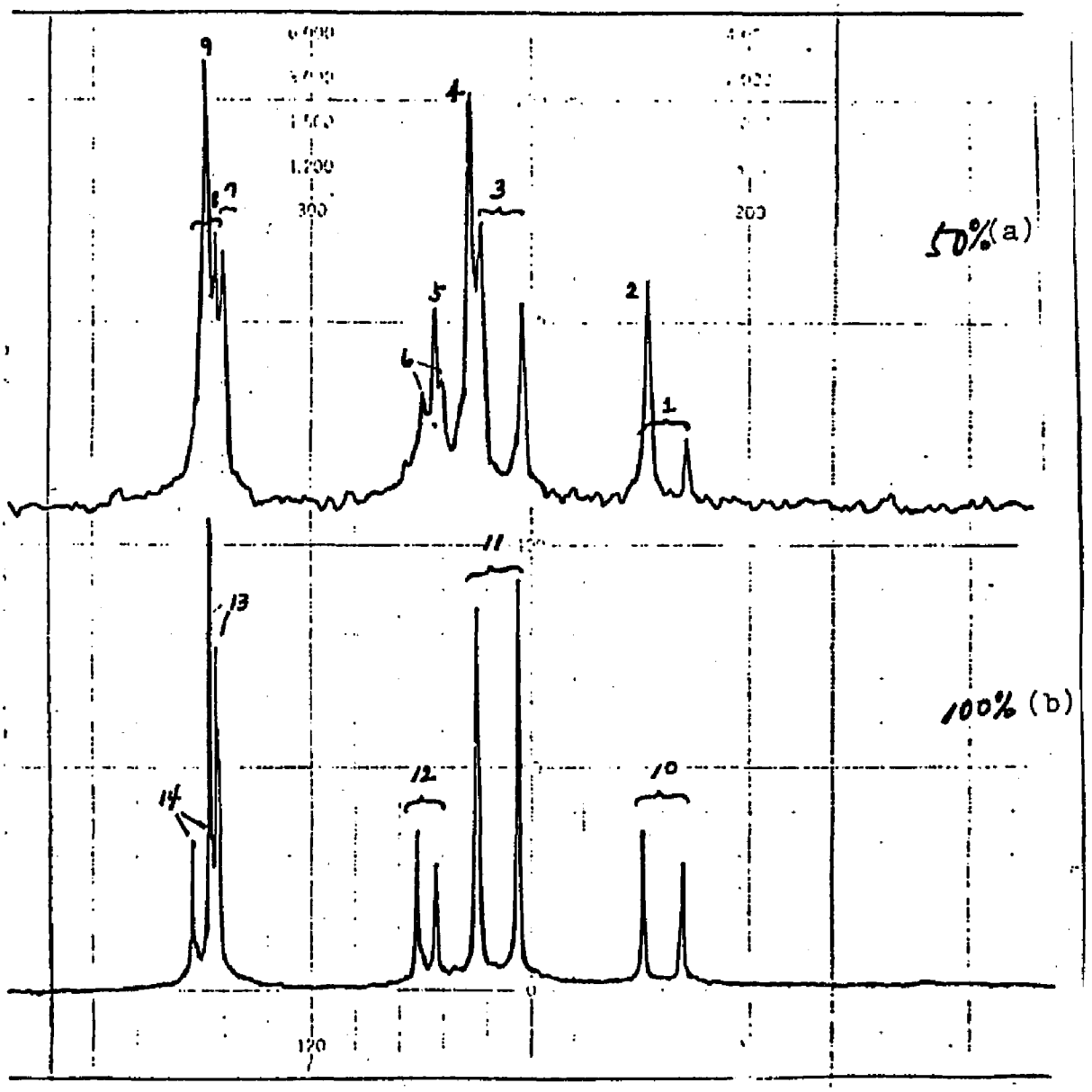

Fig. A11. The -HC-CH- Region of Proton Noise Decoupled ^{13}C NMR Spectrum at 50 MHz of (a) 50% and (b) 100% Epoxidized 3,7-Decadiene.

TABLE A3

SPECTRUM ASSIGNMENT FOR FIG. A11

Peak Designation	Assignment	Chemical Shift
1.*	OO.ct-δ	56.49
		56.78
2.	OD.cE-δ	56.78
3.*	OO.tt-δ	57.71
	OO.ct-η	58.00
4.	OD.tE-δ	58.08
	OD.tZ-δ	58.08
5.	OD.cE-γ	58.33
6.*	OO.ct-γ	58.28
		58.41
7.*	OO.tt-γ	59.87
		59.92
8.*	OO.ct-θ	59.92
		60.04
9.	OD.tE-γ	59.99
	OD.tZ-γ	59.99

*Diastereoisomeric Sequences

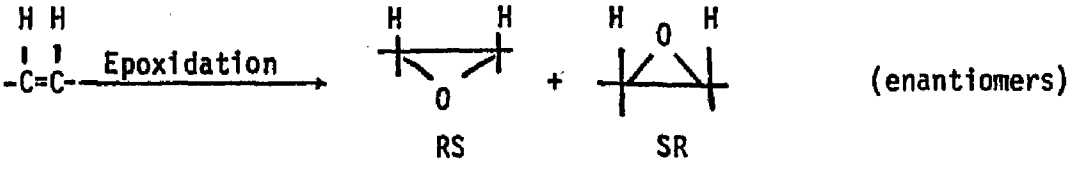

(enantiomers)

The resonance from carbon β-θ are the same for the two stereoisomers for a single epoxy group. However, the spectra for these carbons show a splitting when the two epoxy groups are present.

The spectrum splitting caused by the diastereomers is as follows:

Molecular structure: OO-tt

Carbon Designation	γ	δ	ε
Δppm	0.05	0.29	0.44
			0.51

where the splitting in carbon γ and δ on the  group are relatively small and carbon ε, the $-CH_2-$ group inside the two epoxies shows a larger splitting which helps greatly in the peak assignment for epoxidized TPBD samples. The spectrum splitting caused by the enantiomers is more sensitive than that due to diastereoisomers and is as follows:

Molecular structure: OO-ct

Carbon Designation	β	γ	δ	ε		η	θ
Δppm	0.03	0.13	0.29	0.38	0.37	0.29	0.12
	0.10			0.39	0.43		

Since the OO-ct molecular sequence does not exist in the epoxidized TPBD samples, the spectrum splitting caused by enantiomers are not

important in this research. However, it is new information from ^{13}C nmr spectrum analysis.

Based on the assignments for the model compound, 3,7-decadiene, and a comparison with the spectra for the two solution epoxidized samples, assignment for the resonances found for TPBD crystals epoxidized in suspension were made. Some possible structures of use in this analysis are given in Table A4. The spectra on an expanded scale for the D-CH-, the O-CH-, the D-CH_2- and the O-CH_2- regions for the two solution epoxidized (30% and 78%) and one of the crystal epoxidized sample (UH45) are given in Figs. A12, 13,14,and 15 respectively. The detailed spectral assignments are given in Table A5, 6, 7, and 8, respectively. Finally the expanded spectra for the epoxidized -CH_2- and -HC(O)CH- regions for crystal preparation F1H55 are given in Figs. A16 and A17. As can be seen from Fig. A12 and Table A5, certain sequences such as DDDOD, DODOD and OODOD are only detectable for the solution epoxidized polymer. In the 30% solution epoxidized sample the peak intensities of the pentad sequences such as ODDOO, OODOO and OODOD are too small to be observed; this is also the case for the peak intensities of sequences DDDDD, DDDDO, DDDOD and DDDOO found in 78% solution epoxidized sample.

As can be seen in Table A8, the CH_2's on the epoxidized units are only distinguishable if they are outside an epoxidized run (carbon h) versus being inside the run (carbon i and j) where the diastereo-isomerism causes a splitting. The degree of resolution obtained to date does not distinguish CH_2's in the epoxidized runs above a diad.

In these epoxidized TPBD spectra the resolution for the solution

TABLE A4

SEQUENCES OF INTEREST FOR ANALYSIS OF PROTON NOISE DECOUPLED ^{13}C NMR SPECTRUM (XL-200) AT 50 MHz FOR EPOXIDIZED TPBD POLYMERS

Designation	Resolution		Example
a b	pentad		
-HC=CH-	DDDDD	DODDO	
	DDDDO	DODOD	
	DDDOD	OODDO	
	DDDOO	OODOD	
	ODDDO	OODOO	
c d	triad		
-C-C	DOD		
O	DOO		
	OOO		
	tetrad		
$-CH_2-$	DDDD	DDOD	
e,f,g	DDDO	DDOO	
	ODDO	ODOD	
		ODOO	
Epoxidized	tetrad	DDCD	
	DOOD	ODOD	
$-CH_2-$	DOOO	DDOO	
h,i,j	OOOO	ODOO	

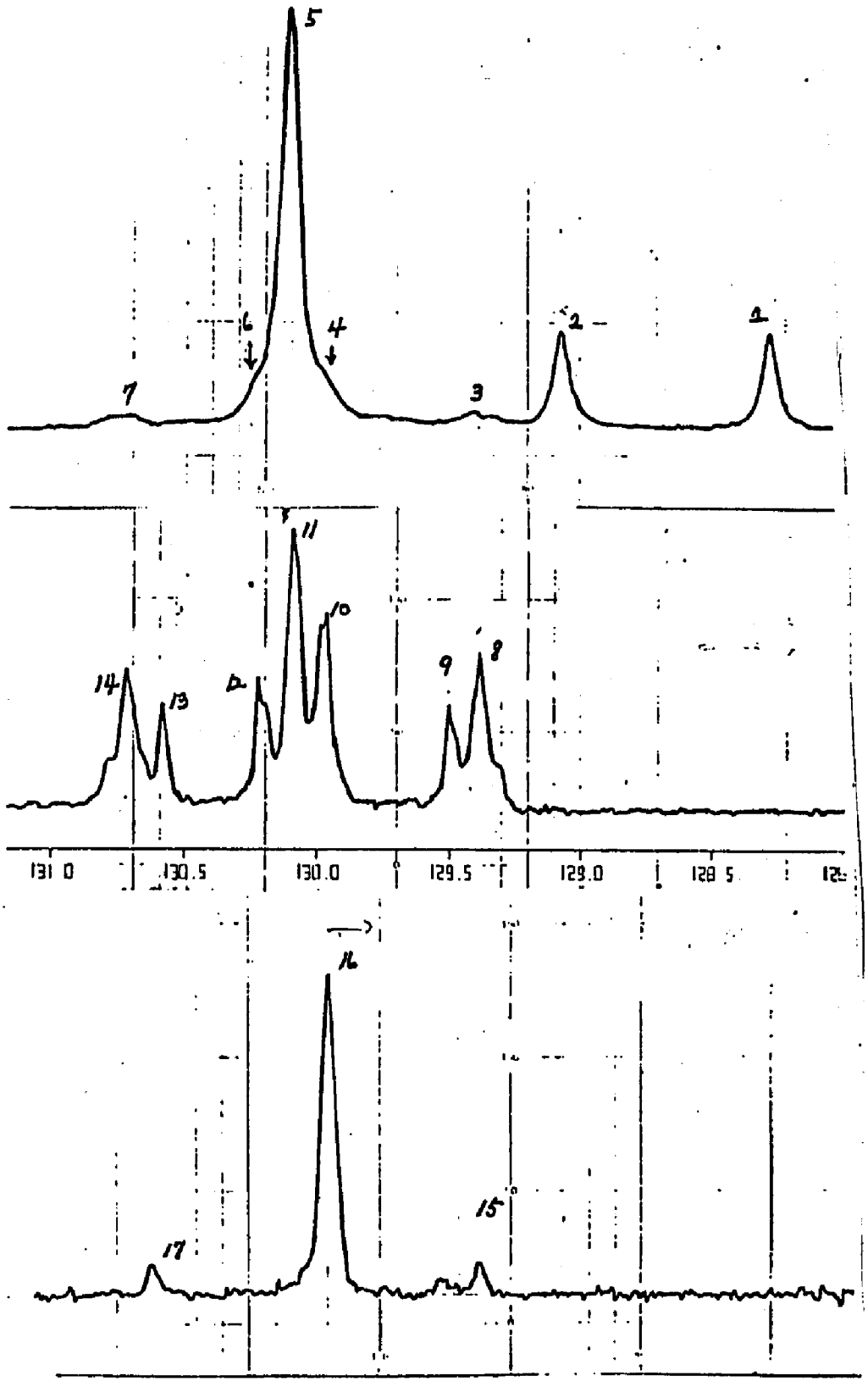

Fig. A12. The -HC=CH- Region of Proton Noise Decoupled ^{13}C NMR Spectrum at 50 MHz of Partially Epoxidized TPBD Polymer Samples.

TABLE A5

SPECTRUM ASSIGNMENT FOR FIG. A12

Peak Designation	Assignment	Chemical Shift
1.	Toluene solvent	128.21
2.	Toluene solvent	129.02
3.	DDDOO-b	129.34
4.	DDDDO-a or b	129.90
5.	DDDDO-a + b	130.06
6.	DDDDO-a or b	130.20
7.	DDDOO-a	130.68
8.	DDDOD-b	129.34
9.	DDDOO-b	129.46
10.	DDDDO-a or b	129.92
	DODOD-a + b	129.92
11.	DDDDD-a + b	130.05
12.	DDDDO-a or b	130.18
13.	DDDOO-a	130.54
14.	DDDOD-a	130.67
15	ODDOO-b	129.43
16.	OODOO-a + b	129.99
	OODOD-a + g	130.04
17.	ODDOO-a	130.65

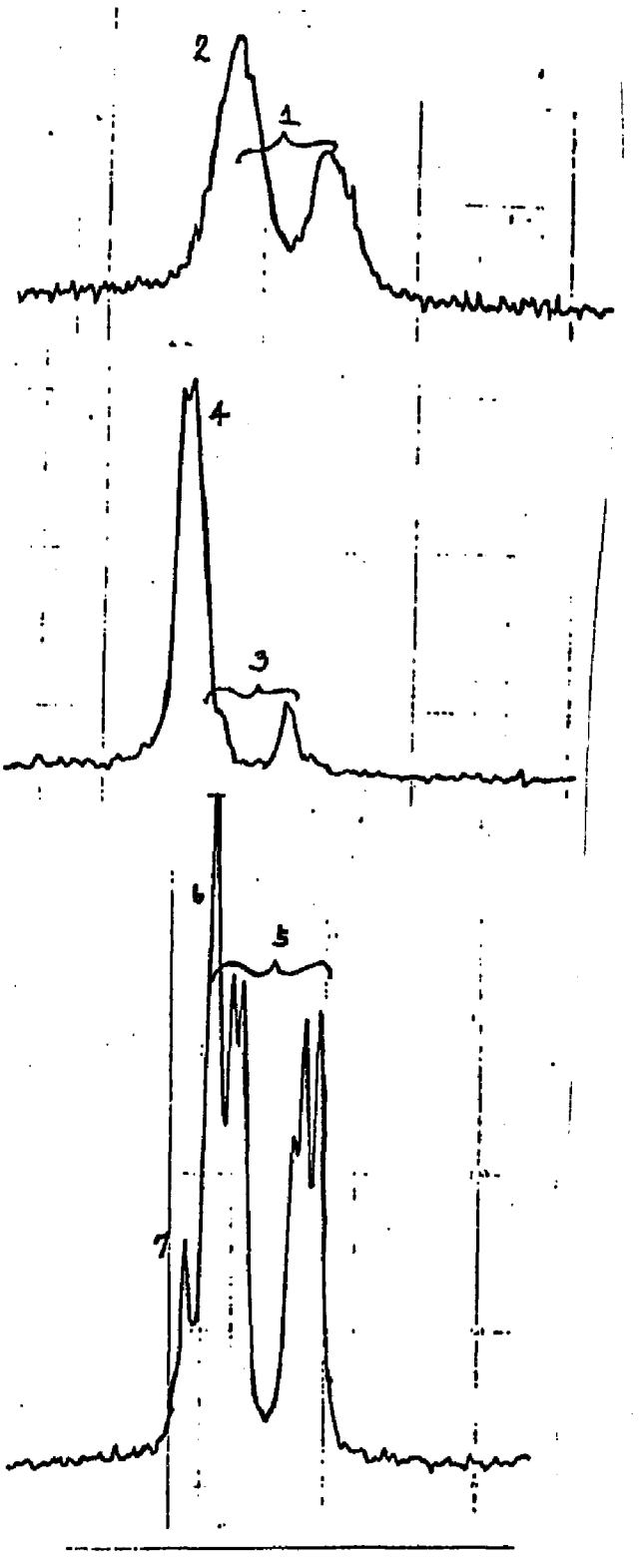

Fig. A13. The -HC$\overset{O}{\diagdown\diagup}$CH- Region of Proton Noise Decoupled ^{13}C NMR Spectrum at 50 MHz of Partially Epoxidized TPBD Polymer Samples.

TABLE A6

SPECTRUM ASSIGNMENT FOR FIG. A13

Peak Designation	Assignment	Chemical Shift
1.	OOO- c + d*	57.90, 58.22
	DOO- d**	58.22, 57.90
2.	DOO- c	58.22
3.	DOO- d**	58.04, 58.34
	OOO- c + d*	58.34, 58.04
4.	DOO- c	58.34
	DOD- c + d	58.34
5.	OOO- c + d*	58.05, 58.33
	DOO- d**	57.98, 58.28
6.	DOO- c	58.33
7.	DOD- c + d	58.34

*Diastereoismer Triads

**Diastereoisomer Pairs

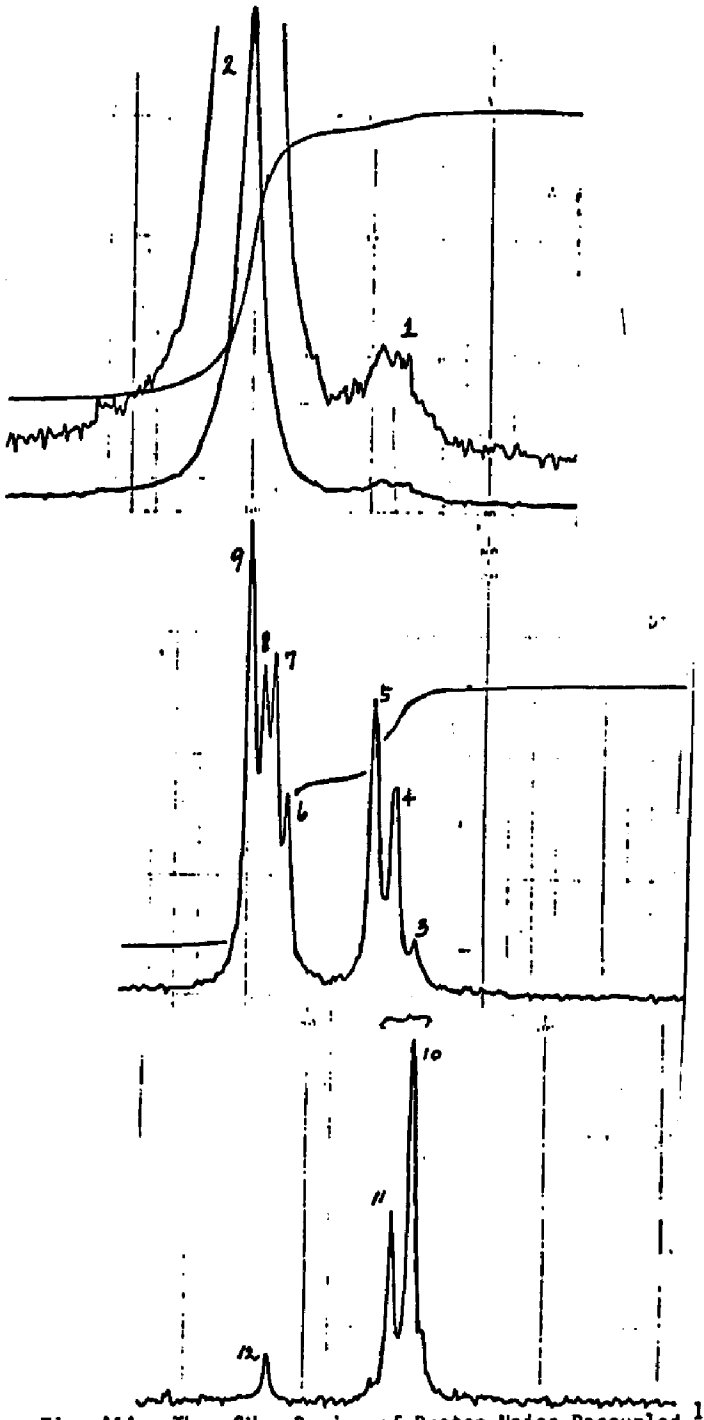

Fig. A14. The $-CH_2-$ Region of Proton Noise Decoupled ^{13}C NMR Spectrum at 50 MHz of Partially Epoxidized TPBD Polymer Samples.

TABLE A7

SPECTRUM ASSIGNMENT FOR FIG. A14

Peak Designation	Assignment	Chemical Shift
1.	DDOO- e	32.21
2.	DDDO- f + g	32.79
	DDDD- f + g	32.79
3.	ODOO- e	32.07
4.	DDOO- e	32.15
	ODOD- e	32.15
5.	DDOD- e	32.24
6.	ODDO- f + g	32.61
7.	DDDO- g	32.71
8.	DDDO- f	32.66
9.	DDDD- f + g	32.76
10.	ODOO- e	32.34
11.	DDOO- e	32.42
12.	ODDO- f + g	32.94

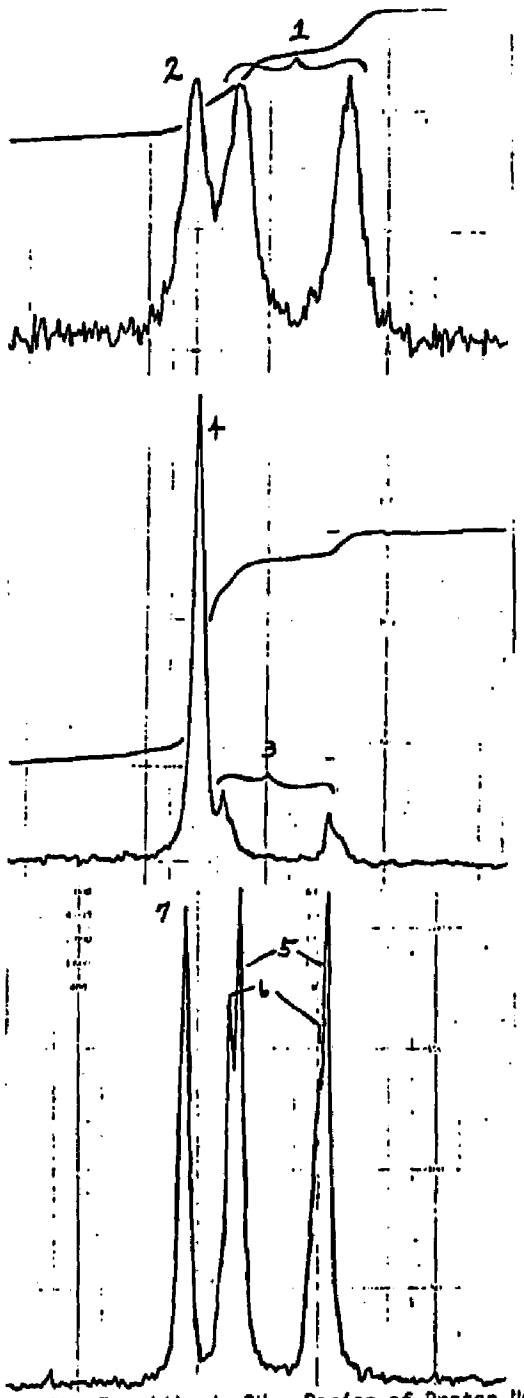

Fig. A15. The Epoxidized $-CH_2-$ Region of Proton Noise Decoupled ^{13}C NMR Spectrum at 50 MHz of Partially Epoxidized TPBD Polymer Samples.

TABLE A8

SPECTRUM ASSIGNMENT FOR FIG. A15

Peak Designation	Assignment	Chemical Shift
1.*	OOOO- i + j	28.47, 28.94
	DOOO- i + j	28.94, 28.47
2.	DDOO- h	29.12
3.*	OOOO- i + j	28.56
	DOOO- i + j	29.00
	DOOD- i + j	29.00
4.	DDOD- h	29.11
	DDOO- h	29.11
	ODOO- h	29.11
5.*	OOOO- i + j	28.46, 28.90
	DOOO- j	28.46, 28.90
6.*	DOOO- i	28.50, 28.95
	DOOD- i + j	28.50, 28.95
7.	ODOO- h	
	DDOO- h	29.07
	DDOD- h	

*Diastereoismer Pairs

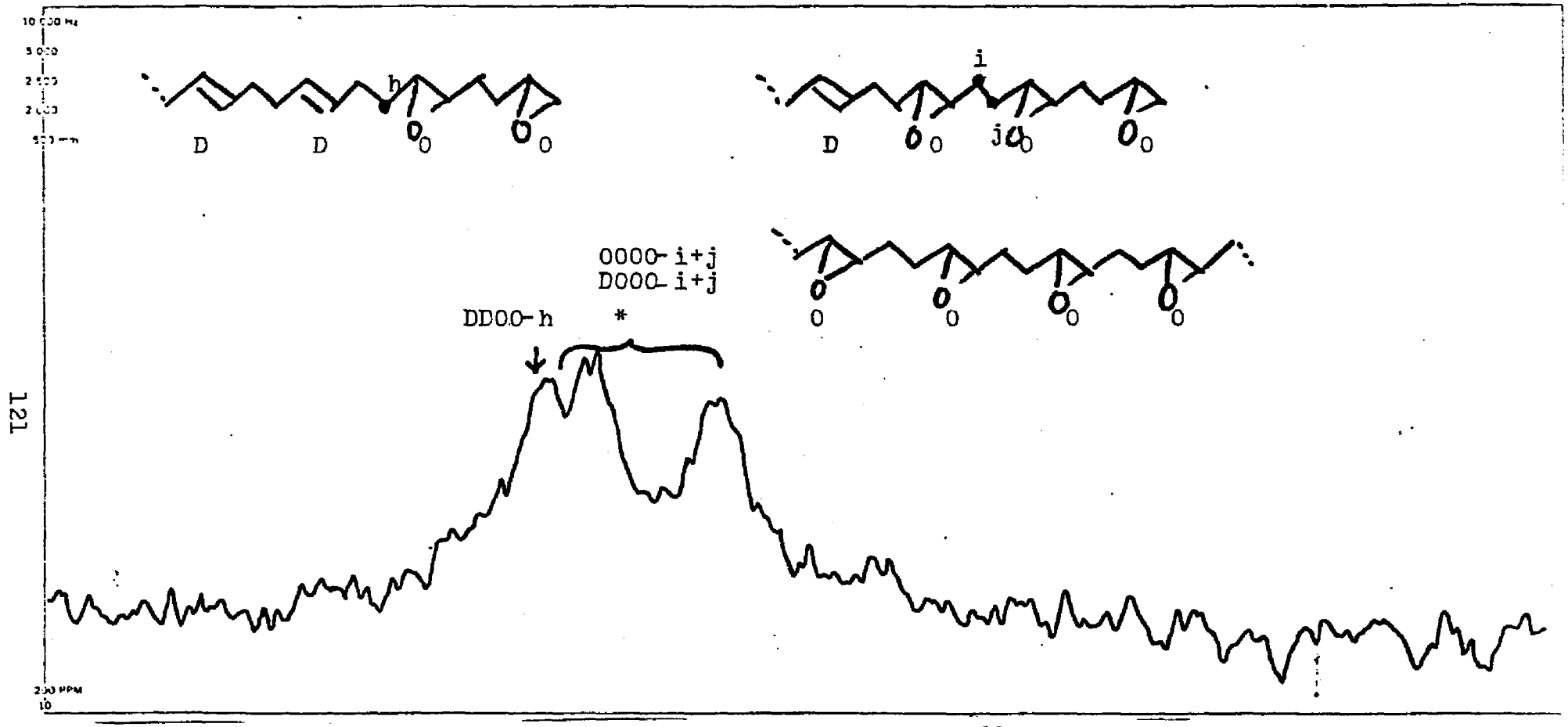

Fig. A16. The Epoxidized -CH_2- Region of Proton Noise Decoupled ^{13}C NMR Spectrum at 50 MHz of Epoxidized TPBD Crystals F1H55. (*Diastereoisomer Pairs)

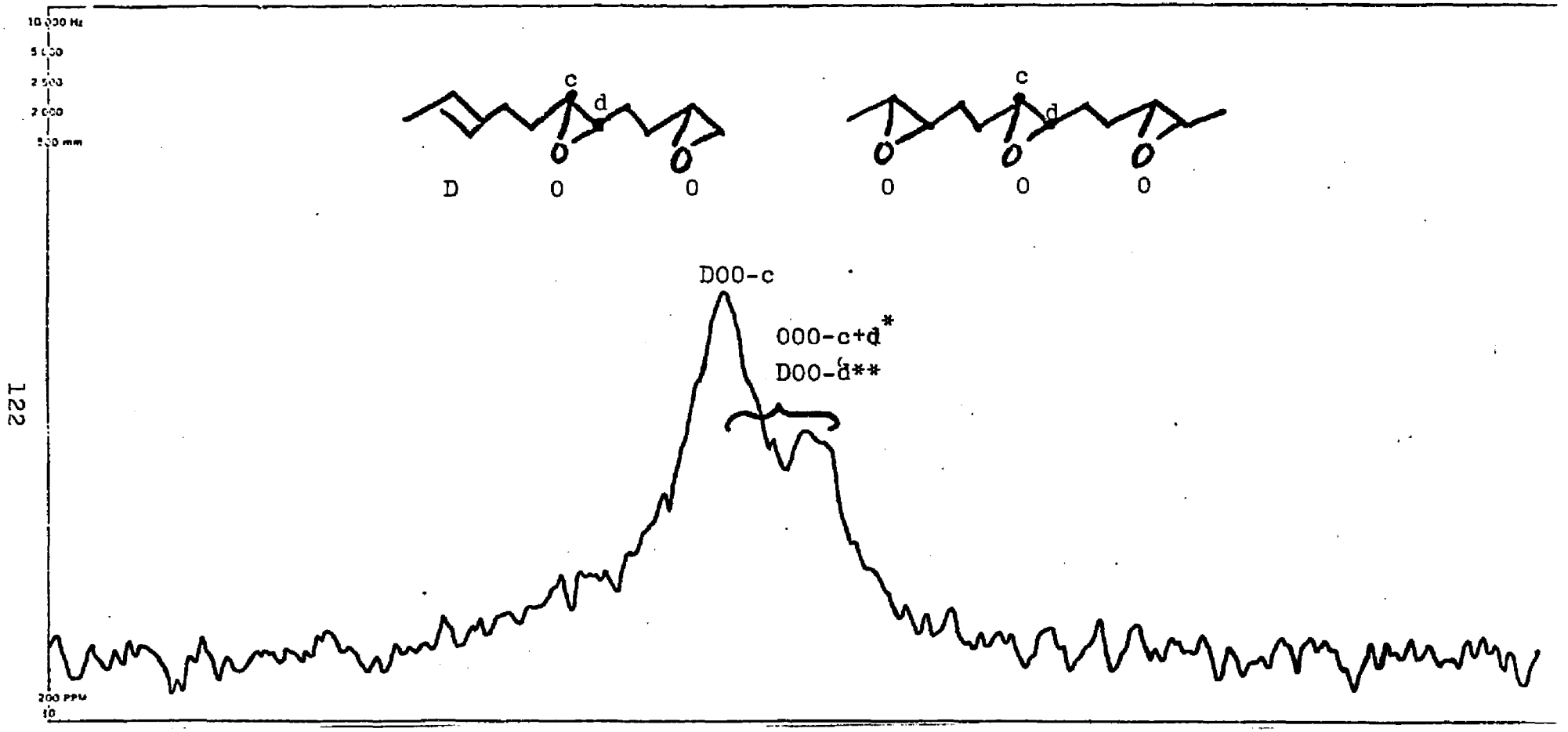

Fig. A17. The Epoxidized -CH- Region of Proton Noise Decoupled ^{13}C NMR Spectrum at 50 MHz of Epoxidized TPD Crystals F1H55. *Diastereoisomer Triads, ** Diastereoisomer Pairs.

epoxidized samples is higher than the crystal epoxidized samples. This could be due to one of the following two reasons: (1) The microdomains of the solution epoxidized samples are homogeneous, and the contribution of the magnetic field homogenity is relatively good for solution epoxidized samples, or (2) a small amount of crosslinking is present in the crystal epoxidized samples. The relatively high viscosity for crystal epoxidized samples (as was found for F1H55) decreases the degree of mobility of the epoxidized polymer molecules in $CDCl_3$ solution.

Calculation of $U_{uncor.}$, the uncorrected average number of monomer units per fold, using equation (10) is carried out from the values of the areas under the three peaks for the CH_2 parts of the epoxidized units given for UH45 in Fig. A15 and for F1H55 in Fig. A16. The area A in equation (10) is that under the two peaks at 28.47 and 28.94 ppm and B is that under the peak at 29.12 ppm.

APPENDIX B

The chain tilt correction in the calculation of U values from equation (7).

In the calculation of the number of monomer unit per chain fold, U, from equation (7):

$$U = \frac{L_c}{R}\left\{\frac{F_s\bar{M}_n}{M_o} - c\right\} \Big/ \left\{\frac{\bar{M}_n(1 - F_s)}{M_o} - \frac{L_c}{R}\right\}$$

where L_c is the crystalline thickness assuming that the c-axis is perpendicular to the lamella as shown in Fig. 21.

In monoclinic TPBD from I crystals the angle is 114°. As shown in Fig. B1 the c-axis is not exactly perpendicular to the lamella. Taking this chain tilt into account in the calculation of U value,

$$L_c' = L_c/\sin \quad = 1.1\ L_c \text{ and therefore}$$

$$U = 1.1\ \frac{L_c}{R}\left\{\frac{F_s\bar{M}_n}{M_o} - c\right\} \Big/ \left\{\frac{\bar{M}_n(1 - F_s)}{M_o} - 1.1\ \frac{L_c}{R}\right\}$$

i.e., it leads to about 10% increase in the calculation of the U value.

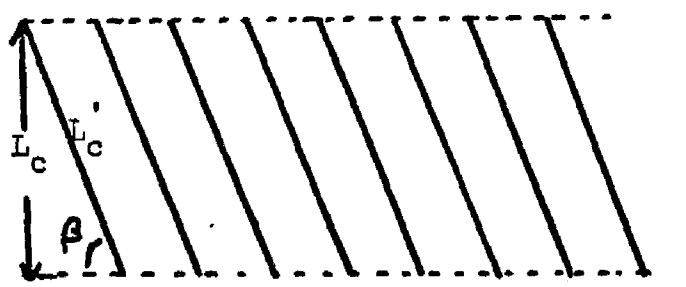

Fig. B1. Chain Tilt in TPBD Form I Crystals

APPENDIX C

Solution of equation (7)

$$U = \frac{L_c}{R}\left\{\frac{F_s\bar{M}_n}{M_o} - c\right\} \Big/ \left\{\frac{\bar{M}_n(1 - F_s)}{M_o} - \frac{L_c}{R}\right\}$$

For a polydisperse system

$$F_s \sum_i^N N_i = U \sum_i^N F_i + NC \quad \text{——} \quad \text{(B1)}$$

and $$(1-F_s) \sum_i^N N_i = \frac{L_c}{R}\left[\sum_i^N (F_i + 1)\right]$$

$$(1-F_s) \sum_i^N N_i = \frac{L_c}{R} N + \frac{L_c}{R} \sum_i^N F_i \quad \text{——} \quad \text{(B2)}$$

From (B1)

$$F_s \sum_i^N N_i/N = U \frac{\sum_i^N F_i}{N} + C$$

$$F_s \bar{N}_n = U \frac{\sum_i^N F_i}{N} + C \quad \text{——} \quad \text{(B3)}$$

From (B2)

$$(1-F_s) \frac{\sum_i^N N_i}{N} = \frac{L_c}{R} + \frac{L_c}{R} \frac{\sum_i^N F_i}{N}$$

$$(1-F_s)\bar{N}_n = \frac{L_c}{R} + \frac{L_c}{R} \frac{\sum_i^N F_i}{N} \quad \text{——} \quad \text{(B4)}$$

From (B3)

$$\frac{F_s \bar{N}_n - C}{U} = \frac{\sum_{i}^{N} F_i}{N}$$

substitute into (B4)

$$(1-F_s)\bar{N}_n = \frac{L_c}{R} + \frac{L_c}{R}\,\frac{F_s \bar{N}_n - C}{U}$$

$$\bar{N}_n = \frac{\bar{M}_n}{M_o}$$

$$(1-F_s)\,\frac{\bar{M}_n}{M_o} - \frac{L_c}{R} = \frac{L_c}{R}\,\frac{F_s\,\frac{\bar{M}_n}{M_o} - C}{U}$$

$$\frac{(1-F_s)\frac{\bar{M}_n}{M_o} - \frac{L_c}{R}}{L_c/R} = \frac{F_s\frac{\bar{M}_n}{M_o} - C}{U}$$

$$U = \frac{L_c}{R}\left\{\frac{F_s \bar{M}_n}{M_o} - C\right\} \Big/ \left\{\frac{\bar{M}_n}{M_o}(1 - F_s) - \frac{L_c}{R}\right\}$$

REFERENCES

(1) Wunderlich, B. "Macromolecular Physics" 1973, Vol. 1, pp.217-266 Academic Press, New York and London.

(2) Keller, A. Phil. Mag. 1957, 8, 1171.

(3) Fischer, E. W. Naturforsch, Z. 1957, 12a, 753.

(4) Till, P. H. J. Polym. Sci. 1957, 24, 301.

(5) Banks, W. and Sharples A. Makromol. Chem., 1963, 59, 233.

(6) Banks, W.; Gordon, M. and Sharples, A. Polymer, 1963, 4, 289.

(7) Geil, P. H. Polymer 1963, 4, 404.

(8) Rybniker, F. and Geil, P. H. J. Macromol Sci., 1973, B7, 1.

(9) Klement, J. J. and Geil, P. H. J. Polymer Sci., 1968, A2, 1381.

(10) Geil, P. H. J. Polymer Sci., 1960, 44, 449.

(11) Padden, F. J. and Keith, H. D. J. Appl Phys., 1965, 36, 2987.

(12) Giannoni, G.; Padden, F. J. and Keith, H. D., Proc. Nat. Acad. Sci. U.S., 1969, 62, 964.

(13) Cormier, C. M. and Wunderlich, B. J. Polymer Sci., 1966, A2, 666.

(14) Keller, A. and O'Connor, A. Disc. Faraday Soc., 1958, 25, 114.

(15) Keller, A. and Bassett, D. C. Proc. Roy. Soc., 1961, A263, 323 (London).

(16) Price, F. P. J. Chem. Phys., 1961, 35, 1884.

(17) Holland, V. F. and Lindenmeyer, P. H. J. Polymer Sci., 1963, A1, 3581.

(18) Holland, V. F. J. Appl. Phys., 1963, 35, 59.

(19) Wunderlich, B. J. Polymer Sci., 1964, A2, 2759.

(20) Kawai, T. and Keller, A. Phil. Mag., 1965, 11, 1165.

(21) Fischer, E. W. and Hinrichsen, Kolloid Z. Z. Polymere, 1966, 213, 93.

(22) Blackadder, D. A. and Schleinitz, H. M. Polymer, 1966, 7 603.

(23) Blackadder, D. A. J. Macromol. Sci. Rev. Macromol Chem., 1967, C1, 297.

(24) Keller, A. Kolloid Z. Z. Polymere, 1964, 197 98.

(25) Holland, V. P. and Lindenmeyer, P. H. J. Appl. Phys., 1965, 36, 3049.

(26) Hoffman, J. D.; Lauritzen, J. I.; Passaglia, E.; Ross, G.S.; Frolin, L. J. and Weeks, J. J. Kolloid Z. Z. Polymere, 1969, 231, 564.

(27) Fischer, E. W. and Lorenz, R. Kolloid Z. Z. Polymere, 1963, 189, 97.

(28) Jackson, J. B.; Flory, P. J. and Chaing, R. Trans. Faraday Soc., 1963, 59, 1906.

(29) Flory, P. J. J. Am. Chem. Soc., 1962, 84 2857.

(30) Roe, R. J. and Bair, H. E. Macromolecule, 1970, 3, 454.

(31) Keller, A.; Martucelli, E.; Priest, D. J. and Udagawa, Y. J. Polym Sci., 1971, A2 1807.

(32) Brown, R. G. J. Appl. Phys., 1963, 34, 2382.

(33) Roe, R. J. J. Chem. Phys., 1970, 53, 3026.

(34) Krimm, S. and Bank, M. I., J. Polym. Sci., 1969, A2 1785.

(35) Keller, A. and Priest, D. J., J. Macromol Sci. Phys., 1968, B2 479.

(36) Keller, A. and Priest, D. J., J. Polym. Sci. Polum. Letters, 1970 8B 58.

(37) Keller, A., Kolloid Z. Z. Polymere, 1967, 219, 118.

(38) Keller, A. and Mitsuhashi, S., J. Polymer Sci., 1963, A1 763.

(39) Holland, V. F. and Lindenmeyer, P. H., J. Polymer Sci., 1962, 57, 589.

(40) Blundell, D. J. and Keller, A., J. Macromol. Sci., 1968, B2 337.

(41) Kawai, T. and Keller, A., Phil. Mag., 1963, 8, 1973.

(42) Hamada, F.; Wunderlich, B.; Sumida, T.; Hayashi, S. and Nakajima A., J. Phys. Chem., 1968, 72, 178.

(43) Bergmann, K. and Nawotki, K., Kolloid Z. Z. Polymere, 1967, 219, 132.

(44) Bergmann, K., Kolloid Z. Z. Polymere, 1973, 251, 962.

(45) Fujimoto, K.; Nishi, T. and Kado, R. Polymer. J., 1972, 3, 448.

(46) Kitarmaru, R.; Horii, E. and Hyon, S. H. J. Polym. Sci. 1977, 15B, 821.

(47) Komoroski, R. A.; Maxfield, J.; Sakaguchi, E. and Mandelkern, L. Macromolecules, 1977, 10, 550.

(48) Schneider, B.; Jakes, J.; Pivcova, H. and Doskocilova, D., Polymer, 1979, 20, 939.

(49) Horii, F. and Kitamaru, R. J. Polym. Sci., Polym. Phys. Ed., 1978, 16, 265.

(50) Manderlkern, L. J. Polym. Sci. Symp., 1975, 50, 457.

(51) Wunderlich, B. and Cormier, C. M. J. Polym. Sci., 1966, A2, 666.

(52) Wunderlich, B., "Macromolecular Physics" Vol. 1 pp. 405-408 Academic Press, New York and London.

(53) Wunderlich, B. and Cormier, C. M. J. Polym. Sci., 1967, A2, 987.

(54) Hellmuth, E. and Wunderlich, B. J. Appl. Phys., 1965, 36, 3039.

(55) Harrison, I. R. J. Polym. Sci. Polym. Phys. Ed., 1973, 11, 991.

(56) Harrison, I. R. J. Macromol. Sci. Rev. Macromol. Chem., 1974, A8, 43.

(57) Harrison, I. R.; Runt, J. J. Polym Sci. Polym. Phys. Ed., 1979, 17, 321.

(58) Peterlin, A. and Meinel, G. J. Polym. Sci., 1965, B3, 1059.

(59) Blundell, D. J.; Keller, A. and Ward, I.M. J. Polym. Sci., 1966, B4, 781.

(60) Williams, T.; Blundell, D. J. and Keller, A. J. Polym. Sci., 1968, A2, 1613.

(61) Priest, D. J. J. Polym. Sci., 1971, A2, 1777.

(62) Keller, A. and Priest, D. J. J. Macromol. Sci., 1968, B2, 479.

(63) Keller, A. and Priest, D. J. J. Polym. Sci., 1970, B8, 13.

(64) Keller, A. J. Polym. Sci. Polym. Phys. Ed., 1975, 13, 2259.

(65) Harrison, I. R. and Juska, T. J. Polym. Sci. Polym. Phys. Ed., 1979, 17, 491.

(66) Stellman, J. M. and Woodward, A. E. J. Polym. Sci. Polym. Letters Ed. 1969, 7, 755.

(67) Stellman, J. M. and Woodward, A. E. J. Polym. Sci., 1971, A2, 59.

(68) Hendrix, C.; Whiting, D. A and Woodward, A. E. Macromol., 1971, 4, 571.

(69) Newman, B.; Stellman, J. M. and Woodward, A. E. J. Polym. Sci. Polym. Phys. Ed., 1972, 10, 2311.

(70) Ng, S-B.; Stellman, J. M. and Woodward, A. E. J. Macromol. Sci., 1973, B7, 539.

(71) Eng, S. and Woodward, A. E. J. Macromol. Sci., 1974, B10, 627.

(72) Evans, H. and Woodward, A. E. Macromol., 1976, 1, 88.

(73) Nagamura, T. and Woodward, A. E. J. Polym. Sci. Polym. Phys. Ed., 1976, 14, 275.

(74) Wichacheewa, P. and Woodward, A. E. J. Polym. Sci. Polym. Phys. Ed., 1978, 16, 1849.

(75) Evans, H. and Woodward, A. E. Macromol. 1978, 11, 685.

(76) Tatsumi, T.; Fukushima, T.; Imada, K. and Takayanagi, M. J. Macromol. Sci. Phys., 1967, B1, 459.

(77) Suehiro, K. and Takayanagi, M., J. Macromol. Sci Phys., 1970, B4, 39.

(78) Iwayanagi, S. Skurai, I. and Sakurai, T., J. Macromol. Sci. Phys., 1968, B2, 163.

(79) Brown, W. R.; Jenkins, R. B. and Park, G. S., J. Polym. Sci., Symp. 1973, 41, 45.

(80) Oyama, T.; Shiokawa, K. and Murata, Y., Polymer J., 1974, 6, 549.

(81) Marchetti, A. and Martuscelli, E., J. Polym. Sci. Polym. Phys. Ed., 1976, 14, 151.

(82) Marchetti, A. and Martuscelli, E. J. Polym. Sci. Polym. Phys. Ed., 1976, 14, 323.

(83) Finter, J. and Wegner, G, Makromol. Chem., 1981, 182, 1859.

(84) Duuren, B. L. and Schmitt, F. L. J. Org. Chem., 1960, 25, 1761.

(85) Garlson, R. G.; Behn, N. S. and Coroles, C. J. Org. Chem., 1971, 36, 24.

(86) Gemmer, R. V. and Golub, M. A. J. Polym. Sci. Polym. Chem. Ed., 1978, 16, 2985.

(87) Hayashi, O.; Takahashi, T.; Kurihara, H. and Ueno, H. Polym. J., 1981, 13, 215.

(88) Hoffman, J. D. and Davis, G. T. J. Res. Natl. Bur. Stand. Sect., 1975, A79A, 613.

(89) Durbetaki, A. J. and Miles, C. M. Anal. Chem., 1965, 37, 1213.

(90) Bovey, F. B. "High Resolution NMR of Macromolecules", 1972, p. 225, Academic Press, New York.

(91) Nagao, R., J. Soc., Rubber Industry, Japan, 1968, 41, 509, (in Japanese).

(92) Geil, P. H. and Reneker, D. H. J. Polym. Sci., 1961, 51, 569.

(93) Wunderlich, B. and Sullivan, P. J. Polym. Sci., 1962, 61, 195.

(94) Mitsuhashi, S. and Keller, A. Polymer, 1961, 2, 109.

(95) Keller, A.; Udagawa, Y.; Wills, H. H., J. Polym. Sci., 1971, A-2, 1793.

(96) Harrison, I. R., Runt, J.; Stanislow, L. J. and Bell, D. A. J. Polym. Sci., Polym. Phys. Ed., 1979, 17, 63.

(97) Bundell, D. J. and Keller, H. H. J. Polym. Sci. 1967, B, 991.

(98) Harrison, I. R.; Runt, J. J. Macromol. Sci. Phys., 1980, B17, 83.

(99) Chu, C. C. Polym. Preprints, 1978, 19, 773.

(100) Wunderlich, B. "Macromol. Phys." 1973 Vol 1, pp. 435-489, Academic Press, New York and London.

(101) Wichacheewa, P. Ph.D. Thesis "The Kinetics of the Epoxidation of Trans 1,4-polybutadiene Crystals in Suspension and Related Studies" 1978, City University of New York p. 104.

(102) Tseng, S.; Herman, W.; Woodward, A. E. and Newman, B. A. Macromol. 1982, 15, 2 338.